2013

Formulation Optimization for Pore Lifetime Enhancement and Sustained Drug Delivery Across Microneedle Treated Skin

Priyanka Ghosh
University of Kentucky, priyankag86@gmail.com

STUDENT AGREEMENT:

I represent that my thesis or dissertation and abstract are my original work. Proper attribution has been given to all outside sources. I understand that I am solely responsible for obtaining any needed copyright permissions. I have obtained and attached hereto needed written permission statements(s) from the owner(s) of each third-party copyrighted matter to be included in my work, allowing electronic distribution (if such use is not permitted by the fair use doctrine).

I hereby grant to The University of Kentucky and its agents the non-exclusive license to archive and make accessible my work in whole or in part in all forms of media, now or hereafter known. I agree that the document mentioned above may be made available immediately for worldwide access unless a preapproved embargo applies.

I retain all other ownership rights to the copyright of my work. I also retain the right to use in future works (such as articles or books) all or part of my work. I understand that I am free to register the copyright to my work.

REVIEW, APPROVAL AND ACCEPTANCE

The document mentioned above has been reviewed and accepted by the student's advisor, on behalf of the advisory committee, and by the Director of Graduate Studies (DGS), on behalf of the program; we verify that this is the final, approved version of the student's dissertation including all changes required by the advisory committee. The undersigned agree to abide by the statements above.

Priyanka Ghosh, Student

Dr. Audra L. Stinchcomb, Major Professor

Dr. Jim Pauly, Director of Graduate Studies

FORMULATION OPTIMIZATION FOR PORE LIFETIME ENHANCEMENT AND SUSTAINED DRUG DELIVERY ACROSS MICRONEEDLE TREATED SKIN

DISSERTATION

A dissertation submitted in partial fulfillment

of the requirements for the degree of Doctor of Philosophy in the

College of Pharmacy

at the University of Kentucky

By

Priyanka Ghosh

Lexington, Kentucky

Director: Dr. Audra L. Stinchcomb, Professor of Pharmaceutical Sciences

Lexington, Kentucky

2013

ABSTRACT OF DISSERTATION

FORMULATION OPTMIZATION FOR PORE LIFETIME ENHANCEMENT AND SUSTAINED DRUG DELIVERY ACROSS MICRONEEDLE TREATED SKIN

Microneedle (MN) enhanced drug delivery is a safe, effective and efficient enhancement method for delivery of drug molecules across the skin. The “poke (press) and patch” approach employs solid stainless steel MN to permeablize the skin prior to application of a regular drug patch over the treated area. It has been previously shown that MN can be used to deliver naltrexone (NTX) at a rate that provides plasma concentrations in the lower end of the therapeutic range in humans. The drug delivery potential of this technique is, however, limited by the re-sealing of the micropores in a 48-72h timeframe. The goal of the current research was to optimize the formulation for a 7 day MN enhanced delivery system for NTX either by adding a second active pharmacological moiety or by optimizing formulation characteristics alone. Three different formulation strategies were explored: formulation pH optimization with NTX; a codrug approach with NTX and a nonspecific cyclooxygenase inhibitor, diclofenac (DIC); and a topical/transdermal approach with NTX and an enzyme inhibitor of the cholesterol synthesis pathway, fluvastatin (FLU). The results indicated that formulation pH cannot be used to extend micropore lifetime, although formulation optimization leads to enhanced transport and thus drug delivery across MN treated skin. The codrug approach was successful in extending the micropore lifetime and further screening of codrug structures and formulation optimization helped in selection of a codrug candidate suitable for evaluation in animal pharmacokinetic studies. Local treatment with FLU helped to keep the micropores open and enabled delivery of NTX for an extended period. The pores re-sealed on removal of treatment within a 30-45 minute timeframe, indicating that infection/irritation should not be a major issue, as in the case of other topical chemical enhancers. Thus, overall it can be concluded that different formulation strategies can be utilized to extend micropore lifetime and enhance delivery of drug molecules across the skin.

KEYWORDS: microneedles, naltrexone, transdermal, formulation strategies, micropore lifetime

Priyanka Ghosh

Student’s signature

April 24, 2013

Date

FORMULATION OPTIMIZATION FOR PORE LIFETIME ENHANCEMENT AND SUSTAINED DRUG DELIVERY ACROSS MICRONEEDLE TREATED SKIN

By

Priyanka Ghosh

Dr. Audra L. Stinchcomb
Director of Dissertation

Dr. Jim Pauly
Director of Graduate Studies

April 24, 2013
Date

DEDICATION

This work is dedicated to my family

ACKNOWLEDGEMENTS

The first and foremost person I would like to acknowledge is my thesis advisor, Dr. Audra Stinchcomb for her constant support and encouragement, not only in the laboratory but throughout every aspect of my graduate studies. She accepted me into the laboratory fresh out of undergraduate studies and helped me grow into a scientist through constant interaction and guidance. I would also like to thank my graduate advisory committee Dr. Peter Wedlund, Dr. Kyung Bo Kim and Dr. Kimberly Anderson. They have been very patient with me and always had valuable input for the continuous progress of my thesis project, be it at committee meetings or anytime I stopped by for advice. I especially would like to thank them for dealing with all my emails, teleconferencing requests and continuous support after we relocated to Baltimore. I would also like to thank my external committee member, Dr. Naresh Shah for taking his valuable time to serve as an external member on my dissertation committee.

Next I would like to acknowledge my entire lab group at University of Kentucky. Dr. Mikolaj Milewski for being the best mentor, guide and friend I could ask for, Dr. Nicole Brogden for being a great friend and support system throughout our numerous hours of work and travels, Dr. Raghotham Reddy Pinninti for helping me understand the basics of organic chemistry and synthesizing the first codrug, Dr. Kalpana Paudel for all the valuable advice, discussions and input including the basic plan for the codrug project, Dana Hammell for help with animal studies and taking care of every other aspect of the lab so that we could just focus on experiments, Jessica Wehle for all her administrative help, and Dr.Courtney Swadley and Dr.Caroline Strasinger for teaching me the basics in the lab. I am grateful to each one of you because being in the lab has taught me not only to to be a good team player, but has helped me immensely in

developing as a scientist. I would also like to thank Dr.Stan Banks for all his help with mass spectrometry and science in general. Very special thanks to Catina Rossoll for taking care of everything for us in the graduate program and never saying no to the strangest of requests.

I would also like to thank everyone in my new lab at Maryland, especially Lijia Chen and Charity Wallace for help with animal experiments, the entire Department of Pharmaceutical Sciences at University of Maryland, Baltimore for accepting me graciously into the graduate program and helping me get settled and move along with my thesis research in every possible way, and Dr. Stephen Hoag for all the helpful discussions and letting me use the DSC and rheometer in his lab.

I would also like to thank our collaborators, DoMin Lee in Dr. Kim's lab and Dr. Kyung Bo Kim for synthesizing the codrugs for my project and the valuable advice, and Dr. Mark Prausnitz and Dr. Vladimir Zarnitsyn for the microneedle fabrication and input. I would also like to acknowledge all the funding sources that are responsible for the work, NIH, CDART at UK, and the graduate school at UK.

All my friends and family in Lexington, India and the rest of the world are tremendously responsible for the completion of my graduate work. I would like to thank Dr. Kamalika Mukherjee and Sucharita Sen for helping me through the ups and downs of graduate school and all my friends in Lexington for the fantastic 3.5 years. Thanks to Megha Roy and Rajasi Biswas for keeping me sane through the last 5 years. And lastly I would like to thank the most important people in my life, my family. My parents, Subhasis Ghosh and Dr. Manju Ghosh, believed in me and inspired me through 20+ years of education and let me travel so far to fulfill my dreams. My brother Dr.Kaustav Ghosh, sister-in-law, Sonia Das and the newest member of our family, my niece Anvita Ghosh (Hiya) have always been there and I never felt distant from home because of them. My brother has always been a role model and source of inspiration in every aspect of my life

and I am really glad that I could follow in his footsteps. I could not have gone through graduate school without each and every one’s constant love, support and encouragement.

TABLE OF CONTENTS

LIST OF TABLES

LIST OF FIGURES

LIST OF ABBREVIATIONS

w/w	weight per weight
w/v	weight per volume
°C	degrees Celsius
µm	micrometer
ACN	acetonitrile
ANOVA	analysis of variance
APCI	atmospheric pressure chemical ionization
API	active pharmaceutical ingredient
AUC	area under the curve
Cl	clearance
cm	centimeter
C_{max}	maximum plasma concentration
C_{ss}	plasma concentration at steady state
COX	cyclooxygenase
DIC	diclofenac
FDA	Food and Drug Administration
FLU	fluvastatin
J	flux
hr	hour
HCl	hydrochloride
HEC	hydroxyethylcellulose
HEPES	4-(2-hydroxyethyl)-1-piperazineethanesulfonic acid
HGP	hairless guinea pig
HPLC	high performance liquid chromatography
IACUC	Institutional Animal Care and Use Committee
IV	intravenous
kg	kilogram
LC-MS/MS	liquid chromatography-tandem mass spectroscopy
log $K_{o/w}$	logarithm of octanol-water partition coefficient
logP	logarithm of permeability coefficient
MeOH	methanol
mg	milligram

min	minute
ml	milliliter
mm	millimeter
mM	millimolar
MN(s)	microneedle(s)
MW	molecular weight
n	number
ng	nanogram
NSAID	non-steroidal anti-inflammatory drugs
NTX	naltrexone
NTXol	6-β-naltrexol
P	permeability
pK_a	acid ionization constant
PG	propylene glycol
PK	pharmacokinetic
PEG	polyethylene glycol
r^2	coefficient of determination
SC	stratum corneum
SD	standard deviation
SDS	sodium dodecyl sulfate
TEWL	transepidermal water loss
T_{lag}	time until appearance of drug in the plasma
T_{max}	time of maximum plasma concentration
UV	ultraviolet
YP	Yucatan miniature pig

Chapter 1

Statement of problem

Oral and parenteral drug deliveries are the preferred routes for most therapeutically relevant drugs. Both the routes have advantages and disadvantages. Oral drug delivery is the easiest mode of treatment for any disease since it doesn't require clinical supervision. The parenteral intravenous administration route is the fastest route to get drug into the systemic circulation. However, common disadvantages of oral drug delivery include reduced bioavaibility due to first pass effects and gastric irritation issues. The need for administration by trained healthcare professional in most cases and needlephobia are some of the disadvantages of the parenteral route. Transdermal drug delivery provides an alternative to pills and injections. Most of the above mentioned disadvantages of oral and parenteral delivery can be taken care of by using transdermal delivery. The stratum corneum (SC), the topmost layer of the skin is the most important barrier to delivery of drugs across the skin. [1] The molecules that can be delivered across the SC are limited by physicochemical properties like size, charge and hydrophobicity. Different enhancement techniques like iontophoresis, electroporation, microneedles (MN), ultrasound, chemical enhancers etc. open up transdermal drug delivery to a whole new class of molecules that are much larger in size, even protein and peptide therapeutics, for example. [2] Most of these systems enhance transport by permeabilizing the SC, either by physical or chemical methods.

MN enhancement has been shown to be effective both in vitro as well as in vivo for a large number of molecules. Some examples include small molecules like naltrexone (NTX), docetaxel, calcein, and lidocaine, to peptides and proteins like insulin and a host of other biotherapeutics. [3-6] The "poke and patch" approach of MN application involves one time application of MN followed by application of a transdermal

patch over the permeabilized skin. It has been investigated over the past decade for a whole range of molecules. The research provided insight into formulation aspects of MN enhanced delivery that is completely different from passive transdermal delivery. [7] The first in-human trial of MN with the above technique further proved the efficacy of MN treatment. [4] Therapeutically relevant levels of naltrexone (NTX) were detected in the plasma using MN compared to no observed plasma concentrations for delivery across intact skin. One major disadvantage, however, was that drug could only be delivered for 48-72h following one time application of MN. [8, 9] The drug delivery potential of the system is severely impaired by the resealing of the micropores or microchannels due to normal physiological processes of the skin. Thus, although the method is able to deliver drug in therapeutically relevant concentrations, reapplications of MN would be required every couple of days to maintain steady state plasma concentrations.

Several mechanisms could be responsible for the healing of the micropores. The rate of pore closure in MN treated skin has been studied utilizing both direct and indirect techniques. Depending on the sensitivity of the technique, the type of skin, as well as the physical characteristics of the MN, the timeframe has been shown to vary anywhere between 30 minutes for unoccluded skin to 72 hours for occluded skin. [10-12] The underlying mechanism has not been studied in extensive detail yet. Recent studies from our laboratory suggest that up-regulation of cyclooxygenase (COX) enzymes in a wound model leads to local subclinical inflammation and a faster rate of micropore healing. Utilizing a nonspecific COX inhibitor, diclofenac (DIC) sodium, it has been shown that the rate of skin re-sealing can be decreased and NTX can be delivered over a 7 day time period. [8, 13, 14]

The main goal of this research project was to understand and optimize formulation characteristics for sustained transport across MN treated skin via the “poke and patch”

approach. The ideal transdermal drug delivery goal would be sustained delivery for 7 days following one time application of the MN. The model compound for the project was NTX. It is a μ-opioid receptor antagonist and is approved for treatment of alcohol and opioid addiction. [15] NTX is an ideal transdermal candidate since it has bioavailability and gastric irritation issues related to the currently approved oral dosage form. [16] The recently approved extended release intramuscular injection form has issues with injection site reactions, and is difficult to remove if there is an emergency opiate requirement. [17] Since it has already been shown that NTX can be delivered for 2-3 days using MN, and development of a 7 day system for alcohol addiction would be ideal, NTX was chosen as the model compound for the current project.

Various mechanisms were exploited for sustained delivery of the model compounds. Formulation pH is known to affect rate of skin recovery following SC removal via tape stripping or acetone treatment. [18] Therefore the role of pH was exploited as a potential pore lifetime enhancement technique in a MN treated skin model. The role of COX inhibitor, DIC as a micropore lifetime enhancer has been established in the literature. However, NTX and DIC are physico-chemically incompatible in coformulation. NTX is a weak base with a most acidic pKa of 7.5 and DIC is an acid with a pKa of 4.2. [19] As a result, it is impossible to formulate the two drugs in high concentrations into a single formulation around a pH of 5, the pH of the outer surface of the skin. [20] Precipitation of diclofenac on co-administration leads to a decreased flux across MN treated skin. [14, 21, 22] A codrug approach was explored in order to solve the formulation issue. Codrugs or mutual prodrugs are formed when two active pharmaceutical moieties are linked together via a covalent linkage to solve a drug delivery problem. [23] Once inside the body they cleave back due to chemical and enzymatic hydrolysis to regenerate back the parent compounds. The third aspect was to explore the mechanism of local inhibition of

lipid synthesis pathways as a mode of delaying recovery of the SC barrier. The correct ratio of SC lipids is the most important factor regeneration of the SC barrier following insult. [24] It has been shown in the literature that enzymes of the lipid synthesis pathway are up-regulated following SC insult and local application of inhibitors led to delayed barrier recovery.[25] Thus topical application of inhibitors was used in a MN treated skin model to evaluate its role in micropore healing.

Chapter 2

Research hypotheses

The overall goal of the project was to optimize the formulation for development of a 7-day transdermal drug delivery system using microneedles (MN). Three different approaches were utilized to enhance micropore lifetime under occlusion following MN treatment. The current studies helped to provide a better understanding of MN-enhanced drug delivery and barrier recovery following MN treatment, as compared to other methods of stratum corneum (SC) disruption.

The research was driven by the following hypotheses:

Hypothesis 1: Formulation pH/ionization state can be utilized to enhance flux of naltrexone (NTX) and delay pore closure across MN treated skin

A pH of 7.4 is known to delay barrier recovery following acetone treatment or tape stripping, as compared to the skin surface pH of 5.0. This is due to decreased activity of β-glucocerebrosidase, an important enzyme of the lipid biosynthesis pathway, at pH 7.4. NTX is a weak base with the most acidic pKa of 7.5. Therefore the drug is more than 99% ionized at pH 5.0 and almost 50% unionized at pH 7.4. Several physicochemical factors like molecular weight, charge/ionization state, hydrophobicity, solubility, etc. influence diffusion of drug across intact skin. The effect of ionization state of the molecule on transport and permeability has been well studied in case of passive transdermal delivery systems. Permeability of ionized molecules across intact skin is lower compared to unionized molecules, due to hydrogen bonding and repulsion of negatively charged molecules across the skin barrier. However, in case of MN enhanced transdermal drug delivery, the mechanism of drug movement is different. Higher solubility of ionized molecules in an aqueous media translates into higher flux, due to

increased driving force in case of MN treated skin. However, the effect of ionization state on movement across micropores has not been studied. It is hypothesized that there will be no significant difference in permeability of ionized molecules across MN treated skin, however higher solubility will translate into enhanced flux using the ionized form of NTX in the lower pH range. On the other hand, pH 7.4 will be effective in delaying micropore closure compared to pH 5.5, thus extending the drug delivery window. Therefore, pH 7.4 will be beneficial for development of a 7-day transdermal system even with comparatively lower flux.

Hypothesis 2: Codrugs of NTX and diclofenac (DIC) can be used for pore lifetime enhancement and sustained NTX delivery

NTX can be delivered transdermally using MN for 2-3 days from a single patch. DIC sodium, a non-steroidal anti-inflammatory drug has been shown to enhance micropore lifetime up to 7 days under occlusion, following one time application of MN, both in animal models and humans. However, NTX and DIC are physicochemically incompatible. NTX is a weak base with the most acidic pKa being 7.5 and DIC is a weak acid with a pKa of 4.2. Therefore at the preferred topical preparation skin surface pH of 4.5-5.5, DIC has limited aqueous solubility and precipitation occurs on simultaneous application of both the compounds. Codrugs or mutual prodrugs are new chemical moieties synthesized by joining two active pharmacological ingredients. This helps in keeping them stable in formulation, and once inside the body, they convert back to parent drugs via enzymatic and chemical hydrolysis. It is hypothesized that synthesis of NTX-DIC codrugs will help solve the drug delivery issue. Once in the skin, local concentration of DIC will keep the micropores open and NTX will be delivered systemically. Structure design optimization will help in selection of a codrug with

optimum stability, solubility, transdermal flux of NTX and skin concentration of DIC for development of a 7-day drug delivery system for NTX via MN.

Hypothesis 3: Lipid synthesis inhibitors can be used to delay resealing of micropores and sustain NTX delivery

The stratum corneum (SC) is the most important barrier to delivery of most drugs across the skin. It is formed of dead keratinized remains of once rapidly dividing epidermal cells bound together by a lipid matrix. The main lipids of the SC are ceramides, fatty acids and cholesterol. A 1:1:1 molar ratio of the SC lipids is crucial for its barrier properties and recovery of barrier function following insult. In a tape stripping/acetone treatment model of SC disruption, inhibitors of the lipid synthesis pathway have been shown to delay recovery of barrier function. MN is an alternate method of SC disruption where small micron-scale needles are used to permeablize the SC. It is hypothesized that local application of fluvastatin (FLU), an inhibitor of the cholesterol synthesis pathway, will delay micropore healing, similar to the tape stripping model and allow NTX delivery over a 7-day period. Since irritation of skin and recovery of the barrier function following removal of treatment are some of the concerns associated with use of biochemical enhancers, follow up studies will be conducted to evaluate these issues. It is hypothesized that on removal of occlusion, the increase in transepidermal water loss will lead to fast and efficient recovery of the SC barrier properties.

Chapter 3

Research plan

3.1 Method development and utilization of impedance spectroscopy to evaluate the effect of formulation pH on micropore healing *in vivo* in a Yucatan miniature pig model

Development of surrogate methods to monitor micropore lifetime in addition to pharmacokinetic studies are imperative for faster screening of drugs and development of delivery systems. Impedance spectroscopy (IM) is a fast, efficient, noninvasive and cost friendly method for measuring the resistance across the skin. Intact skin has the highest resistance with very limited flow of ions, microneedle (MN) treatment leads to formation of micropores and a significant drop in resistance of the skin. Thus, the rate of skin healing or micropore lifetime can be monitored by obtaining regular measurements using IM. The rate of skin healing under occlusion will be monitored at 3 different pH values: pH 5.5, pH 6.5 and pH 7.4 using 3% hydroethylcellulose gels of 0.1M citrate buffer. Three MN treated sites (100 MN pores per site) and one untreated control site will be used for each formulation per experiment. IM readings will be obtained immediately before, following treatment and every 24h up to 100h. Sites will be cleaned with gauze before each measurement, and occluded using an occlusive patch after re application of gel following measurements. Care will be taken to limit the exposure of all sites to air between readings. The data will be analyzed using the following model to obtain micropore resistance. $Z_{total} = \frac{1}{\frac{1}{Z_{box}} + \frac{1}{Z_{skin}} + \frac{0.02}{Z_{pores}}}$. Where Z_{skin} will be obtained from the intact skin value under the same treatment condition at each time point, Z_{box}=200kΩ resistance box and Z_{total} is the raw value obtained on the meter. Admittance (1/Impedance) values will be used to compare pore closure kinetics among formulations.

3.2 Evaluation of the effect of formulation pH/ionization state of NTX on solubility, flux and permeability *in vitro* and modeling of the permeability data across MN treated and untreated skin using the permeability of ionized and unionized form of the drug

Unionized molecules have higher permeability through intact skin compared to their ionized counterpart. However, the effect of ionization state on permeability is not well understood across MN treated skin. Saturated NTX solutions in 0.3M citrate buffer at 6 different pH values over a pH range of 5.5 to 8.5 will be evaluated to determine solubility, viscosity, and transdermal flux across MN treated and intact skin. Viscosity will be determined using a Brookfield DV-III LV programmable cone/plate rheometer and a CPE-40 spindle. Viscosity is quantified since across MN treated skin, high viscosity is known to decrease transdermal flux. Transdermal permeation studies will be carried out using a flow through diffusion cell system and Yucatan miniature pig skin. Drug concentration from solubility and permeation studies will be quantified using reverse phase HPLC. Steady state flux will be obtained from plotting cumulative permeation vs. time for both MN treated skin and intact skin. Total flux and intact skin values will then be used to determine microchannel pathway flux. Flux values across MN treated skin and untreated control will be used to compare formulation across the pH range. Permeability values will also be obtained for intact skin pathway and microchannel pathway. Permeability values for the ionized and unionized form of the drug across the two pathways will be then used to model the permeability data across the pH range. The model will enhance our understanding of differences in drug movement across MN treated skin compared to intact skin

3.3 Proof of concept to evaluate the effectiveness of naltrexone (NTX) diclofenac (DIC) codrugs for sustained drug delivery across MN treated skin

MN enhancement allows NTX to be delivered for 2-3 days across the skin after one time application. DIC helps in further enhancement of the micropore lifetime up to 7 days. Since they are not compatible in formulation, codrugs of NTX and DIC will be synthesized to obtain formulation stability and delivery of NTX from a single patch for 7 days across MN treated skin. A 3-O-ester linked codrug will be synthesized for proof of concept studies. The codrug will be evaluated for formulation stability in a 0.3M acetate buffer pH 5.0 to estimate the conversion in formulation due to chemical hydrolysis. Stability will also be determined in hairless guinea pig (HGP) plasma to evaluate enzymatic hydrolysis in addition to chemical hydrolysis. The codrug will be tested for transdermal flux of NTX and local skin concentration of DIC using a flow through diffusion cell system and Yucatan miniature pig skin. Steady state naltrexone flux will be quantified and compared with optimized NTX formulations for MN treated skin. Changes in skin concentration will be monitored over time and local skin concentration values will be used to correlate *in vitro* data with *in vivo* effect on micropore lifetime. The formulation will be optimized to obtain low viscosity formulations, and salt forms of the drug will be synthesized with the ultimate goal of maximizing solubility and transdermal flux. All in vitro diffusion samples will be quantified using reverse phase HPLC. Finally, a proof of concept pharmacokinetic study will be carried out in a HGP to evaluate the codrug approach as a drug delivery system for MN treated skin. The HGP will be stained with gentian violet/India ink at the end of the study to confirm presence/absence of pores on the skin. Both the dyes stain epidermis but not dead SC, so a grid will only be observed in the presence of micropores on the skin

3.4 Optimization of codrug structures based on physicochemical properties and flux of NTX/ naltrexol (NTXol)

Based on the results from the proof of concept study (3.4), the codrug structure will be optimized for stability in formulation, solubility of codrug, transdermal flux of NTX/ NTXol and local skin concentration of diclofenac. Since a secondary alcohol covalent link is more stable as compared to a phenolic link, due to resonance stabilization of phenol as a leaving group, the 6-O-position of NTXol, an active metabolite of NTX will be utilized to stabilize codrugs. NTXol has a longer half-life in the body and is known to be pharmacologically active in the treatment of alcohol addiction. In addition to ester linkages, carbamate and amide linkages will be explored to join the two codrugs for stability enhancement. Polyethylene glycol (PEG) will be used as the linker molecule to serve the dual role of solubility and stability enhancement. Stability, permeation and skin concentration data will be evaluated to determine a structure permeability relationship for NTX-DIC codrugs as well as selection of a candidate for further *in vivo* evaluation

3.5 Formulation optimization for treatment with fluvastatin (FLU), a 3-hydroxy-3-methyl-glutaryl-CoA (HMG CoA) reductase inhibitor in presence of NTX

Topical applications of inhibitors of the lipid biosynthesis pathway have been shown to delay barrier recovery following tape stripping. FLU is an inhibitor of the cholesterol synthesis pathway. FLU will be used in combination with NTX for micropore lifetime enhancement and development of a 7-day drug delivery system for NTX following MN treatment. NTX permeation and skin concentration of NTX and FLU will be quantified from four different formulations to determine the best method of FLU application for *in vivo* pharmacokinetic studies. NTX flux will be determined across MN treated Yucatan miniature pig skin using a flow through diffusion cell system. Both drugs will be quantified using reverse phase HPLC. Five different treatment groups will be

used with 4 different methods of FLU application and a NTX control. All cells will be MN treated (100 pores total) and 3% hydroxyethlycellulose gel of NTX will be applied either following FLU application or directly after treatment. Drug loading and amount for all vehicles of FLU will be constant; 40µl of 1.5% solution of FLU will be used per diffusion cell. The vehicles to be used for FLU are 200 proof ethanol, acetone, propylene glycol (PG): ethanol=7:3 and PG: ethanol: water=1:3:1. Steady state flux and skin concentration of FLU will be evaluated to choose the most appropriate formulation for *in vivo* pharmacokinetic studies.

3.6 Pharmacokinetic analysis to study the effect of FLU on transport across MN treated skin over a 7 day period

Pharmacokinetic (PK) studies are required to establish the effectiveness of FLU *in vivo* as a micropore lifetime enhancement agent. Following the identification of a method for FLU deposition (3.5), *in vivo* pharmacokinetic studies will be carried out in a HGP model. Three different treatment groups will be used. A treatment group to evaluate the effectiveness of FLU as a pore lifetime enhancement agent, a vehicle control group to evaluate the effect of FLU vehicle on drug delivery, and a control group with only NTX. For all studies, HGP will be treated at 2 sites, 100 MN per site. The sites will be cleaned with ethanol pads and treated with MN. NTX gel will be applied either following FLU/vehicle or directly. The sites will be covered with occlusive patches and Bioclusive™ will be used to hold the patches in place. Blood samples will be obtained at regular intervals of time up to 7 days. Plasma will be separated from blood via centrifugation and stored at -80ºC until analysis. All plasma samples will be analyzed using LC/MS-MS consisting of a Waters Alliance 2695 Separations Module HPLC and a Waters Micromass® Quattro MicroTM API Tandem Mass Spectrometer. Multiple reaction monitoring (MRM) will be carried out with the following parent to daughter ion

transitions for NTX *m/z* 341.8→323.8. The plasma concentration vs. time data obtained will be modeled by fitting data to a non-compartmental model with extravascular input (WinNonlin Professional, version 4.0, Pharsight Corporation, Mountain View, California) to obtain pharmacokinetic parameters, including area under the curve (AUC), maximum concentration (C_{max}), and time to maximum concentration (T_{max}).

3.7 Evaluation of the irritation potential and recovery of the skin following treatment with MN and FLU

FLU is a biochemical enhancer which inhibits or down regulates cholesterol synthesis. Since cholesterol is an important lipid of the SC barrier, down regulation leads to malformation of the SC barrier. Transepidermal water loss (TEWL) and colorimetry will be used in a HGP model to assess the recovery of the skin and irritation potential respectively, following FLU treatment. Five different treatments will be compared: MN+NTXgel+FLU (200 proof ethanol), MN+NTX gel+200 proof ethanol, MN+placebo gel, no MN treatment + placebo gel and occlusion only. TEWL and colorimeter readings will be obtained before and immediately following treatment. The concentration and amount of NTX gel and FLU will be consistent with the PK studies. All sites will be occluded for 7 days, TEWL and colorimetry measurements will be obtained for 30-45 min at all sites or until values return to baseline (pretreatment values) following patch removal.

Chapter 4

Background and literature review

Human skin is one of the most formidable barriers that protects human beings from a vast array of physical and chemical insults on a day to day basis. It is also the largest organ of the body and transport of molecules across the skin delivers them directly into the systemic circulation. [1] Thus on one hand while the skin is very important in protecting the internal homeostasis of the body, on the other hand it can be very effective for delivery of xenobiotics/drugs into the body. Depending on the intended site of action, drug delivery across the skin is divided into two categories. When drug is applied to the skin for local therapy it is known as topical drug delivery whereas when drug is intended for systemic effects it is known as transdermal drug delivery. [1] Both of the mechanisms are equally effective. Topical delivery is useful when the disease is restricted to the outer layers of the skin and deep penetration of drug is not desired because it might lead to unwanted side effects. Transdermal drug delivery (TDD) on the other hand is a potential alternative route for a host of drug molecules that cannot be delivered via the oral or injectable route. Drug is delivered directly into the systemic circulation via the transdermal route thus metabolism in the liver (first pass effects) is no longer an issue. TDD also results in zero order drug release and steady state plasma concentrations over the entire length of the treatment or patch wear time, compared to the peaks and troughs of oral delivery dosing. Transdermal drug delivery is also known to result in better patient compliance. [23]

4.1 The evolution of transdermal drug delivery

The basic principle behind TDD has been utilized for a long time in the form of ointments and plasters with reports of mustard plasters for chest congestion and belladonna plasters as analgesics. [26] The basic mechanism remains the same where

drug is transported across a barrier, the skin in this case, from a region of higher concentration on the surface of the skin to a region of lower concentration or pseudo-sink conditions inside the body. [26] Transdermal drugs were formally introduced onto the market in 1979 with the approval of the scopolamine patch for motion sickness. Subsequently the transdermal market was revolutionized in the 1990's with the introduction of the nicotine patch for smoking cessation. [27] The nicotine patch had a significant positive impact in an addict population that suffered from compliance issues and side effects from alternative nicotine delivery systems. [28] Since then a number of molecules have been introduced into the transdermal market. A wide range of therapeutic areas from hormones like estradiol and testosterone, to pain medications like fentanyl, and attention deficit hyperactivity disorder treatment like methylphenidate, etc are now delivered transdermally. [29] Figure 4.1 shows the total number of drug molecules or combinations approved over the years. A complete list of all transdermal and topical dosage forms indicates that 26 active ingredient/ active ingredient combinations are currently available on the market. [29]

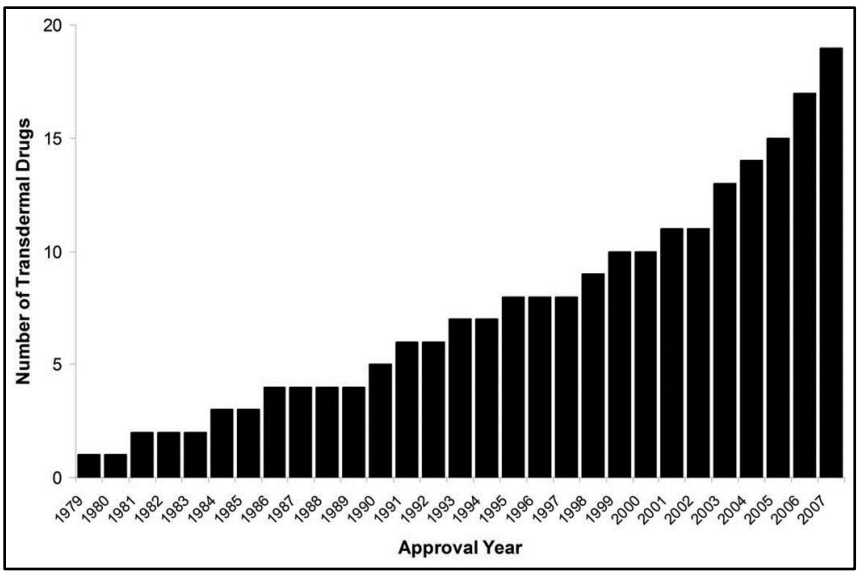

Figure 4.1 Cumulative number of transdermal drugs approved by the FDA since the first approval in 1979. There are currently 19 drugs and drug combinations administered by various delivery methods that are approved in the United States. Data were obtained from the FDA Orange Book.

Reprinted with permission from Nat Biotech 2008;26(11):1261-1268.

In the last few years, there has been a decline in the number of new active pharmaceutical ingredients (API's) being introduced into the transdermal market due to the limited permeability of most molecules across the SC barrier. Physical or chemical enhancement techniques are now being developed to facilitate the permeation of drug molecules across the SC. These techniques disrupt the SC barrier via mechanical/electrical force or chemical modulation and provide an additional advantage over passive transdermal delivery because molecular size is no longer a restriction for delivery across the skin. This was further established with the introduction of Fluzone®, a microneedle (MN) assisted vaccine delivery system, into the transdermal vaccine market in 2012.[29, 30]

4.2 Structure of the skin

The skin is the largest organ of the body and carries out a wide array of functions. [1] It is a formidable barrier to infiltration of chemicals, microbes and is responsible for containment of body heat and water. It is a very sensitive organ due to the presence of a wide array of pressure and tactile receptors. Knowledge of the basic structure of the skin helps to better understand skin function. For drug delivery purposes the structure of the skin is best described using a three layer model. From top down, they are stratum corneum (SC), epidermis and the dermis.

4.2.1 Stratum corneum

The SC is the most important barrier to delivery of drugs across the skin. It is around 10μm in thickness with slight variability across different regions on the body. The SC is 15—20 layers deep and undergoes continuous renewal with an average timeframe of 14 days for complete turnover. This layer is mainly composed of dead keratinized remains of rapidly dividing epidermal cells bound together by a lipid matrix. The major SC lipids are ceramide (50%), cholesterol (25%) and fatty acids (10-20%) by weight. [24] The well-knit cell structure of the SC, with keratinocytes bound in place by the lipid matrix gives it a “brick and mortar” structure. The structure minimizes the excessive loss of water or heat from the body. However, the skin continuously loses water due to insensible perspiration at the rate of 0.5mg/cm^2/h. Under occlusive dressing this leads to excessive water retention or hydration of the skin. [1, 31]

4.2.2 Epidermis

The epidermis is the next layer of the skin after SC, although from a skin physiology perspective the SC is considered a part of the epidermis itself. This layer is around 100μm thick, avascular and is primarily composed of live keratinocytes and a wide array of lipid synthesizing precursors and enzymes. It can be divided into four

layers under a microscope. From outer surface down they are stratum lucidum, stratum granulosum, stratum spinosum and stratum germinatavam. The stratum lucidum forms a flat interface with the SC, whereas the stratum germinatavam forms a papillose interface with the dermis, a characteristic feature of the human skin. [1]The epidermal layer is responsible for self-healing with the help of formation of new cells in the lower layers and progressive maturation ultimately leading to death and integration in the SC. Lipids responsible for formation of the SC are synthesized and undergo differentiation during the epidermal transit of live keratinocytes. [25] Apart from the keratinocytes, the epidermis is also rich in Langerhans cells making it immunologically active, and melanocytes giving individuals their characteristic skin color. [1] Hair follicles and eccrine glands have an epidermal origin thus forming an additional pathway for drug transport across the skin. The epidermis is more hydrophilic and diffusivity of molecules across the viable epidermis is 4 fold higher compared to SC. As a result the epidermis sometimes acts as a barrier to extremely lipophilic molecules.

4.2.3 Dermis

The dermis is about 1000µm thick and is responsible for providing support and nutrition to the top layers of the skin. It is mostly composed of collagen, elastin and reticulum which give the skin its characteristic elasticity and structure. The microcirculatory system serving the skin is located in the dermal region of the skin. In addition to the systemic circulation the skin also possesses an extensive lymphatic system and a network of sensory nerves. The circulatory system of the skin is important for transdermal delivery because it picks up molecules that cross the SC/ epidermal barrier and transfers them directly into the systemic circulation. The major arteries/veins are located in the subcutaneous connective tissue below the dermis but they form a subpapillary network in the dermis and fine branched loops act as a circulatory system at

the interface of the dermis and the epidermis. Blood circulation reaches to within about 150µm of the skin surface and the normal bold flow is about 0.05ml/min/g of skin tissue.[1]

4.2.4 Skin appendages

Hair follicles, sebaceous glands, eccrine glands and apocrine glands form the skin's appendages. Hair is present all over the skin surfaces except for high friction surfaces like the palms of the hands or soles of the feet. The appendages roughly occupies about 0.1% of the total surface area of the body. Hair, like the SC, is also made up of keratin and originates from a hair follicle. Each hair follicle has one or more sebaceous glands responsible for sebum production. Eccrine or sweat glands are also present throughout the skin and are mainly responsible for maintaining the temperature of the internal environment. Apocrine glands are localized to the axilla and anogenital regions. Secretion from the glands mixes with the sebum and leads to the characteristic body odor on bacterial decomposition. [1]

4.2.5 Enzymes in the skin

The epidermal layer of the skin is avascular but metabolically active. The enzymatic activity in the epidermis is very important for drug bioconversion/metabolism. Most enzymes found in the body are also found in the skin, however the amount of each enzyme found in the skin is different from their proportions in the body. Examples include phase I enzymes like cytochrome P450 (CYP), Non-P450, cyclooxygenases (COX), alcohol dehydrogenase (ADH), esterases/ amidases and phase II enzymes like glutathione S-transferase (GST), UDP-Glucoronosyltransferase (UGT) and n-Acetyltransferase (NAT). [32] Distribution studies reveal that xenobiotic metabolizing enzymes like CYP exhibit similar qualitative presence in mouse and human cells. [33] Hydrolytic enzymes like esterase, oxidase and reductase are found 40-120µm from the surface of the skin indicating that these enzymes are present in the basal layer of the

epidermis, and drugs will be potentially metabolized before reaching the systemic circulation.[34-36]

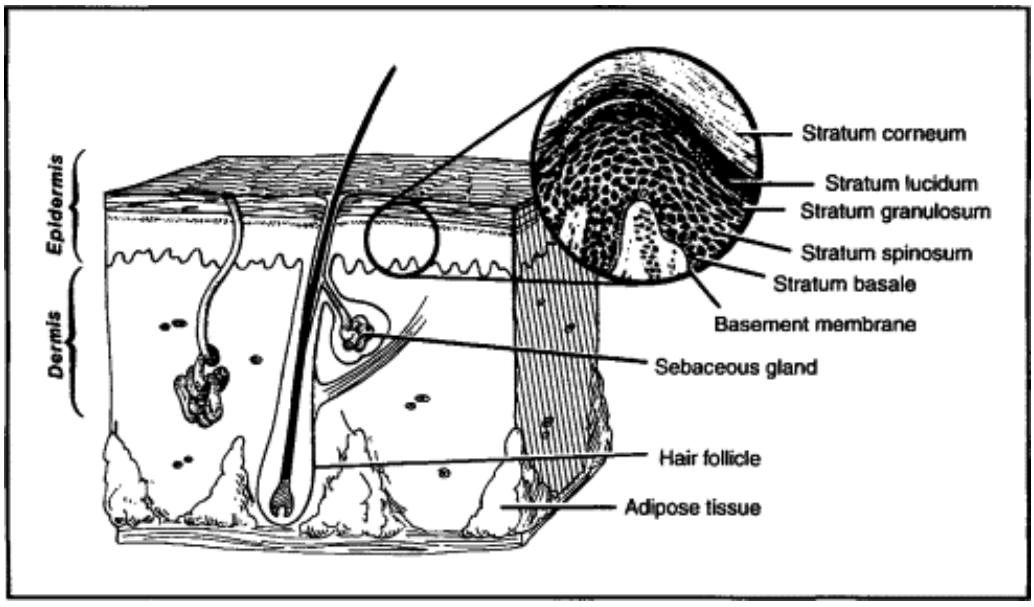

Figure 4.2 Crosssection of skin and epidermis

Reprinted with permission from Mayo Clin. Proc. 1995 70; 6:581-586.

4.3 Passive delivery and the mathematics of passive diffusion

Most transdermal drugs currently on the market are delivered via passive diffusion, i.e. they move across the skin barrier due to a concentration gradient. Such diffusion across the skin can be attributed to three distinct pathways across the skin. [37] The intercellular route is the most important route of drug delivery across the SC. Drug molecules are transported through a tortuous pathway across the lipid matrix of the SC and finally partitions into the more hydrophillic layers of the viable epidermis and subsequently the dermis. This is the preferred route for molecules having a log P ~ 0.5-3.5. For extremely lipophilic molecules (log P> 5), however this poses a problem since molecules partition into the SC but cannot partition back into the hydrophilic environment of the lower layers. The second route is the transcellular pathway where drug molecules

move through the different layers of the skin by partitioning repeatedly between the hydrophobic lipids in the SC and the relatively hydrophilic keratinocytes. The third route is the transfollicular route or the transport of drug molecules through the appendages in the skin, mainly the hair follicles. This is hypothesized as the primary route for transport of polar molecules across the skin. Thus, in spite of the advantages of transdermal delivery, drug delivery across this route is limited to a handful of molecules. [1]

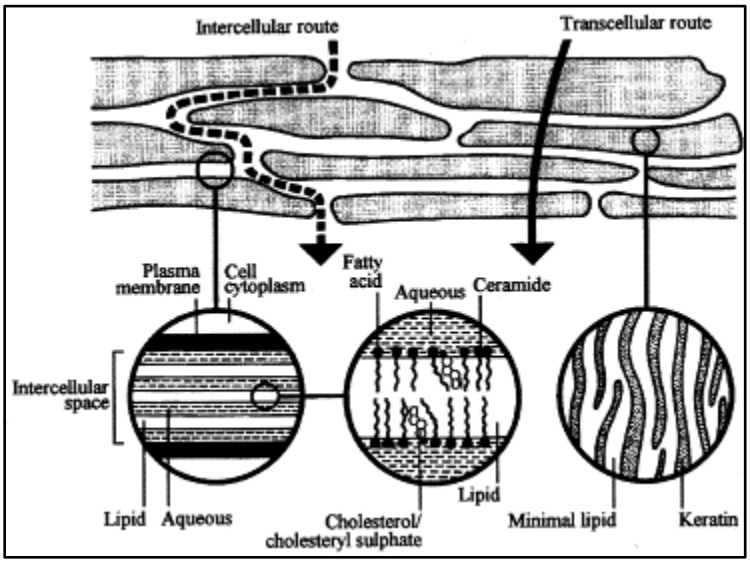

Figure 4.3 Simplified diagram of stratum corneum and two microroutes of drug penetration

Reprinted with permission from European Journal of Pharmaceutical Sciences 2001 9; 14(2):101-114.

Diffusion across the skin barrier is mathematically quantified using Fick's laws of diffusion. [38] For mathematical purposes, the skin barrier in most cases is considered as a single diffusional barrier, with the formulation as donor on the top of the skin and blood as the receiver in the dermis. Depending on the nature of analysis, transport is modeled either as a one dimensional or a multi-dimensional phenomenon. For ease of solution, steady state flux is usually quantified in order to compare formulations. Cumulative

amount of the drug permeated is plotted as a function of time. Steady state flux is estimated using the slope of the steady state portion of the graph

$$J_{SS} = \frac{1}{A}\left(\frac{dM}{dt}\right) = P * \Delta C$$

Where J_{ss} is the steady state flux, A is the active surface area of diffusion, M is the mass transport across the skin, P is the permeability of the molecule and ΔC is the concentration difference between the donor and the receiver. The flow of the receiver can be adjusted to maintain sink conditions at all times so that ΔC is the concentration of the drug in the donor. Therefore, permeability can be calculated for a molecule using the above equation by experimentally determining the steady state flux and donor concentration.

$$P = \frac{D * K}{h}$$

The permeability constant P, can be further analyzed using the above equation. D is the diffusivity of the molecule, h is the thickness of the skin barrier and K is the partition coefficient of the molecule between the SC lipid and the vehicle which in case of transdermal delivery is often estimated using the octanol-water partition coefficient.

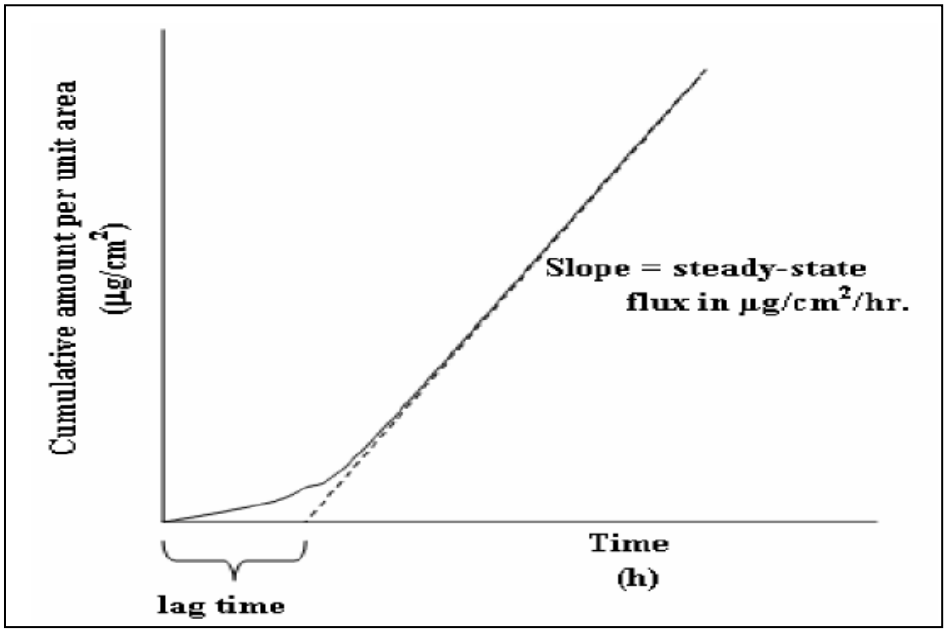

Figure 4.4 Steady state flux and lag time calculation from cumulative amount vs. time plot

4.4 Enhancement techniques

The passive delivery of drugs via the transdermal route is limited by the therapeutic dosage and physicochemical properties of the API. Limitations of passive transdermal delivery have led to the use of physical and chemical enhancement techniques. These techniques employ an additional physical/chemical mechanism to enhance the permeability of the skin for most drugs. Physical enhancement techniques employ a mechanical/electrical force to permeablize the skin while chemical enhancers modify the structure of the skin to enhance permeability.

4.4.1 Physical enhancement techniques

Physical enhancement techniques are employed in order to deliver polar/large molecules, since SC removal shows higher permeation enhancement, or to reduce the lag time following application of a transdermal patch. Some examples of physical

enhancement techniques that have been widely explored include iontophoresis, sonophoresis, electroporation and microneedles (MN).

4.4.1. A Iontophoresis

Iontophoresis uses continuous application of low voltage current for transport of drug molecules across the skin. Molecules move either via electrophoresis or electro-osmosis and the method is most applicable for small charged molecules or larger molecules up to a few thousand Daltons. Compared to passive transdermal delivery where the concentration of the drug in the donor is the driving force, the potential drop across the skin acts as the driving force in iontophoretic delivery. Saturated donor solutions are not used since they lead to a bottleneck effect and flux is optimized using the current applied. [39] There are several advantages of using iontophoresis over other methods of active delivery. At low voltage, it does not change the structure of the stratum corneum for short durations of treatment, thus the skin irritation potential of the method is low and the rate of delivery can be controlled by modulating the potential drop across the skin (microprocessor/ self-control). [2] A current at the rate of 0.05-0.12 mA/cm^2 has been shown to not cause any significant skin irritation for the duration of 30minutes. [40] A few iontophoretic delivery systems have been approved by the FDA in the past. Examples include Iontocaine® and Lidosite® systems with lidocaine, a local anesthetic and epinephrine for topical delivery. However both systems have been discontinued since 2006.[27] Zecuity®, a sumatriptan iontophoretic transdermal system was approved by the FDA in 2013 for acute treatment of migrane. The approval was based on phase III clinical trial data indicating effectiveness of the iontophoretic device containing drug compared to the placebo at 2 hour following treatment. The product will be available in late 2013 from NuPathe. The main disadvantage of the method, however, is if higher voltages are required to achieve therapeutic concentrations, it could lead to

disruption of the lipid structure of the SC, thus leading to irritation and sensitization. Cost associated with the device is significant and commercial failure has resulted in withdrawal of a number of iontophoretic systems in the past.

4.4.1. B Sonophoresis

Sonophoresis employs low frequency ultrasonic waves to enhance the permeability of the skin. Several mechanisms have been investigated to understand the working principle, including thermal effects due to the ultrasound, acoustic streaming and cavitation. It has been concluded that low frequency ultrasound works better for SC disruption and transdermal drug delivery due to higher incidence of cavitation events as well as formation of larger bubbles. Since the effect is not transient, this helps in drug delivery for a number of hours following application of ultrasound to the skin. [27] This system has been primarily investigated for large molecules/biomolecules. Sonophoresis has been shown to be effective for a host of molecules, namely insulin, erythropoietin and heparin *in vitro,* as well as insulin *in vivo* in diabetic rats. [37, 41] Traditionally, high frequency (>1mHz) waves have also been used for local/topical delivery of hydrocortisone for joint pain, but the mechanism of action of high frequency ultrasound is predominantly by thermal ablation and is associated with heating. This can lead to deep tissue damage. [2] The major disadvantages of using sonophoresis is the long recovery time of the SC following treatment, which can lead to infection at the site of treatment and deep tissue damage on incorrect administration of the ultrasonic wave. Further improvement is also required in reducing the cost of manufacturing as well as usage to make it more cost effective and user friendly. [27]

4.4.1. C Electroporation

Electroporation utilizes an electric field to permeablize the skin. High voltage pulses are used over short periods (microseconds to milliseconds) of time to disrupt the

highly ordered lipid bilayer. [27] Unlike iontophoresis, where current is applied continuously for transport of the drug molecules, in electroporation the current is just used to permeablize the skin. The technique has been investigated for large molecules like insulin, lidocaine, vaccines, oligonucleotides as well as DNA. [2] The main advantage of the method is that current is not required for drug transport, thus stability of macromolecules is not affected by the application of the current. Reversibility of treatment i.e. complete regeneration of barrier function following treatment takes anywhere between few second to hours, thus long term effects and infection issues are limited.

4.4.1. D Microneedles

MN assisted transdermal delivery employs small micron-scale needles to permeablize the skin for drug transport in a minimally invasive manner. [42] Small needles are used to create pores or channels across the stratum corneum, the main barrier to passive delivery. [43] The delivery characteristics depend on the nature of the microneedle (solid, hollow, coated or biodegradable) geometry, as well as on the biomechanics of skin penetration, and the density of needles on an array. [42]

MN's were first introduced onto the market in the late 1970's, but the MN's true potential in the drug delivery market was not evident until the development of the microelectronics industry. With the advent and development of the microelectromechanical system (MEMS) industry, the synthesis of MN's became rather inexpensive. For MN fabrication using solid stainless steel, (the MN array used in this project) the array is drafted into AUTOCAD, cut with a laser from a stainless steel sheet, cleaned with detergent and electropolished with glycerin, orthophosphoric acid, and water (6:3:1). The MN array is then cleaned in nitric acid and deionized water to get rid of any loose metal from synthesis. [6] Hollow, coated or biodegradable MN's are usually

synthesized using polymer or glass. The basic mechanism involves synthesis of a master mold of metal and then using polymer or glass to cast the MN itself. For coated MN, the coating is done using a dip coater or individual coating. [44] For biodegradable MN, the polymer mixture used for MN synthesis is premixed with drug and the rate of drug delivery is then controlled by the rate of polymer degradation. The rate of delivery can be optimized by altering the polymer composition. [45] Hollow MN employs an infusion pump to facilitate transport of drug across the skin. Therefore, in this case the MN acts like a normal hypodermic needle but much shorter, such that it does not reach the pain receptors in the dermal layer and therefore does not cause pain. [46], [47]

MN enhanced drug delivery has been studied in detail over the last decade and a half. The physical structure and design of MN has a significant effect on transport across MN treated skin. MN can range from anywhere between 200-1000µm in length. The length of the MN can directly influence the rate of drug delivery. The length of MN can be directly correlated to drug delivery in case of solid MN. However in case of hollow MN complete insertion of MN has been shown to decrease transport. This is due to compaction of underlying tissue. [48] The rate of drug delivery is also influenced by the needle geometry, as well as the needle density. The amount of drug delivered is proportional to the number of MN pores, if the application pressure is constant. [49] However, the “bed of nails” effect plays a role if the needle density is too high. [50] The pressure applied on application in that case is shared over a large number of needles and thus each needle is applied with a lower pressure. The depth and accuracy of microporation is no longer consistent throughout the application area leading to variability in results. The application efficacy of MN can be monitored using dyeing techniques like gentian violet, India ink or calcein staining. The dyes stain the viable epidermis, thus staining is only observed in presence of micropores in the skin.[10, 12].

Impedance spectroscopy and Transepidermal waterloss (TEWL) measurements can also be utilized to verify the efficacy and reproducibility of MN treatment. Impedance spectroscopy measures the resistance drop across the skin following MN treatment and TEWL measures the increase in water loss across MN treated skin. [10, 51]

Mechanistic understanding of the formulation characteristics for MN enhanced transdermal drug delivery systems has helped in identification of parameters that are important for active delivery systems, as opposed to passive delivery. The first important parameter is the route of movement. It has been hypothesized that since MN treatment removes the SC barrier, drug molecules directly permeate into the interstitial fluid. Thus lipid-vehicle partition coefficient of the molecule no longer plays an important role in the movement across the skin since drug permeates into the interstitial fluid in the micropores instead of the SC lipids. However, since the total movement is a contribution of the MN treated skin as well as the intact skin surrounding it, for highly lipophilic molecules that tend to form a depot in the skin, lipophilicity could still affect total flux across MN treated skin. [52] The molecular weight of the drug molecule is no longer a rate limiting step for MN enhanced drug delivery. The diameter of the micropores is significantly higher than the molecular size of macromolecules. Both small molecules like calcein as well as marcromolecules like insulin and vaccines have been successfully delivered across MN treated skin both *in vitro* and *in vivo*. The mechanism of diffusion across the skin has also been investigated for MN treated skin compared to intact skin. Intact skin diffusion takes place following free volume theory in the lipid matrix. Dynamic exchange of drug molecules occurs with regions of free volumes or “holes” within the membrane and diffusivity can be calculated using

$$D = D^0 \exp(-\beta . MV)$$

Where D is the diffusivity of the molecule, MV is molar volume, D^0 is diffusivity of hypothetical molecule having zero molar volume and β is constant. However, for MN treated skin, transport in the interstitial fluid occurs following the Stokes Einstein equation.

$$D = \frac{kT}{6\Pi nr}$$

Where k is the Boltzman constant, T is the absolute temperature; r is the hydrodynamic radius of the solute. This was established using the same drug molecule and varying the viscosity of the formulation to show a linear relationship between permeability and concentration could only be established if the diffusivity across the MN treated skin from the different formulations were normalized for viscosity effects. It was concluded that drug from lower viscosity, aqueous formulations have higher flux across MN treated skin as compared to intact skin. [22] The effect of charge on the molecule has also been studied for MN enhanced delivery. It has been shown that a formulation containing a charged molecule having higher aqueous solubility translated into higher flux across MN treated skin. In intact skin it is known that charged molecules exhibit a lower flux due to binding in the SC, the permeability of charged molecules can be correlated to the hydrogen bonding capability of the molecule. [53] A lower solubility of charged molecules in a lipophilic medium that is typically used for intact skin delivery further decreases the flux of charged molecules across intact skin. [54] Drug loading both in case of solid and hollow MN is an additional parameter that requires optimization for MN enhanced delivery. Typically a saturated solution of the drug is used to maximize activity and thus flux across intact skin. However, for MN treatment, a saturated solution has been shown to cause clogging of the micropores or the MN itself for hollow MN. For solid coated MN the maximum dose is limited by the drug loading on the coated MN array. Thus

optimization of drug loading is an important and additional step in case of MN enhanced delivery instead of using saturated solution for maximum drug transport. [55] Lastly, effect of the lymphatic system on drug uptake in addition to the systemic circulation has been studied for MN enhanced drug delivery. For intact skin, the movement across the SC limits the size of the molecules that can be delivered transdermally. However, when MN is used to remove the SC barrier, macromolecules can be delivered across the skin. Recent studies show the importance of the lymphatic system in uptake of macromolecules following MN enhanced delivery and its effect on both lag time as well as therapeutic efficacy. [56]

Microneedles are already in clinical trials for delivery of large molecules like parathyroid hormone (PTH) and HINI vaccine. It has been established as a efficacious and cost effective way of delivering a wide range of molecules across the skin.[57] Two major concerns with use of this technique in a clinical setting are infection following treatment and pain associated with the MN application. Infection following MN treatment has been studied for a few different MN geometries. All studies indicated that there was no significant risk of infection following MN treatment. [58] Infection, irritation and sensitization were also monitored in all the clinical trials. The results indicated that although mild erythema was noted following MN treatment in some cases, it disappeared within a day or two in most cases (similar changes in the skin was observed for patch application without MN treatment), and infection was not observed in any of the patients due to MN treatment. [59] Several studies were conducted to compare pain due to MN treatment compared to a hypodermic needle. One of the major advantages of using MN is the fact that it is minimally invasive and pain free since the needles are not long enough to reach the free nerve endings in the skin. Visual analog scoring techniques were used to quantify pain in several human studies, using a number of different types

and geometry of MN. [60-62] The studies indicated that in all cases the pain of MN application was significantly lower than a corresponding hypodermic needle positive control. In some cases the pain associated with MN treatment was not significantly different from the negative control and volunteers described the feeling as pressure comparable to “pressing an elevator button” rather than pain. [63] The effect of microneedle geometry on pain has also been evaluated to show that pain increases with increase in length of MN. [64] Thus overall MN’s are a safe, efficient and cost-effective way of enhancing drug transport across the skin.

4.4.2 Chemical/Biochemical enhancement technique

Chemical/ biochemical enhancement techniques utilize an additional or modified chemical moiety to permeablize the skin instead of a physical force. The most important characteristics of chemical enhancers used for transdermal delivery are that they should be pharmacologically inert, nontoxic, rapid onset upon application, fast recovery on removal, and chemically and physically compatible with the drug of interest. [65]

4.4.2.A Chemical enhancers

Conventional chemical enhancers can be subdivided into different groups based on the permeation enhancement mechanisms. There are three major mechanisms by which chemical enhancers permeablize the skin. Lipid disruption/ fluidization of SC, keratin interaction in the SC, increased partitioning and solubility of drug in the SC or a combination of the above.[66] From a chemical standpoint, the enhancers can be broadly divided into surfactants, fatty acids and solvents. [67]

Small molecule solvent enhancers like Azone, dimethyl sulfoxide (DMSO), alcohols and fatty acids fluidize the lipid structure by intercalating into the SC bilayer and increasing the free volume fraction of the SC matrix. Diffusivity of drug increases

following the free volume theory equation and thus leads to flux enhancement. [68] Ethanol, a commonly used penetration enhancer works via this mechanism. Ethanol molecules replace water molecules in the lipid polar head groups as well as the protein regions of the SC, thus increasing the free volume. [69] In addition to SC lipids, DMSO, urea and surfactants interact with the keratin filaments in the SC. This results in alteration of the order of the corneocytes and leads to enhanced transdermal transport. [68] Propylene glycol (PG) is an example of a widely used transdermal excipient that acts as a permeation enhancer by interacting with keratin and decreasing drug tissue binding, thus enhancing flux. [66] An alternative mechanism for solvents like ethanol and PG is by enhancing the solubility of the drug in the SC itself. Drugs for passive transdermal delivery typically have a higher solubility in cosolvent systems of water and PG/ethanol, and since PG/ethanol themselves interact with the SC barrier they enhance the solubility of the drug in the SC. Higher drug concentration in the SC leads to a higher driving force and transdermal flux following Fick's law of diffusion. [68]

One of the major disadvantages of using transdermal penetration enhancers is the irritation potential of these compounds. All of the penetration enhancers work by altering the SC barrier and thus in some cases lead to irreversible damage to the skin. Toxicity is also an issue with use of chemical enhancers, and chemicals that fall into FDA's generally recognized as safe (GRAS) classification are now being investigated as chemical enhancers.

4.4.2.B Biochemical enhancers

Metabolic or biochemical enhancers are chemical moieties that alter biochemical pathways in the skin. They act either by inhibiting enzymes that are responsible for biosynthesis and modifications of the SC lipids or by metabolism of SC lipids and alteration of the barrier function of the skin. [65]

Enzymes of the lipid biosynthesis pathway have also been used as biochemical enhancers. Proper formation of the SC lipids and their integration into bilayers are imperative to the barrier function of the skin. [70] Apart from the regular maintenance and turnover of the SC, lipid biosynthesis is enhanced during repair of the skin following insult. The SC is primarily composed of 3 different lipids, cholesterol, fatty acids and ceramides. [71] A 1:1:1 molar ratio of the SC lipids is imperative to the barrier function of the SC. [72] An important aspect of the SC lipids is that they do not contain significant amounts of phospholipids in the final structure, unlike other bilayers present in the body. Phospholipids are present during lipid biosynthesis; however they are converted into nonpolar species during extracellular processing. [24, 73] The lipid content of the SC is also independent of the lipid composition of the body and only a very small percentage of systemic lipids are incorporated into the SC. The SC lipids are synthesized in the keratinocytes in the basal layer of the epidermis. Following synthesis the lipids migrate through the different layers of the epidermis in trilaminar membrane structures known as lamellar bodies (LB). The LB first appears in the stratum spinosum as ovoid structures and gradually moves towards the interface of the stratum corneum and the stratum granulosum. Once the lamellar body reaches the SC interface, release of lamellar body contents takes place by a mechanism known as lamellar body secretion. Under baseline conditions the amount of lamellar body secretion is regulated by the amount of lipids required for maintenance of the barrier function of the skin. Following secretion, lamellar body lipids undergo extracellular processing with the help of hydrolytic enzymes secreted by the lamellar body. This step converts the lamellar body contents into nonpolar lipids that get incorporated into the SC as shown in the Figure 4.5. [73]

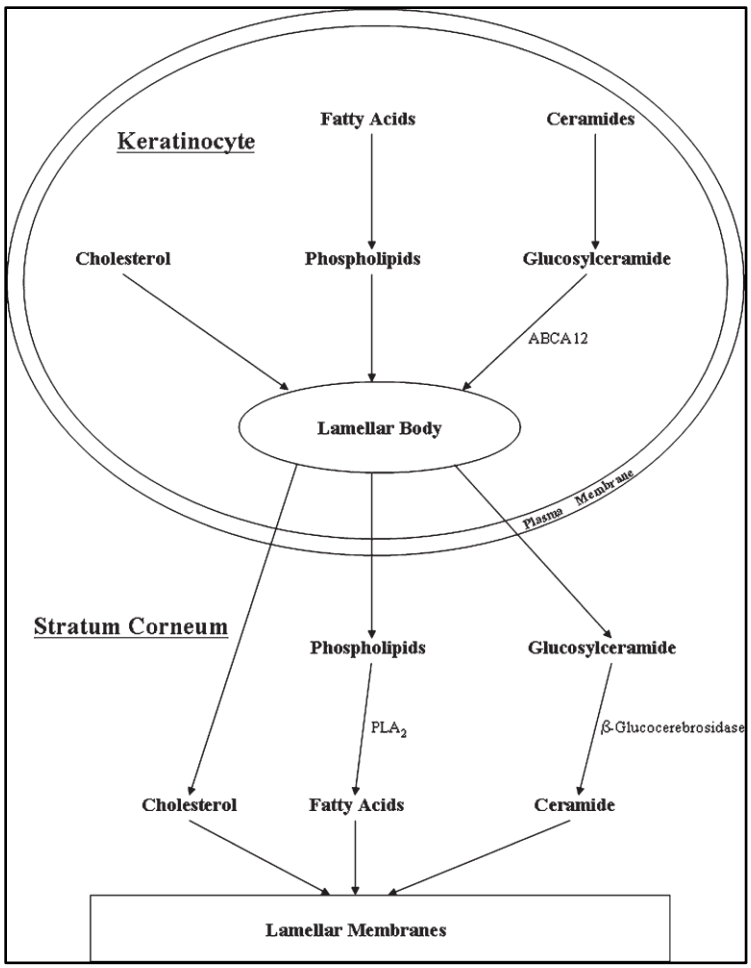

Figure 4.5 Formation of permeability barrier

Reprinted with permission from J Lipid Res 2009 Apr;50 Suppl:S417-22

A host of enzymes are responsible for synthesis and post translational modification of the lipids. When the skin undergoes insult such as normal wear and tear or tape stripping/acetone treatment an up regulation of the mRNA and the enzymes are observed for all the lipid biosynthesis pathways in the skin. [74] Changes in the expression of all the enzymes, HMGCoA synthase, HMGCoA reductase, farnesol pyrophosphate synthase, squalene synthase, acetyl CoA carboxylase, fatty

acid synthase and serine palmitoyl transferase, have been studied in a barrier disruption model via tape stripping. It has been shown that all the enzymes are upregulated following tape stripping. Thus, formation or regeneration of the SC can be altered by inhibiting one or more enzyme of the above pathway as well as by altering lamellar body release. Inhibitors of the enzyme targets have been explored to evaluate their role in skin healing and recovery. Some of the molecules used for inhibiting the lipid biosynthetic pathways are fluvastatin and lovastatin for the HMGCoA reductase, TOFA for acetyl CoA carboxylase and β-chloroalanine for serine palmitoyl transferase. Use of the inhibitors has prolonged the time required for return of barrier properties or proper formation of the SC barrier, evaluated using transepidermal water loss (TEWL) and transdermal delivery of lidocaine HCl and caffeine. [75]

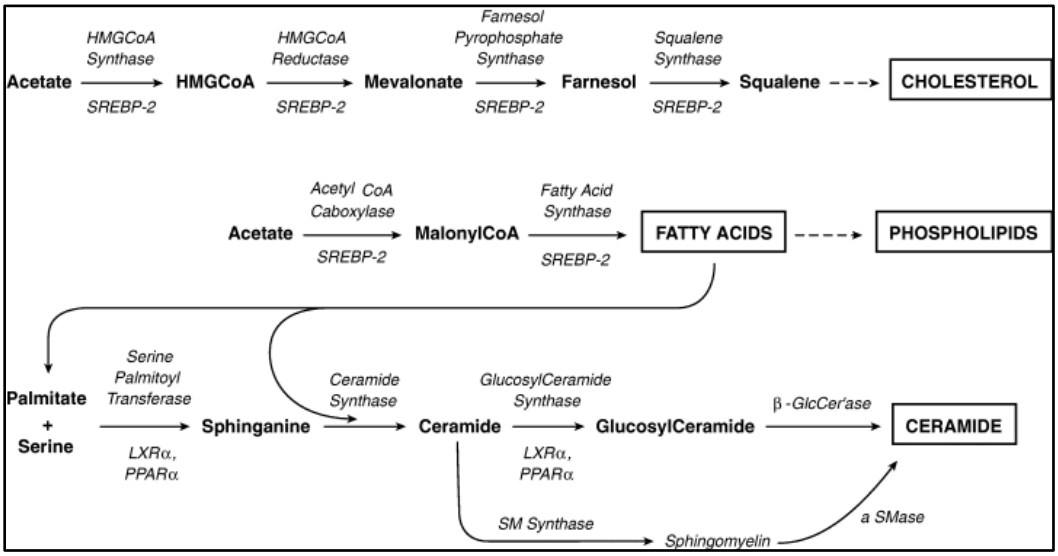

Figure 4.6 Metabolic pathways leading to synthesis of cholesterol, fatty acids, and ceramides

Reprinted with permission from Journal of General Internal Medicine 2005 May: 20(5): 183-200

Trypsin and magainin peptide have also been investigated and reported in the literature recently as potential biochemical enhancers. Trypsin is a serine protease, typically used in a transdermal research laboratory for separation of the stratum corneum from the viable epidermis. Trypsin has been used to increase permeation of large molecules like insulin and dextran across the human skin.[76, 77] The mechanism of action of trypsin has been characterized using infrared spectroscopy to show that trypsin alters keratin in the SC. The transformation of alpha to beta keratin results in decreased barrier properties of the skin and enhanced permeation of drugs. [77] Magainin, a 23 residue naturally occurring pore forming peptide, has been investigated as a biochemical enhancer for transdermal delivery of fluorescein and granisetron. The mechanism of action of magainin is via electrostatic interaction between the charges on the drug molecule and the peptide. [78] This has been confirmed using spectroscopy and changing the pH of the formulation to alter charges on the magainin peptide and thus the interaction potential with drugs.

The major advantage of using a biochemical enhancer is that they are typically required in very small quantities for enzyme inhibition or alteration of chemical structure, and the effects can be easily reversed. The biochemical enhancers lead to a change in the expression pattern of the enzymes responsible for proper formation of the SC barrier. On removal of treatment, the normal turnover processes in the skin lead to regeneration of the SC which can take up to a maximum of 14 days. During drug delivery under occlusion, the changes observed in the expression pattern of the enzymes are smaller and on removal of treatment the increase in TEWL acts as a signal for rapid release of LB contents. Release of preformed LB contents lead to regeneration of the barrier function within 30 minutes and complete recovery occurs within 24hours.

4.2.C Prodrugs and codrugs

The third mechanism for chemical enhancement involves modification of the chemical structure of the drug itself. Prodrugs or codrugs are modified chemical structures of the API that undergo conversion to one or more active drugs within a biological system, such conversion usually involving metabolism. These new chemical moieties are known as prodrugs when the additional moiety/promoiety used for structural modification is pharmacologically inactive. They are known as codrugs when two API's are linked together using a covalent linkage for enhancing delivery. [79] Codrugs and prodrugs are pharmacologically inactive and can be cleaved back to parent drugs efficiently in the body by chemical and enzymatic hydrolysis. The structure modification helps in solving drug delivery issues like chemical instability in formulation, low solubility, and metabolism of the parent drugs leading to toxicity issues. It also helps in better permeation and absorption across biological membranes. Codrugs have an additional advantage in some cases where they can be used as combination therapy with synergistic activity. [23, 80]

Five to seven percentage of drugs approved worldwide can be classified as prodrugs. [81] A functional group on the drug molecule is usually used to link a pro-moiety or a second molecule to form a codrug or prodrug. Some examples of functional groups commonly used are shown in the following Figure 4.7.

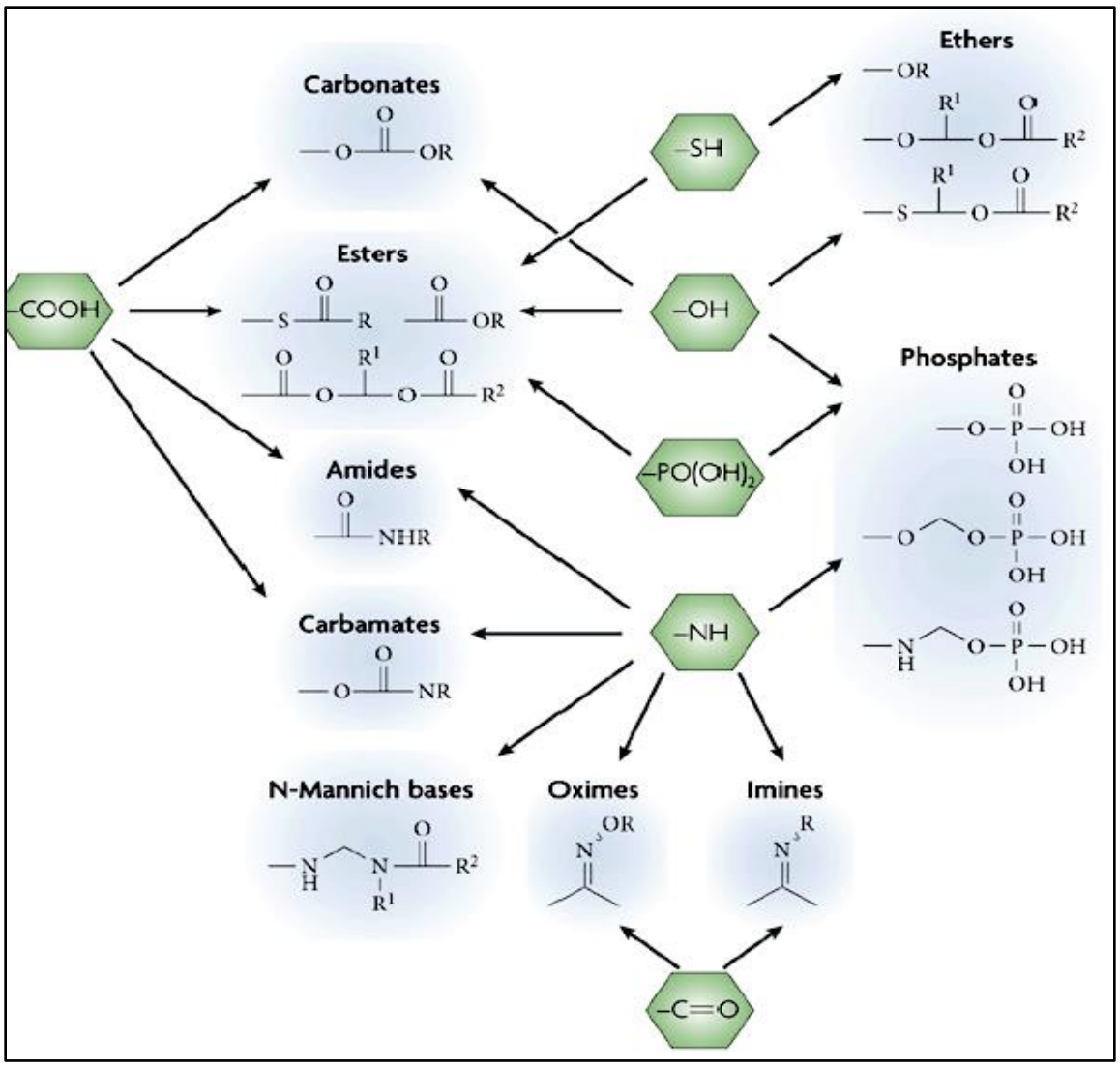

Figure 4.7 Common functional groups on parent drugs that are amenable to prodrug design (shown in green). Most prodrug approaches require a 'synthetic handle' on the drug, which are typically heteroatomic groups.

Reprinted with permission from Nature Reviews Drug Discovery 7, 255-270 (February 2008)

Some examples of blockbuster prodrugs currently on the market include simvastatin, lovastatin, omeprazole and enalapril. [80] Ester prodrugs are the most common and are used to enhance permeability by masking charged groups on the API.

They are preferred due to well documented presence of a number of esterases such as carboxylesterases, acetylcholinesterases, butyrylcholinesterases, paraoxonases and arylesterases in different organs of the body. In addition, chemical modification of carboxylate or hydroxyl group utilized for ester prodrugs are comparatively easy [81] Prodrugs and codrugs have also been investigated for the topical (ocular and dermal) and transdermal market, in addition to the oral route although there are no transdermal prodrugs on the market yet. In addition to solving problems of stability and solubility, dermal prodrugs/codrugs can be designed to deal with skin irritation and sensitization issues. Steroids, NSAID's, opioid antagonists and anticancer agents are some of the therapeutic areas where this strategy has been studied. [23] For passive delivery, prodrug/ codrug structures were optimized for lipophilicity and enhanced permeation. Since most of the new moieties need to undergo bioconversion for activation, esters, carbamate, carbonate and amide linkages are preferentially chosen. The presence of esterase, amidase and protease enzymes is well documented in the epidermal layer of the skin. [82-85] Codrugs for topical delivery are designed with the dual role of enhancing permeation of one or both molecules and synergistic activity. A few examples of topical/transdermal codrugs that have been evaluated include NTX and bupropion for smoking cessation and alcohol addiction [86], retinyl ascorbate and ascorbic acid for oxidative stress, and 5-fluorouracil and triamcinolone acetonide for actinic keratosis. [87, 88] One limitation of the prodrug/ codrug approach via the transdermal route is the increase in molecular weight which limits permeability across intact skin. As a result, prodrugs have been studied in addition to a physical enhancement technique (MN). Since drugs move directly into the interstitial fluid following MN treatment, the prodrugs were optimized for high aqueous solubility and showed higher permeation compared to parent drugs across intact skin *in vitro*. [21] Thus the prodrug/codrug approach is an efficient method for drug delivery enhancement.

4.5 Recovery of the skin following insult/micropore lifetime

Physical and chemical enhancement techniques lead to damage of the SC barrier. Understanding the recovery mechanism following such insult is important for optimizing transdermal drug delivery systems using enhancement techniques. The skin is a self-regenerating organ and the SC undergoes complete renewal every 2 weeks. In addition to the basal level of SC turnover, a defense mechanism is in place following insult or injury to the skin. Depending upon the extent of the insult, the mechanism of skin recovery can be classified into different phases: the inflammatory phase, tissue formation and tissue remodeling. [89] The inflammatory response is the first phase for any wound healing model. This phase lasts for 3-4 days following initial insult and enzymes responsible for SC turnover are up regulated and immunological response takes place during this phase. It is marked by infiltration of platelets and platelet derived growth factors, vascular endothelial growth factors, vasoactive mediators and chemotactic factors. A series of cytokines are also released from the macrophages and keratinocytes, and are responsible for transforming growth factors required for initiation and propagation of wound healing. [90] The next phase is the proliferative phase where migration and proliferation of epidermal cells take place to regenerate back the barrier, lasting for 10-14 days. This phase is marked by proliferation of fibroblasts and other cells responsible for wound healing. The last phase is remodeling and lasts for 6-12 months during which collagen formation and remodeling of the barrier takes place. [91]

4.5.1 Timeframe of SC recovery

Depending on the depth and extent of the wound, all or some of the above phases might lead to full recovery of the barrier function of the skin. Influence of a number of external and internal factors on the rate of recovery have been investigated in SC disruption models via acetone or surfactant treatment or tape stripping. Lamellar

body secretion plays an important role in the recovery of the SC. Within the first 15-30 minutes following SC disruption, lamellar body contents are released from a pool of preformed lamellar bodies. Over the next 30 minutes to 6h, synthesis and release of new lamellar bodies and formation of an organized bilayer structure takes place. Full recovery of the SC takes place within 24h of initial insult. [92] Lipogenesis plays a very important role in the formation of the lamellar body contents. Synthesis and incorporation of the SC lipids are an important step in formation of the lamellar bodies and key enzymes of the lipid biosynthetic pathway act as important modulators of barrier homeostasis.

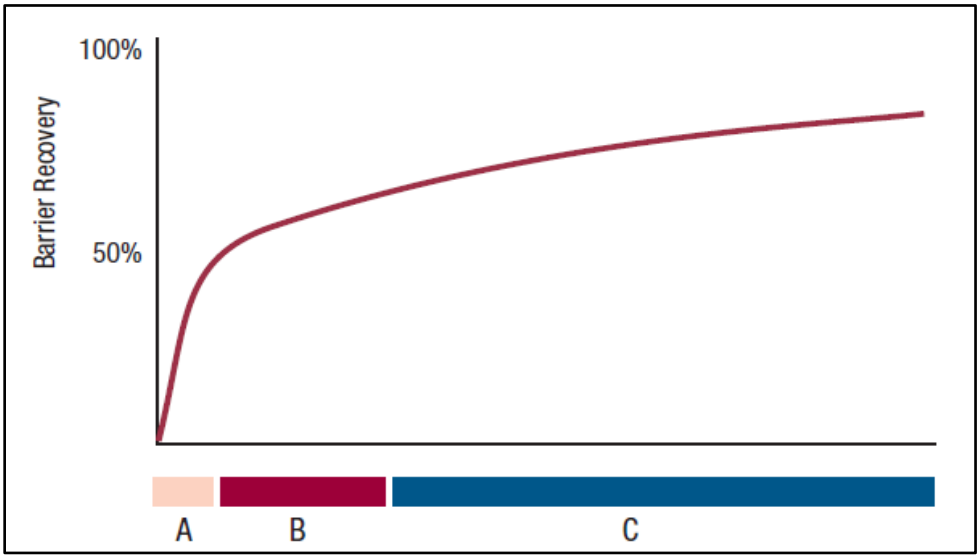

Figure 4.8 Three phases of barrier recovery with distinct metabolic activities occurring after acute barrier disruption. A = Secretion of preformed pool of lamellar bodies (0 to 30 minutes). B = Increased lipid synthesis (free fatty acids, ceramide, and cholesterol) (30 minutes to 6 hours), accelerated lamellar body formation and secretion (2 to 6 hours). C = Increased glucosylceramide processing (9 to 24 hours), increased keratinocyte proliferation and differentiation (16 to 24 hours)

4.5.2 Role of occlusion

Occlusion plays a very important role in recovery of the barrier function of the SC following insult. [93] Transepidermal water loss (TEWL) is a very important signal for recovery of the skin. When the SC barrier is intact, water loss across the skin is minimal due to insensible perspiration, however when the SC barrier is disrupted the TEWL goes up instantaneously and ac as a signal for immediate release of lamellar body contents for regeneration of the barrier. The role of TEWL in the regulation of epidermal lipogenesis has been investigated using occlusive, semi-occlusive dressing and uncovered controls to show that following acetone treatment for barrier perturbation, SC recovers much faster when exposed to air as compared to under occlusion. [94] Barrier recovery following removal of occlusion occurs at the same rate as unoccluded control sites. Thus occlusion does not alter the mechanism of barrier recovery of the skin but the decreased TEWL in case of occlusion slows down the rate of recovery significantly.

4.5.3 Micropore re-sealing

The nature of barrier disruption following MN treatment is not well understood. However, understanding the rate of micropore closure or re-sealing is an important aspect of MN enhanced drug delivery. The rate of micropore closure controls the timeframe of drug delivery across MN treated skin. Several techniques have been employed to monitor the rate of micropore closure in animal models and humans. [95, 96] The techniques range from staining studies using methylene blue and India ink, to calcein imaging and immunohistochemistry.[8, 12, 97] Visualization techniques such as laser scanning microscopy, [98] confocal microscopy, [12] and optical coherence tomography are utilized to look at dye or drug permeation. [99] Surrogate markers like TEWL measurements, impedance spectroscopy and more direct measurements using pharmacokinetic studies are also employed. [4, 9-11, 14, 51]

A number of factors play an important role in micropore closure. Occlusion plays a very important role in micropore re-sealing, comparable to wound healing indicating that TEWL is an important signal for closure of micropores. [10, 12] It has been shown that while under occlusion microchannels remain open for a period of 48-72h, they close within 30 minutes to 4hours when exposed to air. [4, 8, 9, 12] Rate of healing is dependent on the animal model used and the microneedle geometry as well. Sensitivity of the method of detection used to monitor micropore re-sealing also contributes significantly to the variability in the reported timeframe. For example, the TEWL measurements in HGP following treatment with solid stainless steel MN resulted in micropore closure in 15-30 minutes, whereas it took 3-4 hours in rat skin using maltose microneedles. The needle geometry has also been shown to affect the time required for micropore healing [10, 12] Impedance spectroscopy was used to demonstrate that MN length, geometry, and number of MN per array had an effect on the observed timeframe of micropore closure under occlusion. The differences were however not observed using TEWL or impedance spectroscopy when all sites were exposed to air. The results suggest that hydration of the skin following occlusion also plays a role in micropore lifetime in addition to the observed TEWL values. [11] An exhaustive list of all pore lifetime monitoring techniques and time frame of micropore closure has been reported. [14]

Pharmacokinetic studies provide a more direct approach for measurement of micropore lifetime since the drug delivery window is the most important aspect of micropore closure. Studies in HGP and humans with NTX as the model compound have shown that drug can be delivered for 48-72 hours following MN application. [4, 8]

4.6 Pore-lifetime enhancement strategies

Multiple factors are responsible for barrier recovery following SC disruption. Since the exact nature or extent of insult following MN treatment is not very well understood, a number of strategies can be employed to enhance micropore lifetime and allow transdermal delivery of drugs across skin beyond 48h. The goal is to optimize enhancement strategies to extend the transdermal drug delivery window to 7 days following one time application of MN.

4.6.1 Formulation pH

The pH of the formulation can be used to optimize drug delivery. Stability, solubility, and irritation issues are pH dependent. The outer surface of the skin has a pH of 4.5-5.5, due to the presence of free fatty acids, lactic acid in the sweat, as well as microbial colonization. The “acid mantle” of the skin is very important for maintenance of normal physiological functions of the skin including the barrier properties. A pH gradient of pH 5 to pH 7.4 is observed as one proceeds from the surface of the skin to the dermal layer. [100] The pH of the skin is also very important in restoration of barrier function following injury. The role of pH has been studied in both surface and full thickness wounds. It has been shown that SC barrier disruption using acetone treatment has a rate of barrier recovery that is faster at an acidic pH as compared to pH 7.4. [18] The role of β-glucocerebrosidase, an important enzyme of the ceramide synthesis pathway, has been investigated (refer to Figure 4.5) and it has been shown that the enzyme has an acidic pH optimum. Therefore, decreased activity of the enzyme at pH 7.4 is responsible for decreased or malformation of SC lipids/lamellar body contents leading to slower barrier recovery. [101, 102] The effect of pH on barrier recovery was only observed when the “acid mantle” of the skin was destroyed. Once the initial recovery processes restored the normal pH of the skin elevated formulation pH no longer played a role in barrier

recovery. Since the actual nature of disruption following MN treatment has not been well studied, the state of the acid mantle is not known. The role of pH 7.4 in micropore healing will therefore provide a better understanding of the nature of the insult and effect on the “acid mantle” following MN treatment.

4.6.2 Inhibition of the cyclooxygenase (COX) pathway

The arachidonic acid (AA) pathway or the COX pathway is responsible for the formation of both pro-inflammatory and anti-inflammatory cytokines. Since inflammation is the first phase of wound healing, inhibition or alteration of the pathway might lead to changes in the rate and extent of wound healing. The COX enzymes act on AA to form the downstream products, prostaglandins and thromboxanes. Two different isoforms of the COX enzymes are primarily found in the body, COX-1 and COX-2. [103] COX-1 is a housekeeping enzyme. It is constitutively expressed and is responsible for maintaining homeostasis and normal function of the body. COX-2 on the other hand is an inducible enzyme and COX-2 mediated prostaglandin synthesis is usually related to non-physiological conditions like fever, pain, inflammation, cancer, etc. [104] The enzyme also plays a role in cellular repair and proliferation. Inhibition of the COX enzymes either selectively or using non-steroidal anti-inflammatory drugs (NSAID) leads to a decrease in formation of prostaglandins and thromboxanes. Some of the most commonly used NSAID’s include ibuprofen, diclofenac and aspirin for pain and inflammation. Specific inhibition of the isozymes is desired in some cases to reduce side effects associated with NSAID therapy. Celecoxib is one of the most commonly used COX-2 specific inhibitors.

The role and effect of COX enzymes have been extensively studied in a skin tumor model. It has been shown that both COX 1 and COX 2 expression are altered in a skin cancer model. Diclofenac is an NSAID used in the treatment of skin cancer. The

mechanism of action is by reducing proliferation through induction of apoptosis via a prostaglandin (PGE2) mediated pathway. [104] In other tumor models, however, the COX-2 inhibitor celecoxib has been shown to act in a COX-2 independent mechanism to prevent tumor growth. [105, 106] The role of COX enzymes has also been investigated in a skin wound healing model, and up regulation of both COX 1 and COX 2, or specifically COX 2 have been shown in the literature. [107-110] Wound healing studies also show that intraperitonial injection of COX inhibitors affects the rate of wound healing in cutaneous tissue. [108]

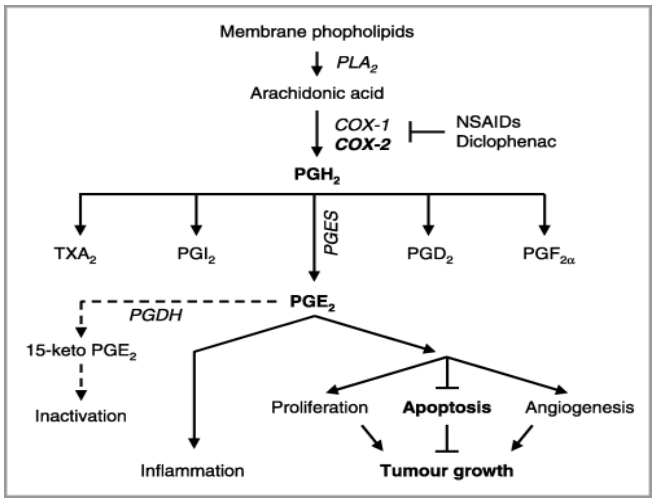

Figure 4.9 COX-1/2-mediated synthesis of prostaglandins. The initial step in prostaglandin synthesis is the formation of arachidonic acid (AA) from membrane phospholipids by phospholipase A_2 (PLA_2).Cyclooxygenase-1 (COX-1) and inducible COX-2 mediate the synthesis of prostaglandin H2 (PGH_2) from AA, which itself gives rise to several other prostaglandins (TXA_2, PGI_2, PGE_2, PGD_2, PGF_{2a}), due to the activities of specific prostaglandin synthases (PGES). PGE_2 exerts important functions in inflammation and tumour growth. Inactivation of PGE_2 occurs via conversion to 15-keto PGE_2 by the enzyme15-prostaglandin dehydrogenase (PGDH)

Reprinted with permission from British Journal of Dermatology 2007, 156(s3), 25-33

With regard to drug therapy, the COX enzymes are important because this is where the NSAIDs exert their pharmacological effects, through specific and non-specific inhibition of the COX enzymes. Diclofenac sodium is used for the treatment of actinic keratosis, the premalignant stage of squamous cell carcinoma. It is available in oral as well as topical formulations. Three different topical formulations are available Voltaren® gel (1% diclofenac sodium), Solaraze® gel (3% diclofenac sodium, 2.5% hyaluronic acid and Pennsaid® (1.5% diclofenac sodium solution).

The effect of Solaraze on micropore lifetime enhancement was evaluated in both hairless guinea pigs (HGP) and humans. In both cases it was shown that daily or alternate day application of topical diclofenac allowed 7 day drug delivery of NTX across MN treated skin. [8, 14] However, the drawbacks were decreased NTX flux across the micropores due to application of diclofenac, as well as requirement for frequent administration. Therefore, to solve the drug delivery problem the codrug approach has been evaluated. Transdermal penetration of a series of NSAID's show that diclofenac has the highest penetration at 0% ionization, however a number of different NSAID's and specific COX 1/ COX 2 inhibitors can be used once the codrug approach is validated. [111]

4.6.3 Lipid biosynthesis inhibitors

Lamellar body formation and secretion is one of the most important steps in barrier recovery. Both mRNA and protein levels of key enzymes of the lipid biosynthesis pathway like cholesterol (HMG CoA reductase), fatty acid (acetyl CoA carboxylase) and ceramide (serine palmitoyltransferase) are up regulated following skin insult. [74] It has been shown that local applications of inhibitors of the above enzymes, fluvastatin (FLU), 5-(tetradecycloxy)-2-furancarboxylic acid (TOFA) and β-chloroalanine (BCA) respectively lead to a decreased rate of barrier recovery and increased drug absorption following acetone treatment. [75] Topical application of a 1:1:1 molar ratio of cholesterol, fatty acid

and ceramide leads to complete recovery indicating that the mechanism of action is by decreasing the free availability of SC lipids for lamellar body synthesis and barrier formation. [73] The role of occlusion in neutralizing the effects of these changes has also been investigated to show that although the extent of upregulation of the key enzymes are lower, significant changes in levels of the enzymes are still observed. Thus for a system under occlusion, inhibitors of the lipid biosynthetic pathways might still work to delay barrier recovery and extend the drug delivery window. Since most transdermal drug delivery systems utilize occlusive or semi-occlusive patches this strategy can be utilized for delivering drugs.

FLU is a competitive inhibitor of HMG CoA reductase. It is available in an oral dosage form and is prescribed for lowering of blood cholesterol levels. The dosage of FLU ranges from 20-80mg/day and the oral bioavaibility ranges from 9-50%. [16] Local applications of significantly lower amounts of FLU should not lead to any unwanted systemic effects. A host of other inhibitors of both the cholesterol synthesis pathway and the other lipid synthesis pathways can also be used to extend micropore lifetime.

4.6.4 Alternate strategies

The role of ions in barrier recovery and proper formation of the SC barrier has been investigated. Local extracellular Ca^{+2} ion concentration is an important regulator of lamellar body secretion. A calcium ion gradient is maintained in the skin with high local concentration of calcium ions at the SC-SG interface. Disruption of the barrier leads to loss of the epidermal calcium gradient and faster release of lamellar body contents. It has been shown that barrier recovery can be inhibited following disruption by increasing the local concentration of calcium and potassium ions. [112] This mechanism has been evaluated in a HGP model for micropore lifetime enhancement. It has been shown that local application of different salt forms of calcium, in addition to NTX didn't lead to

significant enhancement of micropore lifetime. The results can be explained in terms of the local concentrations of calcium and the duration of the studies. In all previous studies, the effect of barrier recovery was monitored for a few hours. Following MN treatment the local concentration of calcium can change faster over time due to diffusion, and maintenance of a high enough concentration to decrease the rate of barrier recovery for 7 days is thus difficult. [14]

Additionally, cytokine mediated pathways play a very important role in barrier regeneration since a host of cytokines are released from keratinocytes as well as via activation PGE2/ PGD2 in the COX pathway. [113]

4.7 The disease state and model drug

Alcoholism or alcohol dependence is defined as "a primary, chronic disease with genetic, psychosocial, and environmental factors influencing its development and manifestations" by the American Medical Association (AMA). [114] It is responsible for approximately 80,000 deaths per year and is the third leading cause of lifestyle related deaths in the country. [115] Alcohol users can be classified into three groups based on the degree of usage. The classifications are: current use is 1 drink, binge use is 5 or more drinks at least once and heavy use is 5 or more drinks on 5 or more occasions during a 30 day period. [116] The groups are not mutually exclusive but binge or heavy drinking individuals can qualify for alcohol use disorder (AUD) if it adversely affects physical, mental, personal, social or occupational function.

The main problem with alcoholism lies in the fact that it is a chronic relapsing disorder and although therapies are available, compliance is an issue for this patient population. The pharmacology of alcohol/ethanol induced addiction is not very well understood, but it affects a number of different pathways in the brain. Some of the

neurotransmitters that are of importance include dopamine, serotonin and opioid peptides. Release of these neurotransmitters or activation of their receptors lead to the rewarding effects of alcohol. [117] An ideal treatment would be something that lowers craving, blocks reinforcing properties and is free of adverse effects.

4.7.1 Current treatment options

Different treatments have been developed over the years for alcohol addiction. Pharmacotherapy or behavioral therapy or combinations of both are used for treatment of AUD. [118] Some of the behavioral approaches used are cognitive-behavioral therapy, motivational enhancement therapy and Alcoholics Anonymous and 12-step facilitation therapy. [119] Among pharmacotherapies, the oldest drug for alcoholism is an aversive medication known as disulfiram. The drug acts by blocking the metabolism of alcohol at the acetaldehyde stage, leading to increased acetaldehyde plasma concentration on consumption of alcohol in the presence of disulfiram in the system. This leads to severe nausea, pain and vomiting on alcohol ingestion. Clinical trials show that disulfiram only prevents consumption due to the side effects, but is not beneficial in decreasing craving or the rate of relapse. [16] Another medication used for alcoholism treatment is acamprosate.. The mechanism of action is not completely understood but it is known to interact with the N-methyl-D-aspartate (NMDA) receptor system. [120] Acamprosate has been shown to be effective in numerous clinical trials in recently detoxified alcoholic individuals. [121] One advantage of acamprosate is it does not interfere with the reinforcement pathway of alcohol. [122] The third drug used for treatment of alcoholism is NTX. NTX is the most widely used alcohol dependence pharmacotherapy.

NTX is a μ-opioid receptor antagonist, used for alcohol and opioid addiction. It was FDA approved in 1994 for alcohol addiction. It works by attenuating the reward associated with the ethanol induced mesolimbic dopaminergic pathway for alcohol

addiction. [123] In the presence of NTX, the increase in levels of tyrosine hydroxylase mRNA in the ventral tegmental area associated with ethanol use is not observed. [123] From a physicochemical standpoint NTX is a free base (pKa-7.5, 9.2 and log P -2) [19] It is currently available in the United States in two different dosage forms. ReVia® (NTX hydrochloride) is a 50mg oral tablet and once daily dosing is recommended for most patients. [124] NTX is also available as an extended release intramuscular injection form. The 30 day dosage form contains 380mg of NTX and the drug is incorporated into 75:25 biodegradable polylactide-co-glycolide microspheres. [125] For patients to be eligible for treatment with NTX they need to be opioid free for 7-10 days before the beginning of treatment and be willing to take the medication on a regular basis. Both of the dosage forms currently on the market have limitations. The oral dosage form has oral bioavaibility ranging from 5-40%, leading to extensive and variable first pass effects, causes gastric irritation and hepatotoxicity. [16] According to Vereby et al, a 2ng/ml plasma concentration of NTX is required for 85.6% narcotic blockade following a 25mg IV injection of heroin. [15] Peaks and troughs ranging from 10ng/ml to 1 ng/ml are observed in the plasma concentration following oral dosing requiring a once daily treatment regimen. The IM injectable NTX was approved to solve some of the issues related to the oral formulation. However, Vivitrol® has extensive injection site reaction issues leading to the issuance of a FDA alert. [126] Dose dumping and difficulty of removal of the IM dosage form in case of emergency opiate requirement are some of the other issues. Consumption of opioid in presence of Vivitrol in the system can lead to accidental overdose and has been associated with death in some cases. Vivitrol also has a 25ng/ml peak plasma concentration following administration, and gradually decreases to around 3ng/ml at 4 weeks.

Further analysis of the metabolism and pharmacokinetics of NTX in humans reveals that NTX is metabolized by dihydrodiol dehydrogenase to form 6β-naltrexol (NTXol), the major active metabolite. [127]. Both NTX and NTXol plasma levels can be correlated to alcohol consumption levels. [128] NTXol has a longer half-life in the plasma as compared to NTX, but a significantly higher plasma concentration of NTXol is required for therapeutic efficacy as compared to NTX. [15]

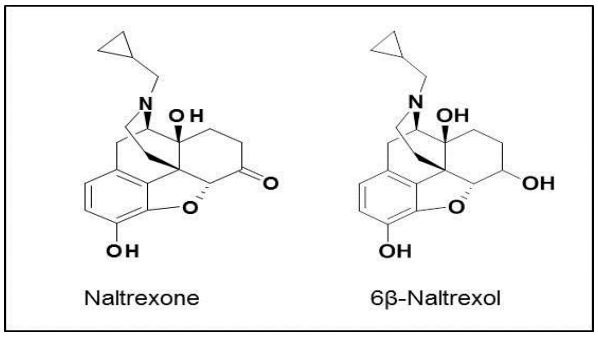

Figure 4.10 Structure of NTX and NTXol

4.7.2 Issues with NTX therapy

NTX is typically prescribed for highly motivated patients since opioid consumption during treatment can lead to overdose and death. It works very well in a compliant population, however subject compliance is one of the major issues with NTX therapy. It has been shown that NTX treatment efficacy increases in compliant subjects receiving additional behavioral therapy. [129] NTX satisfies almost all the characteristics of a good addiction medication. The drug reduced relapse to 23% in NTX treated group compared to 54.3% in a placebo treated group, where relapse was defined as consumption of alcohol on 5 or more days within a week during the 4 week study period [130, 131] blocks reinforcing properties and the “high” associated with alcohol use is lower on

treatment with NTX [132], and most of the side effects are associated with the route of delivery.

Transdermal drug delivery could be a potential alternate route for NTX. Variable bioavaibility and hepatotoxicity issues can be resolved via transdermal delivery, steady state plasma concentrations are seen with transdermal delivery compared to the peaks and troughs of oral and IM delivery, compliance is higher in an addict population [28], and patches can be removed very easily in case there is a need for emergency opiate treatment. However, NTX cannot be delivered in the therapeutic plasma level range by passive transdermal delivery. [4] Prodrugs and codrugs of NTX have been synthesized to enhance permeability, and although some of them enhanced flux, the enhancement was not enough for therapeutic efficacy in humans. [82-86] MN were used as a physical enhancement technique and it was shown that NTX can be delivered at a rate to provide low therapeutic plasma concentrations by using 4 MN patches [4]. Recently Vivitrol® has been shown approved for opioid dependence and NTX has shown efficacy in treatment of tobacco addiction and amphetamine addiction as well. [133]

Thus NTX is an excellent model compound for optimization of pore lifetime enhancement strategies and development of a 7 day transdermal drug delivery system.

Chapter 5

Effect of formulation pH on transport of naltrexone species and pore closure in microneedle-enhanced transdermal drug delivery

5.1 Introduction

The contents of this chapter have been published in Molecular Pharmaceutics (April 2013) except figure 5.1. Skin is the largest and the most accessible organ of the body. The extensive vasculature in the dermal region of the skin ensures rapid uptake of any compound that permeates across the skin barrier into the systemic circulation, thus making the skin a very attractive drug delivery target. [1, 2] However, in order to protect an individual's internal environment from infiltration of xenobiotics as well as excessive water loss, the stratum corneum (SC), the topmost layer of the skin is specifically designed to protect the human body. [134] A very small subset of pharmacologically active molecules can successfully cross the SC (passive delivery) in therapeutically relevant concentrations. [2, 37] Research in the field of passive transdermal delivery has focused primarily on small molecular weight (<500Da) unionized compounds with a octanol/water partition coefficient (log P)~2 to help in transport and partitioning across the SC, the most important barrier to passive transport. [1, 135] Active transdermal drug delivery systems on the other hand employ some kind of physical enhancement technique to permeablize the SC or reduce the barrier effect of the SC. Research and development in the field of active drug delivery systems over the past two decades have greatly enhanced the number of molecules that can be delivered transdermally. It has also opened up a whole new area of research since active transdermal systems focus on transport across the lower epidermal and dermal layers, which are more hydrophilic than the SC and could benefit from water-soluble drug candidates. [2, 27, 136]

The current study focuses on microneedle (MN) enhanced transdermal drug delivery as a model of active drug delivery systems. Other active drug delivery systems may include iontophoresis, ultrasound, microdermabrasion, or electroporation. MN's are small micron-scale needles that are used to permeablize the skin by creating micropores or microchannels across the SC. [42] Once the SC barrier is removed, drug can directly pass into the interstitial fluid and the lower layers of the skin. MN can vary in length anywhere from 200μm to a few millimeters. There are four different methods of MN application, "poke/press and patch" where solid MN are used to permeablize the skin followed by application of a drug patch, coated MN where drug is coated onto the surface of the MN and used as the drug delivery medium, dissolving MN where drug is loaded into the polymer used for MN synthesis, and hollow MN where drug is pushed through micron-scale needles with the help of an infusion pump. Several researchers have looked at the effects of needle length, needle shape, material, etc. on the mechanical/structural integrity of MN. [64, 137] Additional studies have focused on transport and drug delivery across MN treated skin both *in vitro* as well as *in vivo.* It has been shown that a large number of molecules can be successfully delivered using a MN system. Some examples include naltrexone, calcein, insulin, parathyroid hormone, etc. [44, 54, 59]

Formulation and pore closure kinetics for MN enhanced drug delivery had not been investigated in great depth until recently. The effect of charge/ionization state was investigated by Banks et al. to show that an ionized form of the drug exhibited a higher flux using naltrexone (NTX) and naltrexol. For intact skin, it is known that unionized molecules generally exhibit faster transport, but in MN treated skin the primary permeation route is completely different and the faster transport of ionized molecules was an important finding. In the Banks study it was concluded that the faster transport of

ionized molecules could be attributed to enhanced solubility. [54] Another aspect of MN formulation that has been investigated is the effect of formulation viscosity. Milewski et al. showed that a lower viscosity formulation translated into faster flux compared to a higher viscosity propylene glycol (PG) rich formulation utilizing the same concentration of drug in the donor. The results in that study could be explained by assuming a Stokes-Einstein equation for diffusivity of drug through the MN pores instead of the free volume theory that is used for intact skin. [22] The third aspect of donor formulation investigated was the effect of saturation on transport across MN pores. For intact skin, delivery from a saturated solution translates into the maximum driving force and hence the fastest flux. However, in MN enhanced delivery it has been shown that the highest flux is achieved using a sub-saturated solution due to pore clogging and viscosity effects. [22, 138, 139]

MN enhanced delivery maximizes drug transport by creating micropores (or microchannels) across the skin. However, these micropores begin to close under the influence of normal physiological functions. Thus the efficacy of sustained-release MN enhanced delivery is greatly limited by the lifetime of the micropores. Recent literature reports have shown the effects of MN geometry, occlusion, and skin type on the rate of pore closure. Several direct and surrogate markers have been used by different groups for closure rate comparison, such as transepidermal water loss (TEWL), impedance spectroscopy, dye imaging, and pharmacokinetics. [9-12, 54] By and large, a pore closure timeframe of 48-72 hours under occlusion and around 10-15 minutes without occlusion has been observed. Several factors may contribute to the closure of micropores. The formation of the SC depends on the availability of SC lipids, their processing and release from lamellar bodies. [70] Deeper tissue wound healing is a multi-step process which involves inflammation, proliferation and remodeling. [140] The role of pH in healing of superficial wounds due to tape stripping or acetone treatment has been previously

studied using TEWL in rat skin. The results from those studies showed that healing of the skin is delayed at a higher pH of 7.4.[18] The results can be explained in terms of activity of β-glucocerebrosidase across the pH range of the study from 5.5-7.4. β-glucocerebrosidase is an important enzyme in the ceramide synthesis pathway, [101] and exhibits an activity maximum around pH 5, with substantially decreased activity at pH 7.4 [102]. Since ceramides constitute 50% of the SC structure by weight, and a molar ratio of 1:1:1 of ceramides: cholesterol: fatty acids is an important factor for proper formation of the SC barrier, at a higher pH the rate of healing is significantly slower over a 6 hour timeframe. [24, 73] The effect of surface pH in chronic wounds has also been studied. [141, 142]

There are several factors that can contribute to transport and pore closure during MN enhanced delivery. The effect of formulation pH was examined in this study. The model compound of choice was NTX (molecular weight- 341.4, log P- 2.0, pKa- 7.5, 9.16). [143] It is a μ-opioid receptor antagonist used in alcohol and opioid addiction [144]. ReVia®, the original daily oral formulation has bioavaibility issues as well as gastrointestinal side effects. [145] Vivitrol®, the extended release 28-day formulation has injection site reactions, and it is difficult to remove if emergency opioid treatment is required. [17] Hence, NTX is a good model compound for a sustained release transdermal patch formulation. NTX does not reach a therapeutically relevant plasma concentration via passive transdermal delivery, so MN enhanced drug delivery was used for development of an active transdermal patch. The first human study with NTX and MN showed that while utilizing MN, drug could be delivered in the lower therapeutic plasma level range for 48-72h, no detectable level of the drug was obtained in plasma for the control non-MN treated subjects. [4] Subsequent efforts were directed towards improving the NTX formulation for better transport, as well as enhancement of pore lifetime by using diclofenac sodium towards the development of a 7 day transdermal system, the

ideal transdermal drug delivery goal. [8, 9, 14, 21, 22, 139, 146, 147] In this study the effect of formulation pH will be evaluated for transport and in depth analysis of permeability via the microchannel pathway and intact skin pathway. A mechanistic understanding of the relation between ionization state and transdermal flux will help in development of active transdermal systems for a host of different molecules that can potentially benefit from a multiday sustained release dosage form. Since the factors contributing to micropore closure are not very well understood yet, studying the effect of formulation pH on micropore closure kinetics will help determine if this can be used as a possible mechanism for pore lifetime enhancement for development of 7-day drug delivery systems. The current study was carried out to fulfill research goal 3.1 and 3.2.

5.2 Experimental section

5.2.1 Chemicals

Naltrexone base was purchased from Mallinckrodt (St. Louis, MO). Citric acid monohydrate was purchased from Fisher chemicals (Fairlawn, NJ). Water was purified using a NANO pure Diamond™, Barnstead water filtration system. 1-Octanesulfonate, sodium salt was obtained from Regis Technologies, Inc. (Morton Grove, IL). Trifluroacetic acid (TFA), triethylamine (TEA) and acetonitrile (ACN) were obtained from EMD chemicals (Gibbstown, NJ). Sodium hydroxide was obtained from Sigma (Saint Louis, MO). Natrosol® (hydroxyethlycellulose) was obtained from Ashland (Wilmington, DE). Seventy percent ethanol was obtained from Ricca chemicals (Arlington, TX)

5.2.2 Donor solution preparation

All donor solutions for *in vitro* permeation studies were prepared in citrate buffer (0.3M). Citric acid monohydrate was mixed with nanopure water to obtain a base solution. The pH was then adjusted with sodium hydroxide to obtain solutions at 6 different pH values. NTX base was

added to 3ml of each solution in excess, vortexed, sonicated for 10 minutes, and were left in a shaker water bath at 32°C overnight. The pH adjusted saturated drug solutions were used as donor solutions for all studies. (pH 5.76, pH 6.30, pH 6.43, pH 6.72, pH 7.56, and pH 8.26)

All donor gels for *in vivo* pig studies were prepared in citrate buffer (0.1M). Citric acid monohydrate was used to prepare a base solution. The pH was adjusted to pH 5.5, pH 6.5 and pH 7.4 using NaOH (3M). The solutions were left overnight and the pH was also measured on the next day to make sure changes did not occur. Three percent hydroxyethlycellulose (HEC) was added to each solution as a gelling agent. The gels were stored at 32°C for the entire length on the study.

5.2.3 pH measurements

The pH of all *in vitro* donor solutions were measured using a VWR® sympHony® (SB70P) pH meter and VWR® sympHony® Glass Combination pH Electrode. All solutions were measured following pH adjustment, after overnight incubation with drug, and immediately before dosing.

5.2.4 Solubility determination

The apparent solubility of NTX base in solutions with different pH values was determined immediately prior to dosing. Five hundred µl of each donor solution was filtered using a 0.2µm, 500µl centrifugal filter. Ten µl of the filtered solutions was used to spike 10ml of ACN. Concentration of drug was analyzed using a HPLC (method reported in quantitative analysis section) after appropriate dilutions. All solubility determination experiments were carried out in triplicate.

5.2.5 Viscosity measurements

Viscosity was measured using a Brookfield DV-III LV programmable cone/plate rheometer and a CPE-40 spindle. Each filtered donor solution viscosity was measured at three different torque values within the range of 10-100% torque. The temperature was maintained at 32°C using a circulating water bath throughout the study.

5.2.6 *In vitro* diffusion studies

Full thickness Yucatan miniature pig skin was used for all *in vitro* experiments. The skin was removed from euthanized animals under a University of Kentucky IACUC approved protocol. The skin was obtained from the dorsal region of euthanized animals, dermatomed to a thickness of 1.4-1.8mm after removal of all subcutaneous fat and frozen (at -20°C) until use. Skin samples were thawed on the day of the study. For MN treatment, the skin was placed on a wafer of Sylguard® 184 silicone elastomer to mimic the underlying tissue. MNs for this study were obtained from Dr. Mark Prausnitz's laboratory at the Georgia Institute of Technology. A 5 MN in plane MN array was used for *in vitro studies*. Each MN (triangular in shape) was 750 µm long, 200µm wide (at the base) and 75 µm thick (thickness of metal used) and the inter needle spacing was 1.35µm. Each square piece of skin was pierced 20 times to create a total of 100 MN pores (Skin was rotated by 90° following 10 MN insertions so as to create non-overlapping pores). The skin was then placed in a horizontal flow through diffusion cell with an active diffusion area of 0.95cm^2. Untreated skin was placed directly onto the diffusion cells. Three to four cells were used per treatment group for all experiments. A PermeGear flow through (In-line, Riegelsville, PA) cell was used for *in vitro* diffusion studies. Water adjusted to pH 7.4 containing 20% ethanol was used as the receiver solution. The flow rate of the receiver solution was adjusted to 1.5ml/h to maintain sink conditions. The temperature of the cells was maintained at 32°C, the temperature of the

outer surface of the skin. Transepidermal water loss (TEWL) measurements were obtained to make sure that untreated skin had values <5g/m^2/h indicating no damage. Each cell was charged with 250µl of saturated donor solution and receiver solution was collected in 6h increments for a total of 48h. Drug concentration was quantified using a HPLC assay for NTX. A cumulative amount vs. time plot was generated and flux was determined from the steady state portion of the curve using Fick's first law of diffusion.

$$J_{TOT}\ or\ J_{SS} = \frac{1}{A}\left(\frac{dM}{dt}\right) = P * S_{TOT}$$

J_{TOT} or J_{SS} is the steady state flux or total flux, A is the diffusional surface area (0.95cm^2), M is the total mass transport across a membrane (skin in this case) and t is time. P is the apparent permeability coefficient and S_{TOT} is the saturation solubility of the donor. The driving force for diffusion is the concentration gradient across the barrier. However, in this case since the receiver solution is maintained at sink conditions throughout the experiment, the driving force is the solubility of the drug in the donor. Flux enhancement is the ratio of flux across MN treated skin to flux across non treated skin for the same formulation. At the end of the experiment, the skin was removed and dissected into small pieces. Skin concentration of drug was measured by extracting drug from the tissue into ACN overnight at 32°C and analyzing the solution by HPLC after appropriate dilutions.

5.2.7 Quantitative analysis

The drug concentration in the receiver solution was measured using a HPLC assay. The HPLC system consisted of Waters 2695 separation module, Waters 2489 dual wavelength absorbance detector and Waters Empower™ software. A Perkin Elmer Spheri5 VL C18 column (5µ, 220 x 4.6mm), C18 guard column (15 x 3.2mm) was used. The mobile phase consisted of 70:30(v/v) of ACN: 0.1% TFA containing 0.065% 1-octane sulfonic acid sodium salt, adjusted to pH 3.0 with TEA aqueous phase. The

wavelength used for quantification was 280nm. The injection volume for all samples was 100 µl and the retention time for NTX was 2.1 ± 0.1 min. Samples were analyzed within a 100–10000 ng/ml linear range of standard curve ($r^2 \geq 0.99$)

5.2.8 *In vivo* studies with impedance spectroscopy

Impedance spectroscopy was used to look at pore closure kinetics in the Yucatan miniature pig. All animal experiments were approved by the University of Kentucky IACUC. The pig skin was cleaned with soap and water a day before the treatment. On the day of the treatment, all sites were marked, 3 sites for MN treatment and 1 site for intact skin control for each formulation. The site for the reference electrode was in the center and equidistant from all measurement sites. The impedance setup consisted of an impedance meter (EIM-105 Prep-Check), 200 kΩ resistor in parallel (IET labs, Inc.), reference and measurement electrodes. A large electrode (70mm diameter) with conductive gel (Superior StarBurst® electrode with PermaGel) was used as the reference electrode. A Ag/AgCl gel electrode (S & W Healthcare Corp. Series 800, 50mm diameter total area, 10 mm active electrode diameter) was used as the measurement electrode. Baseline measurements were obtained in duplicate at all 12 sites [51]. Active sites were cleaned with an ethanol swab, allowed to dry and treated twice with a 50 MN array (to give a total of 100MN insertions). The sites were measured again for post-MN treatment value; 200µl of gel was then applied to each site and covered with an occlusive patch. [148] The non-treated control sites were occluded after application of gel as well. All patches were secured using Bioclusive dressing (Systagenix Wound Management, Quincy, MA). For each subsequent measurement the patch was removed and the active site was cleaned with gauze, measurements were obtained followed by reapplication of gel and patch. Single measurements were obtained for all post treatment measurements to minimize the exposure of the active site to air and gel on the

measurement electrode. Data was analyzed using the following equation for calculation of Z_{pores} (impedance of pores),

$$Z_{total} = \frac{1}{\frac{1}{Z_{box}} + \frac{1}{Z_{skin}} + \frac{0.02}{Z_{pores}}}$$

Where Z_{skin} was obtained from the intact skin value under the same treatment condition at each time point, Z_{box}=200kΩ resistance box and Z_{total} is the raw value obtained on the meter. Admittance (1/Impedance) values were used to compare pore closure kinetics among formulations. All data were reported as mean ± SD.

5.2.9 Statistical analysis

Data for all experiments are reported as mean ± standard deviation. Statistical analysis of data was carried out with Students' t-test and one way ANOVA with Tukey's posthoc pairwise tests, if required, using GraphPad Prism® software. $P<0.05$ was considered to be statistically significant.

5.3 Results

5.3.1 pH and viscosity measurements

The pH of all *in vitro* donor formulations was measured before and after addition of drug. Changes in formulation pH were observed for all solutions following the addition of the drug. The change was more significant for formulations at the lower end of the pH spectrum. The viscosity was also measured for all formulations to account for the effect of viscosity on MN enhanced transdermal flux. The lower pH formulations were more viscous, which can be attributed to the higher concentration of drug in those formulations. Viscosity decreased significantly with increase in formulation pH ($p<0.05$), except at pH 6.72 and pH 7.56 ($p>0.05$). Table 5.1 lists the changes in pH and viscosity

for all formulations. The pH of each solution at dosing was used for all subsequent results and calculations.

5.3.2 Solubility measurements

The solubility of NTX was quantified in all *in vitro* donor solutions. Figure 5.2 shows the measured experimental values of solubility at 32°C for the 6 different pH conditions compared to the predicted values from Scifinder® at 25°C. The measured values were higher compared to the predicted values across the pH range.

5.3.3 *In vitro* diffusion studies

Flux was determined across MN treated skin as well as non-treated control for each of the 6 formulations (Figure 5.3). The flux values indicated that there was a significant difference in flux across MN treated skin among the formulations ($p<0.05$), except for pH 5.76 compared to pH 6.3, and pH 7.56 compared to pH 8.26. Flux values across non-treated control skin were not significantly different from each other among the formulations ($p>0.05$). Significant flux enhancement was obtained due to MN treatment at pH 5.76, pH 6.30, pH 6.43 and pH 6.72 as compared to intact skin control ($p<0.05$).

Skin concentration and lag time were calculated from the *in vitro* studies. Table 5.2 lists the flux enhancement, skin concentration, and lag time of NTX across MN treated and non-treated skin. Flux enhancement was higher in lower pH/higher solubility formulations compared to the higher pH/lower solubility formulations. Skin concentration data for MN treated skin mimicked the flux profiles; formulations exhibiting higher flux had higher concentration of the drug in the skin. Skin concentrations for MN treated samples were significantly different from each other for all formulations ($p<0.05$) except between pH 5.76 and pH 6.3, and pH 7.56 compared to pH 8.26. Skin concentrations for

non-treated skin were not significantly different from each other ($p>0.05$). The lag time calculations showed that MN treatment significantly reduced the lag time compared to non-treated control for all formulations except pH 7.56. Lag time also increased with increase in pH for MN treated skin ($p<0.05$).

5.3.4 *In vivo* studies for pore closure kinetics

In vivo studies were conducted in a Yucatan miniature pig model to look at the effect of formulation pH on closure of micropores. Three different pH values were evaluated for impedance studies. The average raw values for pre and post MN treatment were 84.59 ± 17.82 and 25.87 ± 0.88, respectively. Significant differences between pre and post MN treatment impedance values were obtained for all sites (data not shown) ($p<0.05$). Figure 5.4 shows a plot of admittance values vs. time. The admittance values were significantly different between pH 5.5 and pH 6.5, and pH 5.5 compared to pH 7.4 at 24h ($p<0.05$). There was no significant difference in admittance values between pH 5.5 and pH 7.4 beyond the 24h time point ($p>0.05$).

5.4 Discussion

The current study was designed to look at the effect of formulation pH on transport and pore closure across MN treated skin. Formulation plays a significant role in any drug delivery system by having an effect on stability and solubility from the physicochemical standpoint, to ease of use from a clinical standpoint. Since this study focuses on effect of pH, the choice of the buffer was important and it was based on previous publications that studied the effect of pH on wound healing. [18] The 3 pKa values associated with citrate buffer are 3.13, 4.76 and 6.4 and it is widely used in the pH range of 3-7. A single buffer species was chosen for all pH values to reduce variability in the data due to formation of a second NTX species following overnight incubation in saturated buffer solutions. *In vivo* studies were conducted at a buffer

concentration of 0.1M, comparable to previous literature. Higher buffer strength of 0.3M was used for *in vitro* studies since the buffer strength of 0.1M was not suitable in the presence of high concentrations of NTX base in solution. Changes in the final pH of the formulations following incubation with drug were noted and used for all subsequent calculations. Solubility of NTX base in the donor formulation was higher, compared to predicted values from Scifinder®. The difference in solubility can be explained in terms of the temperature difference. The predicted values were at 25°C, while the experimental values were at 32°C. The solubility could also be higher due to formation of NTX citrate following overnight incubation. The data reported in this paper is in agreement with previously published literature on solubility of NTX salts at 32°C [139]. Previous researchers also reported that saturation solubility is reached around pH 5.0; therefore the range of data in the current study is sufficient to explore the effect of formulation pH on flux and permeability for NTX.

The *in vitro* results showed that MN enhancement translated into significant flux enhancement at pH 5.76, pH 6.3, pH 6.43 and pH 6.72. The flux across MN treated skin was not significantly different from non-treated control for pH 7.56 and pH 8.26. Thus it can be concluded that formulation pH had an effect on flux enhancement across MN treated skin. The enhancement ratio of 11.24±2.9 at pH 5.76 indicated that using a lower pH formulation is advantageous in terms of flux enhancement across MN treated skin. Since flux enhancement directly translates into higher plasma concentration, this will lead to smaller patch sizes or fewer numbers of MN treatments in an individual.

MN enhanced drug delivery employs two distinctly different routes for drug movement, the microchannel pathway through the micropores created across the skin/SC barrier and passive diffusion through the intact skin pathway around the microchannels. However, since the SC is the most important barrier to movement for a

large number of molecules, removing the SC barrier theoretically enhances permeability by 100-1000 times. [1] The only exceptions to this rule are highly lipophilic molecules that form a depot in the SC and release slowly over time. Thus, the total flux (J_{TOT}) can be considered to be a sum of the flux values across two parallel routes, relative contribution of the MN pathway (J_{MCP}) and intact skin pathway (J_{ISP}) flux values towards the total flux can be obtained using the following equation. [22]

$$J_{TOT} = J_{MCP} + J_{ISP}$$

J_{ISP} is obtained from the intact skin (non-treated) control cells for each pH value. Subtracting the J_{ISP} from the total flux of MN treated cells at each pH value gives J_{MCP}. Figure 5.5 shows the relative contribution of the two different pathways towards the total flux across the pH range. At formulation pH 5.76 NTX is 98% ionized (pKa 7.5), while at pH 7.56 NTX is 50% ionized. Figure 5.5 shows that J_{MCP} is 91% of total flux at pH 5.76 and decreases to 13% at pH 7.56. As the percentage of ionized molecules decreased in formulation, the contribution of the J_{MCP} towards the total flux decreased. This can be explained in terms of the movement of ionized and unionized molecules across the skin. The MN treated skin drug permeates directly into the interstitial fluid in the microchannel pathway, a hydrophilic environment that facilitates permeation of hydrophilic molecules. Since solubility of the ionized form of the drug is significantly higher in an aqueous formulation, it translates into faster flux across MN treated skin at a lower pH. On the other hand, unionized molecules move faster through intact SC since charge on the surface of the molecule hinders its movement and partitioning. [1] Skin concentration data exhibited a similar profile to flux for MN treated and non-treated skin. Thus, the higher flux at lower pH values is not an effect of saturation of the skin with NTX. Lag time measurements were obtained from the steady state profiles to compare formulations. The average lag time for non-treated skin was around 20h, while the lag time for the pH

5.76 condition in MN treated skin was 5h. Significantly shorter lag times of low pH formulations in MN treated skin would be beneficial for development of a drug delivery system, since shorter lag times translate into shorter time to steady state plasma concentrations.

Permeability of drug across the skin barrier via the two different pathways would provide a better understanding of movement by eliminating the effect of solubility. Therefore, total permeability (P_{TOT}), microchannel pathway permeability (P_{MCP}), and intact skin pathway permeability (P_{ISP}) were calculated using the following equations.

$$J_{TOT} = P_{TOT} * S_{TOT}$$

$$J_{MCP} = (f_{MCP} * P_{MCP} * S_{TOT})$$

$$J_{ISP} = (f_{ISP} * P_{ISP} * S_{TOT})$$

J_{TOT}, J_{MCP} and J_{ISP} were previously calculated values from Figure 5.5. The values of f_{MCP} and f_{ISP} were the fractional area of the treated skin exposed to active MN delivery and passive delivery, respectively. f_{MCP} has been estimated to be 0.02 or 2% of the total area and f_{ISP}~1, based on prior literature. [146] The total permeability of NTX across Yucatan pig skin as well as permeability via the two different routes was calculated. Figure 5.6 shows permeability values of NTX from each of the 6 different formulations. P_{MCP} was not calculated for pH 8.26 since the J_{MCP} calculation model does not allow for MN pathway flux calculation for that particular data point. The data showed that P_{MCP} was not significantly different among the formulations across the pH range ($p>0.05$). On the other hand, P_{ISP} values for the higher pH formulation at pH 7.56 and pH 8.26 were significantly higher ($p<0.05$), compared to the rest of the formulations. Thus P_{ISP} is affected by the change in ionization state of the molecule in formulation, and permeability of the unionized form of NTX is higher across intact skin compared to the ionized form. P_{MCP} is

not influenced by the change in ionization state of the molecule indicating that transport across the MN pathway is independent of the ionization state. The flux enhancement observed at the lower pH formulations is solely a function of the higher solubility of the ionized form of the drug. At the higher pH values the flux/permeability is solely a function of the unionized species of the drug. This is evident from the fact that at pH 7.56 and pH 8.26 there is no significant difference between the P_{TOT} and P_{ISP}. The effect of charged and uncharged species on flux had already been studied before for MN treated skin. However, the current study looks at the role of speciation across the pH range to evaluate the effects in MN treated and non-treated skin, while controlling for important factors like viscosity of formulation, thickness of skin, etc.

Modeling the data in terms of permeability of the ionized and the unionized form of NTX would help in the mechanistic understanding of drug transport across MN treated and non-treated skin. [149] The following model is used for calculating P_{MCP} and P_{ISP}. The total solubility of any molecule in solution is a function of the intrinsic solubility (S_{un}) and the solubility of the ionized form (S_i) of the molecule which is pH dependent. This assumes that only one pKa of NTX (pKa 7.5, associated with the protonation of the tertiary amine) is relevant for solubility calculations in the range of the experimental data. S_{un} (0.48mg/ml) was obtained from Scifinder® and S_i was calculated using the pKa and the pH values.

$$S_{TOT} = S_i + S_{un}$$

$$S_{TOT} = S_{un}\left(1 + \frac{H^+}{K_a}\right)$$

The S_{un} and S_i can then be used to calculate P_{MCP} and P_{ISP} utilizing the following equations.

Model 1

$$J_{MCP} = (f_{MCP} * P_{MCP} * S_{TOT})$$

$$J_{MCP} = \{f_{MCP} * (P_{MCPi} * S_i)\} + \{f_{MCP} * (P_{MCPun} * S_{un})\}$$

$$J_{ISP} = (P_{ISP} * S_{TOT})$$

$$J_{ISP} = (P_{ISPi} * S_i) + (P_{ISPun} * S_{un})$$

Model 2

$$J_{MCP} = (f_{MCP} * P_{MCP} * S_{TOT})$$

$$J_{MCP} = \{f_{MCP} * (P_{MCPi} * S_i)\}$$

$$J_{ISP} = (P_{ISP} * S_{TOT})$$

$$J_{ISP} = (P_{ISPun} * S_{un})$$

The permeability of the ionized (P_{MCPi}) and unionized (P_{MCPun}) form of NTX across the microchannel pathway, and ionized (P_{ISPi}) and unionized (P_{ISPun}) form across the intact skin pathway were estimated using the experimental data. The permeability at pH 5.76 was used for the completely ionized form of the drug, and pH 8.26 was used for the completely unionized form of the drug. Since the P_{MCP} could not be calculated for pH 8.26, P_{ISP} at pH 8.26 was used for the P_{MCPun} and P_{ISPun} values. The model assumes that the products of ionized permeability and unionized solubility and vice versa are negligible for both equations. Flux values calculated using the above equations were divided by the total calculated solubility to get calculated permeability values. Model fitting was done using Scientist® version 3.0 and least squares fitting to experimental data. From the fitted data, goodness of fit was r^2>0.8 for estimation of microchannel pathway permeability and r^2>0.9 for estimation of intact skin pathway permeability. The

results indicated that the model can be used to predict permeability of a molecule both across MN treated and non-treated skin. In Figure 5.7 the black dashed line is the calculated permeability from model 1. The black solid line is the calculated permeability considering only the ionized species for microchannel pathway and unionized species for intact skin pathway (model 2). From the model, the permeability across MN treated skin is best predicted using the completely ionized form of the drug. Total permeability across the MN pathway is better predicted by model 1 indicating that it is a function of both the ionized and the unionized form of the drug. For model 2, the predicted permeability at pH 7.26 due to the ionized component alone is much lower compared to the experimental values indicating that at the higher pH values unionized molecules have a significant contribution towards the MN pathway flux. The intact skin permeability value can be predicted by estimating permeability for the ionized and unionized form of the drug, or only the unionized form of the drug. There is no significant difference in the predicted values with/without taking the ionized species into consideration i.e. between model 1 and model 2. P_{ISPi} values at the lower end of the pH range estimated to be negative by model 1 were forced to zero in Figure 5.7. From Table 5.3 it can also be seen that permeability of the completely ionized species (P_{ISPi}) for the intact skin pathway is estimated to be negative, indicating that negligible permeation of the ionized species takes place via the intact skin pathway for this particular molecule. Thus model prediction of flux based on pH of formulation can be used for a whole range of molecules by estimating the permeability of the ionized and unionized species for the particular molecule experimentally. For the intact skin pathway, different equations can be used to predict permeability of the unionized species, such as the Potts and Guy equation, etc. [150, 151] Once permeability is known flux can be calculated using total solubility values since the model shows that there is no significant difference between model 1 and model 2 for intact skin. For MN treated skin, a single experiment will be required to determine

the permeability of the completely ionized component across the membrane of choice. Using a combination of the P_{MCPi} and the intact skin permeability, flux can then be predicted across the pH range using the above model. Thus the data can be used to minimize wet lab experiments and facilitate selection of candidates for MN enhanced and passive transdermal delivery based on their solubility and estimated permeability across the pH range.

Barrier recovery is one of the most important aspects of enhanced transdermal delivery systems like MN. The rate of healing of the skin determines the rate of delivery across the skin. Previously published reports have investigated the role of various factors in skin wound healing in different wound models ranging from acetone treatment to tape stripping and full thickness wounds. The role of pH was investigated in an acetone treated model of acute barrier perturbations and it was reported that barrier recovery was slower at pH 7.4 over a 6h period. The slower rate of recovery was attributed to lower activity of β-glucocerebrosidase and post secretory processing of lipids into lamellar membrane structures. [18] However, this is only true when the SC barrier is completely destroyed and the skin loses its acidic environment. As the skin starts to recover and the acid mantle is reinstated the effects of external formulation pH are no longer observed. MN barrier disruptions are not well understood in terms of the pH environment of the wounds or barrier recovery. Thus the *in vivo* experiments in this paper were important to determine whether an external pH would have an effect on the rate of healing by affecting enzyme activity or post secretory processing over a prolonged period of time (7 days), thus extending the micropore lifetime. Impedance spectroscopy is a fairly new technique developed to look at wound healing or pore closure for MN channels, compared to TEWL. It has been used extensively to look at pore closure in rat models and humans. [11] Method development studies for impedance spectroscopy were also conducted to look at use of different electrodes, pressure of

application, etc. in hairless guinea pigs, Yucatan miniature pigs, and humans. [51] The current results showed that there was a significant difference between pH 5.5 and pH 7.4 at the 24 hour time point, but there were no significant differences in admittance values at 54h and 72h. Thus using a pH 7.4 formulation would not be beneficial for multiday pore lifetime enhancement in the current MN treatment model. The presence of certain cations, like calcium and potassium, has also been shown to have an effect on the rate of recovery indicating that ionic strength may also have an effect. [112] In the current study citrate buffer was used and the pH of the buffer was adjusted with NaOH to eliminate effects of the different ions on barrier recovery. Interestingly the counter ion did not play a role in barrier recovery following iontophoresis. [152]

5.5 Conclusion

The aim of the current study was to investigate the role of formulation pH on transport and recovery of MN treated skin. The in vitro results indicated that there is a significant flux advantage of using a lower pH, higher solubility (for a weak base) formulation for the development of a 7-day patch system. Modeling the data based on permeability gives an in depth understanding of the relative movement of the ionized and unionized form of the drug across MN treated and non-treated skin. The model can be further used for other drugs by obtaining permeability coefficients for the ionized and the unionized forms. The in vivo impedance spectroscopy data showed that there was no significant effect on barrier recovery/pore closure kinetics when using a higher pH formulation over the span of 4 days.

Table 5.1 Formulation characteristics of 6 different formulations (n=3 for all viscosity measurements)

pH of buffer	pH of formulation (after addition of drug)	Viscosity (cP)
2.3	5.76	4.01 ± 0.03
3.5	6.30	3.47 ± 0.02
4.5	6.43	2.57 ± 0.01
5.5	6.72	2.20 ± 0.02
6.5	7.56	2.22 ± 0.07
7.4	8.26	1.98 ± 0.0

Table 5.2 Diffusion parameters for 6 different formulations across MN treated and non-treated pig skin. (n=3-4)

pH of buffer	pH of formulation (after addition of drug)	Flux enhancement	Skin concentration (μmol/g)		Lag time (h)	
			MN treated	Non treated	MN treated	Non treated
2.3	5.76	11.24 ± 2.90	5.15 ± 0.48	2.11 ± 1.14	5.01 ± 2.76	21.26 ± 0.16
3.5	6.30	6.11 ± 1.87	5.22 ± 0.46	2.12 ± 0.15	6.41 ± 0.80	16.27 ± 0.68
4.5	6.43	3.55 ± 1.07	3.99 ± 0.54	2.98 ± 1.31	6.09 ± 3.12	18.24 ± 3.76
5.5	6.72	4.24 ± 0.59	2.96 ± 0.38	1.09 ± 0.18	10.89 ± 0.67	21.64 ± 1.34
6.5	7.56	1.15 ± 0.46	1.44 ± 0.29	1.43 ± 0.12	19.24 ± 2.21	22.59 ± 0.26
7.4	8.26	0.96 ± 0.37	0.79 ± 0.22	0.96 ± 0.15	20.85 ± 2.32	24.76 ± 1.12

Table 5.3 Experimental and calculated permeability values from Model 1 and Model 2

	Experimental	Model 1	Model 2
P_{MCPi} (cm/h)	$3.10 \times 10^{-3} \pm 3.25 \times 10^{-4}$	$3.92 \times 10^{-3} \pm 1.18 \times 10^{-3}$	$4.75 \times 10^{-3} \pm 1.18 \times 10^{-3}$
P_{MCPun} (cm/h)	$1.66 \times 10^{-3} \pm 2.70 \times 10^{-4}$	$5.89 \times 10^{-3} \pm 4.0 \times 10^{-3}$	--------
P_{ISPi} (cm/h)	$6.06 \times 10^{-6} \pm 1.51 \times 10^{-6}$	$-(1.45 \times 10^{-4}) \pm 1.05 \times 10^{-4}$	---------
P_{ISPun} (cm/h)	$1.66 \times 10^{-3} \pm 2.70 \times 10^{-4}$	$1.75 \times 10^{-3} \pm 1.96 \times 10^{-4}$	$1.66 \times 10^{-3} \pm 2.02 \times 10^{-4}$

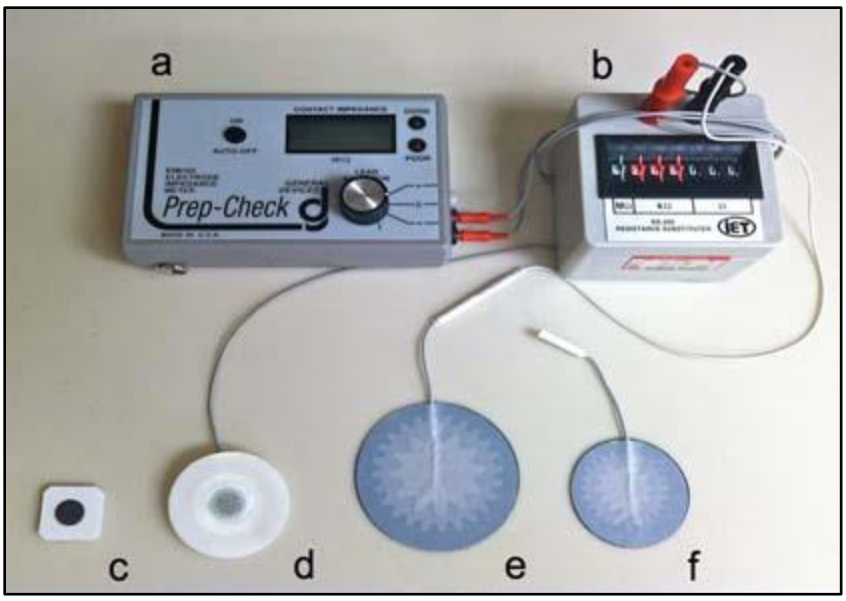

Figure 5.1 Impedance setup used for all human and animal studies. (a) Prep-Check impedance meter, (b) 200 kΩ resistor in parallel, (c) dry Ag/AgCl measurement electrodes, (d): gel Ag/AgCl measurement electrodes, (e) reference electrode for Yucatan miniature pig and human studies, and (f) reference electrode used for hairless guinea pig studies

Reprinted with permission from Journal of Pharm. Sci 2013; 102(6):1948-1956.

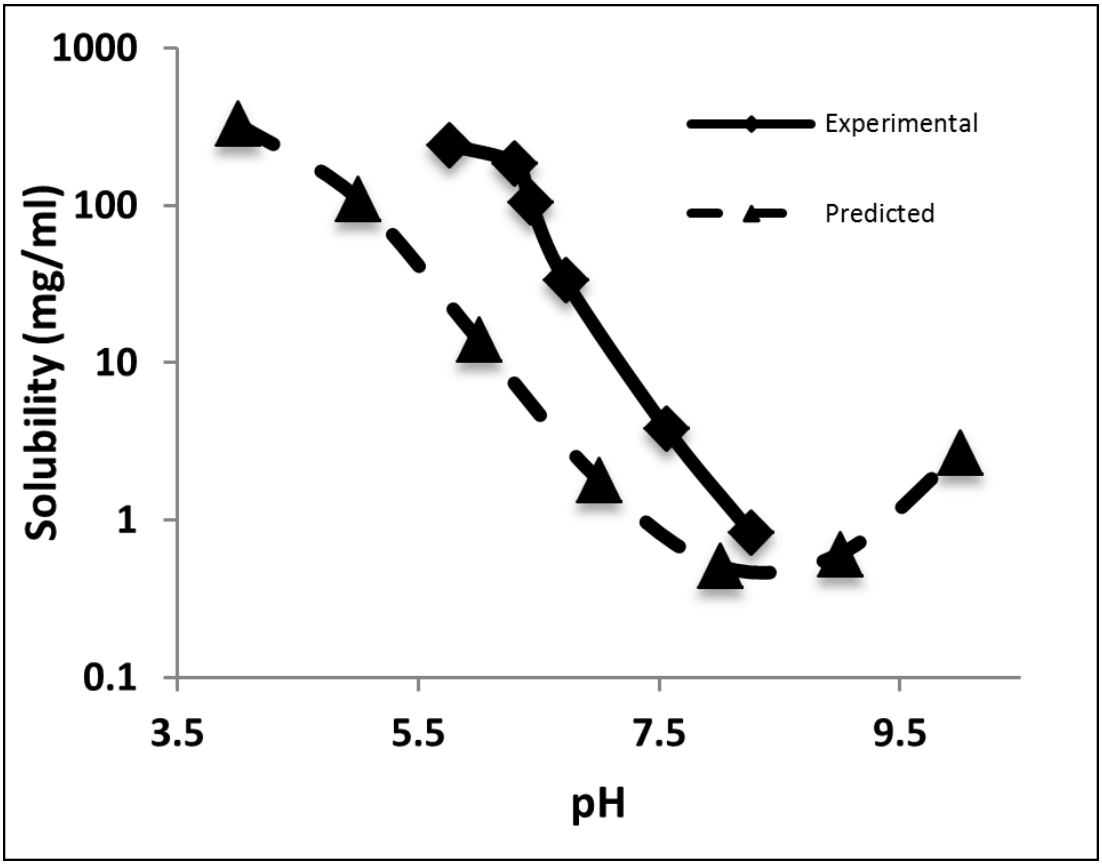

Figure 5.2 Solubility of NTX base in citrate buffer (0.3M) at 6 different values at 32°C. The dashed line represents the predicted values from Scifinder® in the pH range of 4-10 at 25°C. (n=3 for solubility determinations)

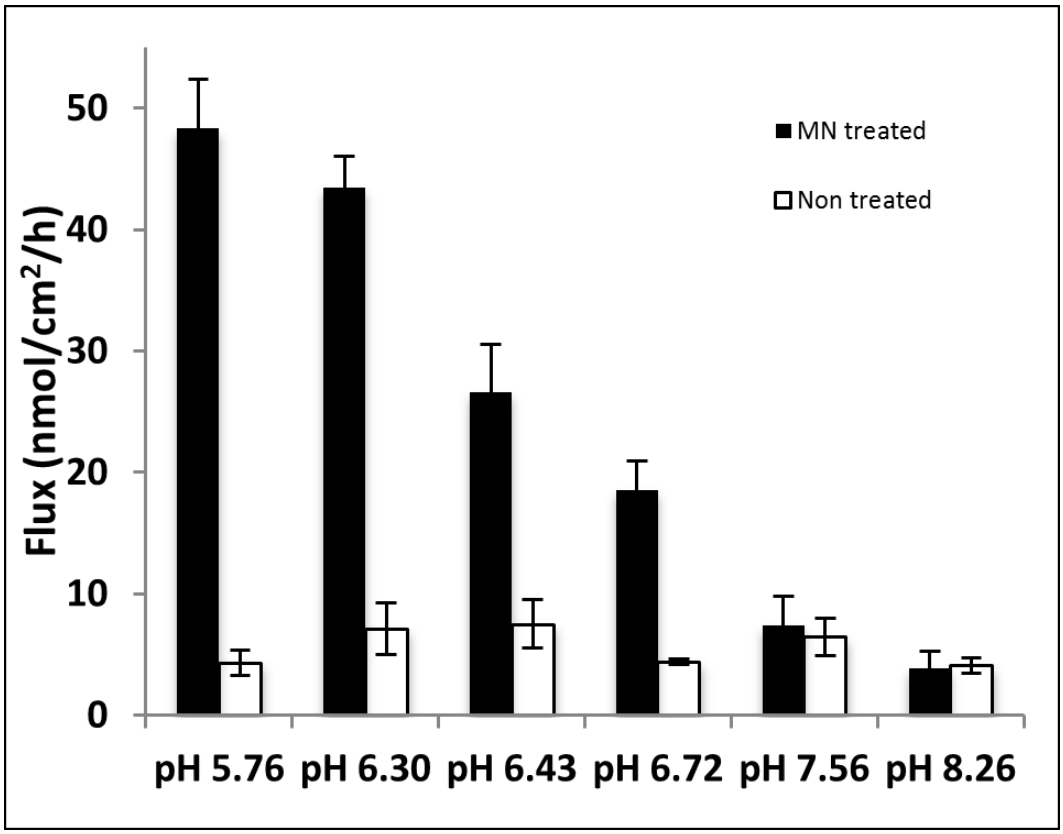

Figure 5.3NTX flux across MN treated and non-treated pig skin from 6 different formulations (n=3-4). MN treated flux was significantly higher compared to non-treated skin for pH 5.76, pH 6.3, pH 6.43 and pH 6.72 ($p<0.05$)

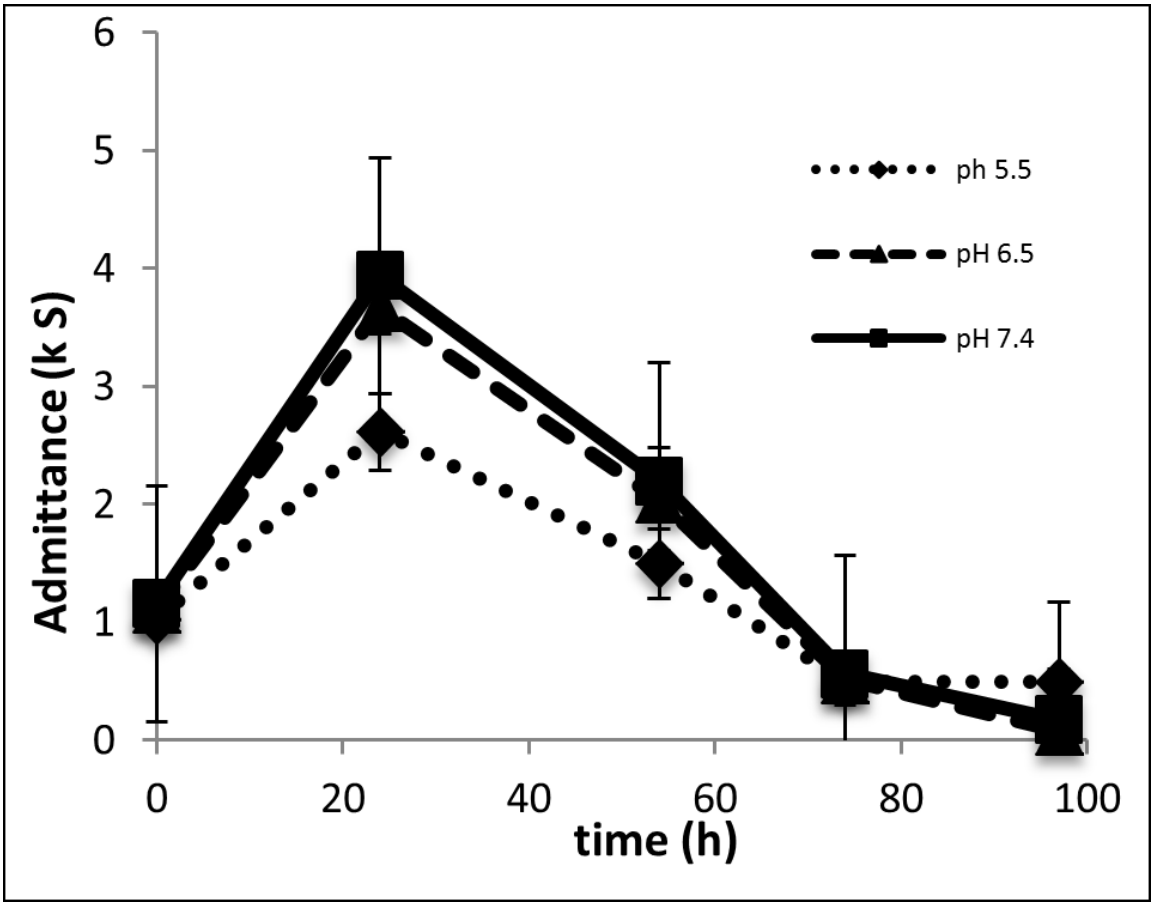

Figure 5.4 Admittance values vs. time for 3 different pH values. Admittance values were not significantly different from each other between the formulations ($p>0.05$) except for the 24h time point (pH 5.5 and pH 7.4; pH 5.5 and pH 6.5 $p<0.05$)

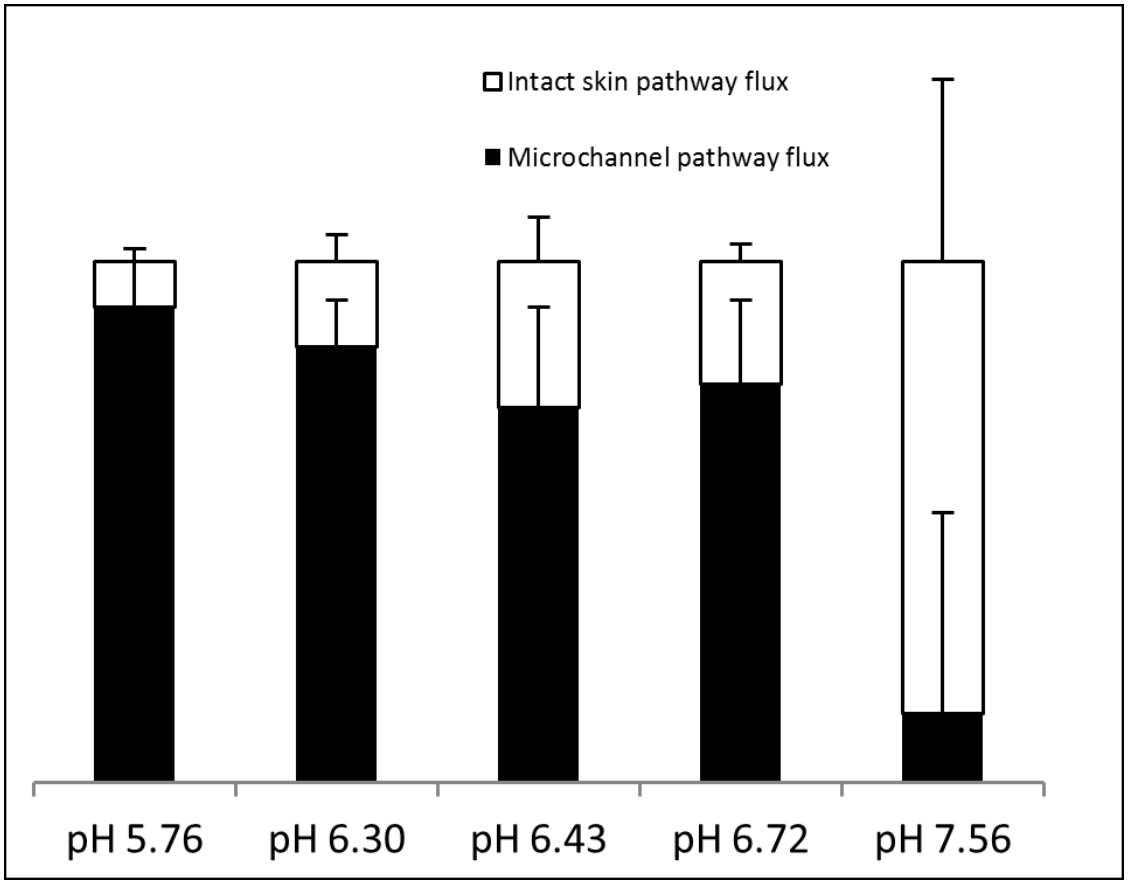

Figure 5.5 Relative contributions of microchannel pathway and intact skin pathway towards total flux from 5 different formulations

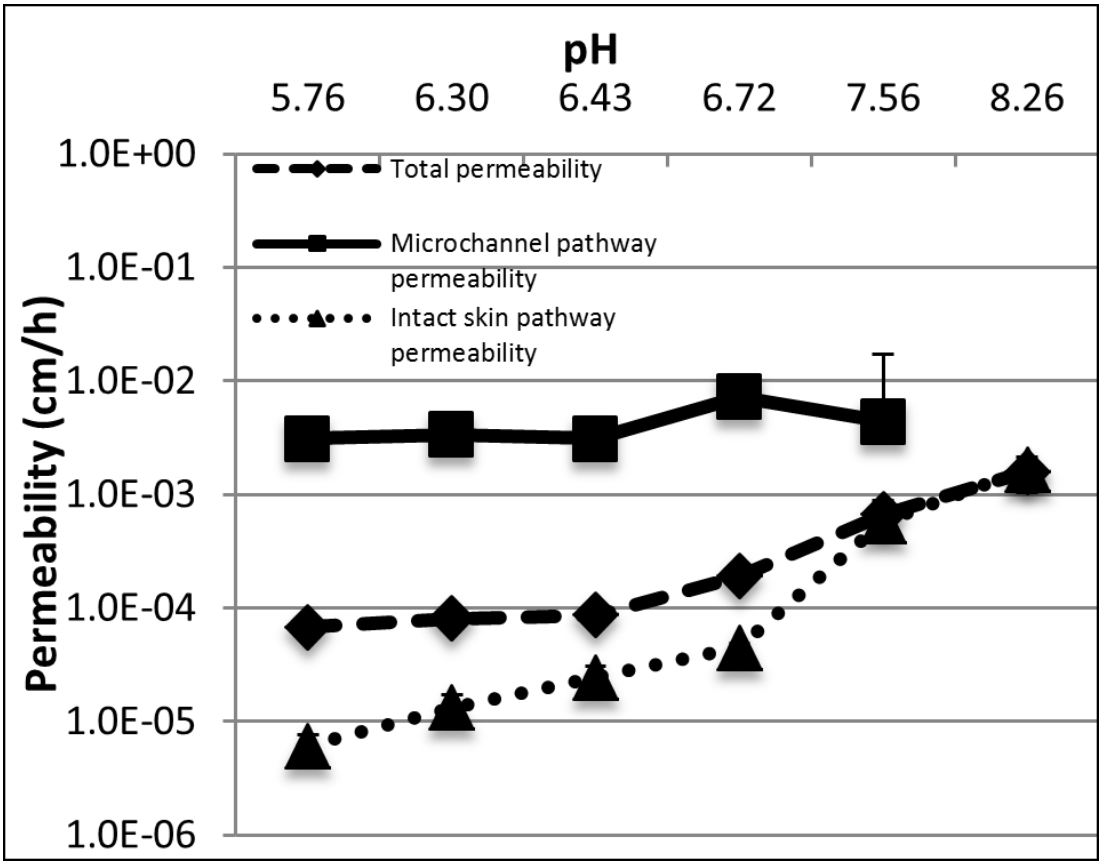

Figure 5.6 Calculated permeability of NTX across microchannel pathway and intact skin pathway from experimental data

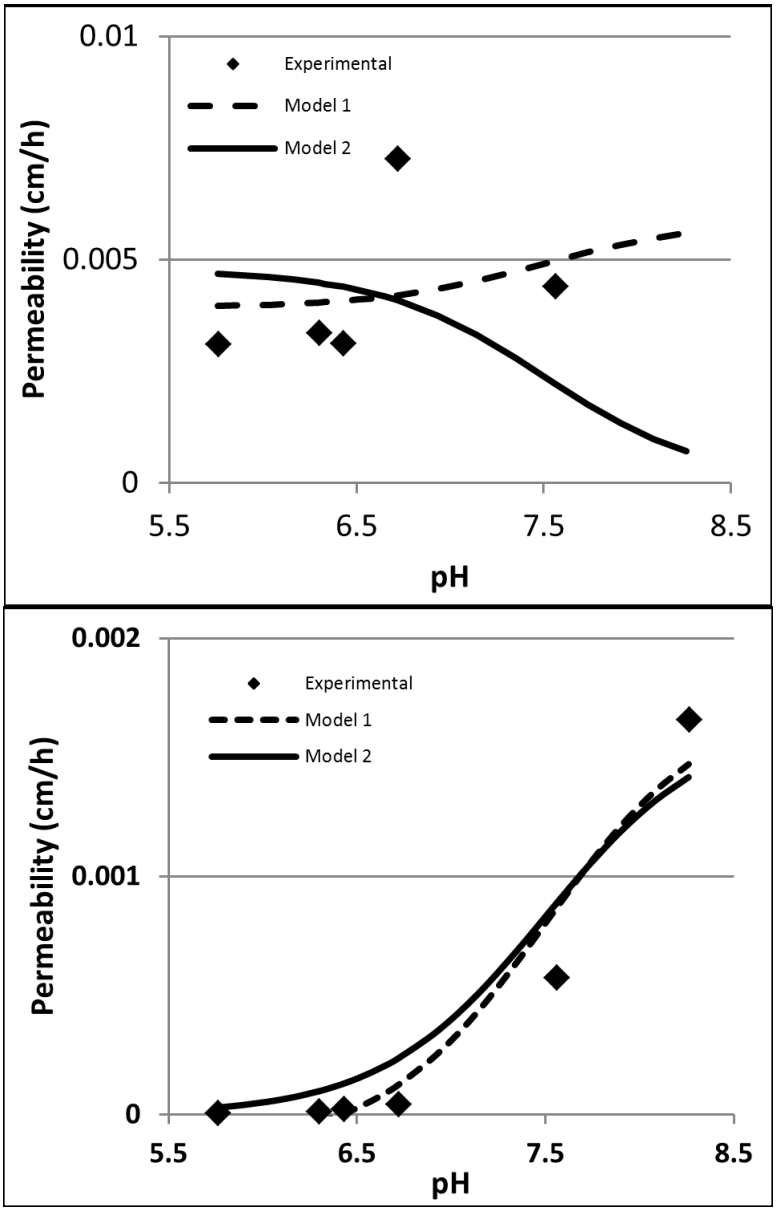

Figure 5.7 Permeability estimation of NTX species through the microchannel pathway (a) and intact skin pathway (b). The dashed line is the calculated value of permeability based on Model 1. The solid line is calculated permeability based on Model 2. The points are the experimental parameters. Model selection criteria's for model 1 and model 2 respectively, MN treated skin -0.74 and -0.88, intact skin 2.05 and 2.00

Chapter 6

Development of a codrug approach for sustained drug delivery across microneedle-treated skin

6.1 Introduction

The contents of this chapter have been published in Journal of Pharmaceutical Sciences. [147] Transdermal drug delivery is a potential alternative route for a host of drug molecules that are difficult to deliver via the oral or parenteral route. It avoids first pass effects, hepatotoxicity, gastric irritation issues, as well as needle phobia. However, only small, lipophilic molecules can be delivered by passive diffusion alone across the stratum corneum (SC), the main barrier to transdermal drug delivery. Hence, physical and chemical enhancement techniques are used to enhance the variety of molecules that can be delivered via this route. Physical enhancement techniques include iontophoresis, electroporation, low frequency ultrasound, and microneedle (MN) enhanced delivery. Chemical enhancement techniques include chemical enhancers and the prodrug/codrug approach. [2, 27] A codrug or a mutual prodrug is a new chemical entity formed when two pharmacologically active molecules are linked together via a covalent linkage. The structural modification is usually utilized to enhance drug delivery properties like stability, solubility or permeability of one or both drugs. [23] In this study MN enhanced delivery was combined with a codrug approach to develop a seven day sustained release patch system. MN delivery is a minimally invasive physical enhancement technique. The pain-free method used in this research was the “poke (press) and patch” approach [42] where solid stainless steel MN arrays are used to create micropores (also referred to as microchannels) across the SC. The MN array is then removed and a matrix/reservoir type patch is applied to deliver drugs through the micropores. Pain associated with the application of these MNs is negligible when compared to a hypodermic needle, [60, 64]

which could potentially lead to better patient compliance, one of the major drawbacks of addiction therapy. [131] Naltrexone (NTX), the model compound (M.W of 341.41, log P of 2.0), is one of the leading FDA-approved pharmacotherapies for alcohol addiction. It is a μ-opioid receptor antagonist and is known to decrease alcohol craving in recovering addicts. [153] The drug exerts its mechanism of action by attenuating the ethanol induced stimulation of the mesolimbic-dopaminergic pathway. [123], [154] Currently, NTX is marketed as a 50-100 mg once daily oral formulation, ReVia® (Naltrexone Hydrochloride). The oral therapy has compliance issues in addicts. [129, 155] It also has an oral bioavaibility ranging from 5-40% and is associated with side effects like hepatotoxicity, nausea, and vomiting [145]. The intramuscular injectable 28 day controlled release formulation of NTX; Vivitrol™ was approved by the FDA in 2006. Injection site reactions and difficulty of depot removal in case of emergency opiate treatment, in addition to the aforementioned issues are some of the major drawbacks of this dosage form. [17, 156] 6-β naltrexol is the major metabolite of NTX in humans and has a longer half-life of 13 hours in plasma compared to that of 4 hours for NTX. It has been shown to be an effective therapy for alcohol abuse as well. [128] Recent clinical data suggests that NTX might be a treatment option for smoking cessation as well as amphetamine and methamphetamine abuse. [133]

NTX cannot be delivered in relevant therapeutic concentrations transdermally by passive diffusion alone. Some of the earlier efforts in this area of research have looked at delivery of NTX via the prodrug and codrug approach. The results indicated that although significant flux enhancement was achieved in some cases, it was not enough to deliver the molecule in therapeutically relevant concentrations. [83, 84, 86] Using MN it has been shown both *in vitro* as well as in humans *in vivo* that NTX can be delivered at the lower end of the therapeutic plasma level range of 2 ng/ml. [4, 15, 54] However, one of the issues with this approach is that the micropores begin to close between 48-72 hour under occlusion. [4, 10, 12] When exposed to air following one time application of the MN the

micropores heal within a 30 minute timeframe. Therefore, in order to develop a 7 day patch system, pore lifetime enhancement techniques need to be employed along with MN for successful therapy.

Different techniques can be used to delay barrier recovery after MN treatment. The skin is a self-regulating organ and employs different methods for recovery after insult. Cutaneous wound healing itself consists of multiple phases, inflammatory response being the first step. Increased synthesis and secretion of lamellar body contents and transformation into bilayers are also a part of the recovery process. [92, 113, 157] Occlusion alone can also delay the recovery process by decreasing the water flux across the barrier, one of the major signals for recovery of structure and function. [94]

There are several literature reports indicating the increase in expression of both COX-1 and COX-2 following damage to the skin and the role of both enzymes in cutaneous repair. [104, 107-109] Diclofenac (DIC) is a potent non-steroidal anti-inflammatory drug (NSAID) that nonselectively inhibits both COX-1 and COX-2 thereby preventing formation of downstream products like prostaglandins and thromboxane, thus decreasing inflammation. [158] It is currently available on the market as an oral as well as a topical formulation, and is the first choice of NSAID for this project. Previous experiments showed that daily application of Solaraze gel® (3% diclofenac sodium, 2.5% hyaluronic acid) after one time application of MN was able to allow delivery of NTX over the seven day time period in hairless guinea pigs (HGP).[8] Daily application is irrational for a proposed 7-day patch system and coformulating the drugs at high concentration at a pH optimum of 5 (pH of the outer layer of the skin is 4.5-5.5) [20] is difficult because the drugs have different physicochemical properties. Naltrexone is positively charged at pH 5 since the most acidic pKa associated with the amine group is 7.5. Diclofenac on the other hand is neutral or negatively charged with a pKa of 4.2 associated with the carboxylic acid group. Solubilities of both compounds are also different by orders of magnitude in the pH

5 range as shown in Figure 6.1. These incompatibilities lead to the codrug approach. Combining the two molecules via a covalent linkage helps in formulating them together in a single formulation. Separate application of the two pharmacologically active components leads to precipitation of diclofenac on top of the skin and affects the flux of naltrexone across MN treated skin significantly. The 3-O-ester-codrug (Figure 6.2) contains a biolabile ester linkage that can be cleaved by hydrolytic enzymes (e.g. esterase) as soon as it reaches the viable epidermal region of the skin; in order to release the parent compounds. [32, 82, 159] Once in the skin the more lipophilic DIC will act locally to keep the pores open while NTX is delivered systemically. The overall objective of this research is to show that the codrug approach can be used to reduce the inflammatory response in combination with occlusion for delayed barrier recovery following MN treatment, so that the ultimate goal of a seven day patch system can be achieved. The study was carried out to evaluate research goal 3.3. The codrug was synthesized by Dr. Raghotham Reddy Pinninti from Dr. Audra Stinchcomb's laboratory at the University of Kentucky.

6.2 Materials and methods

6.2.1 Chemicals

Naltrexone HCl was purchased from Mallinckrodt (St. Louis, MO), diclofenac acid from AK Scientific, Inc. (Mountain View, CA) and diclofenac sodium salt from TCI America (Portland, OR). Water was purified using a NANOpure DIamond^{TM}, Barnstead water filtration system. Hanks' balanced salts modified powder; propylene glycol and ethanol (200 proof) were purchased from Sigma (St. Louis, MO). 4-(2-Hydroxyethyl)-1-piperazineethanesulfonic acid (HEPES), sodium bicarbonate, sodium acetate, acetic acid and gentamicin sulfate were obtained from Fisher Scientific (Fair Lawn, NJ). 1-Octanesulfonate, sodium salt was obtained from Regis Technologies, Inc (Morton Grove,

IL). Trifluroacetic acid (TFA), triethylamine (TEA) and acetonitrile (ACN) were obtained from EMD chemicals (Gibbstown, NJ). Natrosol® (hydroxyethlycellulose) was obtained from Hercules. Chemicals for codrug synthesis were purchased from Alfa Aessar (Ward Hill, MA)

6.2.2 Synthetic procedure for codrug

The synthesis of naltrexone-diclofenac codrug in the current study was carried out by Raghotham Reddy Pinninti from Dr. Audra Stinchcomb's lab group. Diclofenac sodium salt was dissolved in a 1:1 (ethyl acetate: water) mixture and acidified with concentrated hydrochloric acid. The organic layer was separated and the aqueous layer was treated with ethyl acetate twice. The combined organic layer was dried on anhydrous sodium sulfate and rotary evaporated to remove reaction solvents. Diclofenac free acid was activated with DCC (N, N'-Dicyclohexyl carbodiimide) and DMAP (4-Dimethylaminopyridine) in anhydrous tetrahydrofuran. After two hours, an equivalent amount of NTX was added in dry tetrahydrofuran. Combined reactants were allowed to stir over night under nitrogen atmosphere. After completion of the reaction, solvents were removed under reduced pressure and the reaction crude mixture purified by flash silica gel column chromatography eluting with 80% ethyl acetate and 20% cyclohexane. The codrug was obtained in **56%** yield. The codrug was dissolved in 1, 4-dioxane and an equimolar amount of 2M hydrochloric acid in dioxane was added and refluxed for 1.5 hours, and precipitated with hexanes to get the hydrochloride salt of the codrug.

6.2.3 Quantitative analysis

NTX, DIC and the codrug concentrations in all samples were quantified using a high pressure liquid chromatography (HPLC) assay, which is a modified version of the previously reported NTX assay. [22] The HPLC system consisted of a Waters 717 plus auto-sampler, a Waters 600 quaternary pump, and a Waters 2487 dual wavelength

absorbance detector with Waters Empower™ software. A Perkin Elmer Brownlee™ Spheri 5 VL C18 column (5 µ, 220 x 4.6 mm) and a C18 guard column (15 x 3.2 mm) were used with the UV detector set at a wavelength of 280 nm. The mobile phase consisted of 70:30 (v/v) ACN: (0.1% TFA with 0.065% 1-octane sulfonic acid sodium salt, adjusted to pH 3.0 with TEA aqueous phase). Samples were run at a flow rate of 1.5 ml/min with a run time of 8.5 min. The injection volume used was 25µl for receiver samples and 100µl for the skin disposition samples. For the plasma samples the mobile phase consisted of 50:50 (v/v) ACN: (0.1% TFA with 0.065% 1-octane sulfonic acid sodium salt, adjusted to pH 3.0 with TEA aqueous phase). Samples were run at a flow rate of 1.0 ml/min with a run time of 37 minutes and injection volume of 25 µl.

6.2.4 Chemical and enzymatic stability

Chemical and enzymatic stability was determined for the codrugs. For chemical stability studies, the codrug was put in prewarmed 0.3M acetate buffer (pH 5.0) after solubilization in <5% ACN, if required, at 32ºC in an incubator. Samples were withdrawn at regular intervals and injected into the HPLC after appropriate dilutions. Enzymatic stability studies are important for estimation of conversion of codrugs in the plasma. For plasma stability studies prewarmed HGP plasma at 37°C was spiked with codrug solution and samples were withdrawn at regular intervals. One-hundred µl of plasma sample was extracted with 1ml of 1:1 ACN: ethyl acetate, vortexed, and then centrifuged at 10,000 X g for 20 minutes on a bench top Eppendorf Mini Spin®. The supernatant was decanted into a glass test tube and evaporated to dryness under nitrogen. Samples were reconstituted in 100µl ACN and injected onto the HPLC. All stability data was analyzed using pseudo-first order kinetics ($r^2 \geq 0.99$). All stability studies were carried out in triplicate, at a minimum.

6.2.5 *In vitro* diffusion studies

The *in vitro* permeation experiments were carried out to determine the transdermal flux of the parent drugs and the codrug, the permeability coefficients, as well as the concentration of the drug molecules in the skin at the end of the study. For all *in vitro* experiments Yucatan miniature pig (YP) skin was used. YP skin is one of the most relevant models for transdermal studies due to physiological, morphological and biochemical similarities with the human skin.[160] Full thickness skin was obtained by removing the subcutaneous fatty tissue by scalpel dissection, and stored at -20°C. All pig tissue harvesting experiments were done under IACUC approved protocols at the University of Kentucky. A PermeGear flow-through (In-Line, Hellertown, PA,) diffusion cell system was used for the skin permeation studies. Skin for MN treatment was placed on a wafer of polydimethylsiloxane polymer, which mimics the underlying mechanical support of tissue because of its comparable structural flexibility and elasticity. The skin was pierced 20 times with a 5 MN in-plane stainless steel array (each needle being 750µm long, 200µm wide, 75µm thick and the distance between two needles 1.35mm), making a total of 100 individual and non-overlapping piercings before mounting the skin in the diffusion cell. The needles were manufactured by Dr. Mark Prausnitz's lab group at the Georgia Institute of Technology. MN pores were distributed evenly within the 0.95cm^2 area of skin. Untreated skin samples were mounted directly onto the diffusion cells. The setup was maintained at 32°C using a circulating water bath. Data was collected using a minimum of 3-4 cells per treatment group. The receiver solution was water adjusted to pH 7.4 containing 20% ethanol at 37ºC. Gentamicin sulfate (50mg/L) was also added to the receiver for 7 day studies as an antimicrobial agent. The receiver flow rate was adjusted to 1.5ml/h to maintain sink conditions. Each cell was charged with 0.25 ml of the donor solution and the diffusion cells were covered with a stopper to prevent evaporation of formulation. Samples were collected at regular increments over 48 hours or for the length

of the treatment. Drug was concentrated 10 fold by evaporating 1ml of the collected receiver sample under nitrogen and reconstituting in 100 µl of ACN for quantification. All samples were stored at 4°C until analyzed by HPLC. The skin was removed at the end of the study and the treatment area was minced into small pieces using a scalpel after removing all excess drug formulation from the surface of the skin. Drug was extracted from the samples by immersing the skin pieces in ACN overnight in a shaker water bath at 32°C. Samples were injected into the HPLC after appropriate dilution for quantitative analysis. The donor was also removed and quantified at the end of the study by direct injection onto the HPLC after suitable dilution using ACN. All data was analyzed using Fick's first law of diffusion. $J_{ss}=P*\Delta C$ where J_{ss} is the steady state flux, P is the permeability coefficient and ΔC is the concentration difference between the donor and the receiver. Since the receiver is maintained at sink conditions ΔC is essentially the concentration of the donor. Steady state flux is obtained from the linear portion of the plot of cumulative amount permeated over time.

6.2.6 *In vivo* studies

Fabrication of transdermal patches

The transdermal patches were fabricated by sandwiching a buna nitrile rubber ring barrier to create a reservoir between the skin and the impermeable backing membrane (Scotchpak™ #1109 SPAK 1.34 MIL Heat Sealable Polyester Film). This was done to prevent evaporation of formulation and maintain occlusion of treated sites over the period of treatment. 3M™ double sided tape was used on either side of the spacer to attach the backing on one side and to maintain contact with the skin on the other side.

Dose preparation and application

All animal experiments were approved by the University of Kentucky IACUC. A proof of concept *in vivo* experiment was carried out using 4 % w/w gels of the hydrochloride salt form of the codrug. Gels were formulated by dissolving 4% codrug salt in PG: buffer at pH 5.0(10:90) and 3.0% hydroxyethylcellulose (HEC) polymer (to have a viscous gel formulation). Polymer was dissolved over a 30 minute period to obtain a homogenous gel. The solution was stirred until a viscous gel resulted and then left at room temperature for about 2 hours to remove bubbles and ensure completion of reaction. . The gel was saturated with excess drug solid and therefore was cloudy. MN treated animals were first cleaned topically with isopropyl alcohol, and a 50 MN array was applied twice mutually perpendicular to each other to give a total of 100 pores at each site. Gel doses (0.3 ml) were applied to the dorsal region of the HGP. Bioclusive dressing (Systagenix Wound Management, Quincy, MA) was applied to hold the patch in place and prevent evaporation of the formulation. The patch was re-applied using new formulation at 3.5 days such that more than 54% of intact codrug was always present in formulation. A control experiment was also carried out to look at the effect of NTX HCl alone in the same vehicle on pore closure kinetics. A 9% solution of NTX HCl was used to prepare a 3% HEC gel and all other methods of application were consistent with the codrug gel.

Staining

The patches were removed at predetermined time points and the site was cleaned with sterile gauze. Gentian violet/ India ink was applied as the dye at the MN treated sites and allowed to dry before excess was removed with ethanol and gauze. Both the dyes stain the viable epidermis but not the intact SC. Hence, a grid is observed only in the presence of micropores in the skin, no staining is observed in its absence.

6.2.7 Statistical analysis

Data for all experiments are reported as mean ± standard deviation. Statistical analysis of data was carried out with Students' t-test and one way ANOVA with post hoc Tukey's pairwise tests, if required, using GraphPad Prism® software, version 5.04 software. $P<0.05$ was considered to be statistically significant.

6.3 Results and Discussion

6.3.1 Synthesis

The codrug and its hydrochloride salt were synthesized successfully. The structures were verified using ^{1}HNMR, ^{13}CNMR and HRMS

Codrug

^{1}HNMR ($CDCl_3$, 300 MHz): δ 7.29(m, 2H), 7.19(t, 1H), 6.93(m, 2H), 6.75(d, 1H), 6.60(d, 2H), 6.57(d, 1H), 4. 78(s, 1H), 3.67(s, 2H), 3.12(m, 2H), 2.79(m, 1H), 2.32(t, 2H), 2.27 (m, 2H), 2.05 (m, 2H), 1.69(m, 2H), 1.62, (m, 2H), 0.46(m, 1H), 0.31(m, 2H), 0.30 (m, 2H)

^{13}CNMR($CDCl_3$,(300 MHz): δ 4.22, 4.41, 9.77, 23.31, 31.09, 31.59, 36.45, 38.50, 43.75, 51.01, 59.48, 62.15, 70.28, 90.93, 118.75, 119.52, 122.45, 123.05, 124.19, 124.31, 128.30, 128.97, 129.73, 130.38, 130.64, 131.31, 132.63, 138.09, 142.92, 147.77, 169.98, 207.67

HRMS: Calculated for $C_{34}H_{32}O_5N_2Cl_2$ 618.1688 and found 618.1697

Hydrochloride salt of codrug

^{1}HNMR ($CDCl_3$, 300 MHz): δ9.98 (bs,NH^+) 7.33(m, 2H), 7.13(t, 1H), 6.99(m, 3H), 6.61(d, 1H), 6.57(d, 1H), 4.97(s, 1H), 4.73(s, 1H), 4.10(s, 2H), 3.60(m, 2H), 3.14(m, 4H), 2.92(m, 1H), 2.65(m, 2H), 2.41(d,1H), 1.82(m, 3H), 1.25(m, 2H), 0.84(m, 4H), 0.62(m, 1H)

6.3.2 HPLC method development

HPLC assay development for the parent drugs and the codrug was the first step towards quantification of the data. The retention time of NTX was 2.3 minutes, DIC was 3.5 minutes and codrug was 6.5 minutes. The retention times for the same compounds in plasma samples were 3.3 minutes, 16.0 minutes and 33.0 minutes, respectively. All retention times reported are value ± 0.1 minute. Samples were analyzed within the linear range of the standard curve for all the three compounds from 100 – 10,000ng/mL. The standard solutions exhibited excellent linearity over the entire concentration range employed in the assays, r^2 >=0.99.

6.3.3 Stability studies

Prodrugs and codrugs are traditionally used to enhance solubility, stability or permeability of parent drug molecules. Naltrexone and diclofenac have a physicochemical incompatibility when co-formulated; therefore the codrug approach was employed to enable them to coexist in a single formulation. Bioconversion of these new chemical entities (NCE) to the parent drugs is essential for pharmacological effect. Thus one of the most important steps in development of prodrug/codrug molecules is looking at stability. Formulation stability of prodrugs/codrugs is used to estimate the conversion in the donor medium. The most common mechanism in an aqueous medium is either acid or base catalyzed ester hydrolysis. The enzymatic stability in a biological medium measures the effect of enzymes in addition to the chemical degradation to indicate how fast the parent molecules will be regenerated inside the body. The chemical and enzymatic stability data indicated that the chemical half-life of the codrug in the pH 5.0 buffer was 3.9 ± 0.56 days and the enzymatic half-life in the HGP plasma was 6.4 ± 0.84 minutes. In both studies regeneration of the parent drugs was observed with the degradation of the codrug. The chemical stability indicates that the codrug is not stable

enough in an aqueous formulation for the development of a 7-day transdermal drug delivery system. However, it could still be utilized as a learning tool for understanding permeability, bioconversion of the codrug in the epidermal region of the skin, as well as for proof of concept that the codrug methodology could work to enhance the drug delivery window following one time application of the MN. The plasma stability study indicates that even if intact codrug permeates the skin and reaches the systemic circulation; it would cleave back to the parent drugs almost immediately, thus contributing to the NTX flux. The systemic concentration of DIC should not be of concern since it would be orders of magnitude lower compared to therapeutically relevant systemic doses. The lowest systemic dose of DIC sodium is 50mg twice daily and the oral bioavaibility is 0.55. [16] Therefore, the daily systemic dose is 55mg/day. From a 25cm^2 patch, the flux required to reach the systemic dose will be 288nmol/cm^2/h.

6.3.4 *In vitro* experiments

In vitro permeation experiments were carried out to estimate permeability of the codrug, as well as to examine the rate of delivery and the extent of the parent compound regeneration in the skin. The goal of the first set of *in vitro* experiments was to estimate flux and skin concentration of the base form of the codrug. A 4.5 mg/ml saturated donor solution consisting of codrug in propylene glycol (PG): ethanol: water (43:43:14) was used. Four treatment groups each having 3 diffusion cells (MN treated) were dosed and then cells were removed every 12 hours to obtain the skin concentration of the parent drugs as well as the codrug. An intact skin control was also present for the entire length of the study (48 hours). A steady state flux from NTX and DIC of 0.42 ± 0.12 nmol/ (cm^2/h) and 0.19 ± 0.06 nmol/ (cm^2/h), respectively, was obtained (Figure 6.3). The flux of NTX was significantly higher compared to the flux of DIC ($p<0.05$). The skin concentration data shows that the codrug degraded in the skin to regenerate back to the parent drugs

and the concentration of parent drugs from the codrug increased with time. It also showed that the DIC concentration increased in the skin with time and was higher compared to the NTX concentration at 48 hours. Thus from the results it can be concluded that the codrug cleaved, and NTX flux was obtained from the base form of the codrug, although it was not high enough to produce therapeutic efficacy. Significantly, a higher amount of NTX was found in the receiver while DIC was retained in the skin in higher concentration at 48 hours from this formulation. This difference in flux and skin concentration could be attributed to the difference in physicochemical properties of the drug molecules. While NTX (pKa 7.5, 9.2) is positively charged at the skin surface pH of 5, [20, 19] at least 80% of DIC (pKa 4.2) is negatively charged. The skin is known to possess a net negative charge due to the presence of negatively charged free carboxylic acid groups, which might be responsible for slower migration and higher retention of DIC molecules in the skin compared to NTX. Different rates of migration for positively and negatively charged molecules have been previously observed in the case of active transdermal drug delivery systems utilizing iontophoretic delivery, [161] indicating that similar results could be expected in the current system. The hydrophobicity or log P values of the parent molecules could also have an effect on the rates of migration. NTX having a log P value of 2.0 (optimum log P for transdermal delivery is around 2) should permeate much faster through the different layers of the skin compared to DIC with a log P of 4.5, which will have a tendency to form a depot in the SC layer instead . The hypothesis behind the project is based on the fact that DIC would act locally to enhance the drug delivery window while NTX will have a systemic effect. The characteristics of the molecules listed above would thus be beneficial for the development of a seven day system.

The first set of experiments confirmed bioconversion, but further flux enhancement was required before the codrug could be tested *in vivo* for pore closure kinetics. From the literature it is known that a charged molecular species has higher flux through MN treated skin as compared to a non-treated control. This property is attributed to the enhanced solubility of a charged species in an aqueous donor rather than the molecular species itself. [54] Viscosity of the donor formulation also has a predominant effect on the flux across MN treated skin, where it has been shown that 17-fold flux enhancement was obtained using a low viscosity, aqueous donor compared to a high viscosity propylene glycol (PG) rich donor (concentrations for all donor solutions were maintained at 110mg/ml). On the other hand, there was no significant difference in flux between the low viscosity aqueous donor and the high viscosity PG rich donor across untreated skin. Thus it was concluded that donor solution microviscosity has an effect on transport across MN treated skin. [22] Hence the hydrochloride salt form of the codrug was tested for higher solubility and flux in aqueous donor for subsequent experiments. The hydrochloride salt of the codrug (Mol. Wt. 654.15) was used as the donor solution with a concentration of 39.3mg/ml in 0.3M acetate buffer at pH 5.0. The flux of NTX from the codrug salt was 5.42 ± 1.5 nmol/(cm^2/h). A 13-fold flux enhancement was obtained by using the salt form over the free base form ($p<0.005$), which can be attributed to the solubility enhancement of the salt form in an aqueous donor.

Precipitation issues were observed with purely aqueous donor during *in vitro* experiments with the hydrochloride salt form of the drug, so further experiments were carried out for formulation development by varying the amount of PG in the donor formulation. The different concentrations of PG used were 10%, 25% and 50 % with the salt form of the codrug and it was observed that while there was no significant difference in flux between the aqueous formulation and 10% PG containing formulation ($p<0.05$),

flux decreased significantly for higher concentrations of PG (Figure 6.4). All experiments were carried out with saturated donor solutions. The data was compared using one way ANOVA with Tukey's posthoc analysis for pairwise multiple comparisons. From these results, the 10% PG containing formulation was chosen for *in vivo* studies since there was no significant difference in flux and precipitation issues were much lower.

6.3.5 *In vivo* studies

The *in vitro* studies confirmed permeation and bioconversion, but *in vivo* studies were required to elucidate pore closure kinetics. The HGP is the best small animal model for transdermal drug delivery. [162] Pore visualization studies were conducted to look at the presence/absence of pores under occlusion after one time application of MN. The pores can be clearly visualized with gentian violet in Figure 6.5 (A) immediately following MN treatment. In panel (B) the pores cannot be visualized at day 4 (96 h) following treatment with MN followed by application of NTX HCl gel under occlusion. This is in agreement with previously reported data in pharmacokinetic studies where it has been shown that the micropores close anywhere between a 48-72 h timeline following MN treatment under occlusion, in the absence of additional pharmacological moieties for pore lifetime enhancement. [4, 8] Pores can be visualized by India ink staining in panel 5 (C) where the hydrochloride salt form of the codrug was used following MN treatment indicating that the pores can stay open up to 7 days. Therefore, it can be concluded from the studies that the codrug is effective in keeping the pores open analogous to our hypothesis. Once the patches are removed, on exposure to air the micropores would heal within a 15-30 minute timeframe so that post-treatment infection issues are not a major concern with the codrug-MN approach.

From these studies, it can be concluded that the codrug cleaved back to parent drugs both in stability studies, as well as during *in vitro* studies. The salt form of the

codrug improved solubility and flux significantly in *in vitro* studies. Subsequent *in vivo* studies with the salt form in an optimized 10% PG containing formulation kept the pores open for a 7 day target drug delivery window, but the steady state plasma concentration of NTX from the codrug was not high enough to quantify in the HGP model. This could be predicted from the clearance estimation from previous pharmacokinetic studies with NTX in the same animal model based on the size of the treatment area since,

$$Jss * A = Css * Cl$$

Where J_{ss} is the steady state flux, A is the active treatment area, C_{ss} is the steady state plasma concentration and Cl is the clearance of the compound in a HGP model.

In this case with 4 patches, A was 1.8cm^2 for each patch (total of 7.2cm^2 for 4 patches, 400 MN treatments, J_{ss} was 6.35 nmol/cm^2/h (0.95cm^2,100 MN treatments) from the *in vitro* studies and Cl is 5.6 L/h, [148] which translates to a C_{ss} of 1.5 ng/ml based on number of MN treatments. The LLOQ on the LC/MS assay was 1ng/ml. Hence reliable pharmacokinetic data could not be obtained from this codrug. Physicochemical optimization is required to obtain a molecule that would have higher stability and permeability in a range that can be clinically applicable, thus making the codrug approach applicable for pore lifetime enhancement and delivery. NTX has been used in this research as a model compound; further optimization of these codrugs will help in development of 7 day transdermal systems for a host of other molecules that can potentially benefit from once a week transdermal dosing.

Future codrug designs will explore a variety of different linking groups of diverse susceptibility to hydrolysis including carboxylate ester, carbamate ester and carbonate ester. From previous data, it is known that all the aforementioned linkers are bioconverted in the skin and that the rate of bioconversion depends on the structure of the molecule and type of linker used. A nontoxic extended linker moiety will be used in between, if

required (e.g. polyethylene glycol, alkyl chain). The polyethylene glycol can enhance solubility due to the presence of additional groups with hydrogen bonding capabilities. The alkyl chain can be used to enhance stability of prodrug/codrug molecules due to electron donating effects. [21,146] Different salt forms of the codrug can also be used to enhance solubility as shown in the case of NTX. [139] Different positions on the NTX molecule will also be explored to look at the 6-O secondary alcohol position in comparison to the 3-O phenolic position. Formulation stability could also be enhanced by adding PG to the formulation, since the main mechanism of degradation in formulation is chemical hydrolysis. However, the viscosity will need to be monitored to balance between formulation stability and effect of viscosity on transport across MN pores. Quantitative stability studies based on structures using all of the above would help in identification of a candidate that can be developed as a 7 day drug delivery system.

Flux enhancement parameters, like the ionization form of the drug for solubility enhancement and lower viscosity formulations would be utilized to develop a quantitative structure permeability relationship (QSPR) for compounds that are suitable from a stability standpoint for development of the 7 day system. The theoretical flux range required for NTX to achieve therapeutically relevant concentrations in humans is 12-90nmol/ (cm^2/h) from a 25cm^2 patch, based on the standard oral NTX dosing regimen. Comparisons of the codrug salt formulation with that from the human pharmacokinetic study [4] carried out previously across YP skin showed that there was no significant difference in flux between the two formulations ($p>0.05$). However, this flux is much lower compared to the most optimized low viscosity NTX HCl formulation currently used as a prototype (Figure 6.6). Thus the above flux optimization techniques will be employed to reach the final drug delivery goal of a 2 ng/ml plasma concentration in humans.

The development of QSPR with NTX and DIC as model compounds will help in future development of codrugs for MN enhanced transdermal delivery. Depending on the local concentration and permeability, DIC could be substituted with a host of other NSAIDS. NTX can be replaced with a series of drug molecules that could potentially benefit from 7-day transdermal drug delivery. From a structural standpoint, any drug molecule can be used provided they have an accessible –OH group since all the linkages proposed for this research, carboxylate, carbamate and carbonate require a functional –OH or –COOH group for bond formation.

6.4 Conclusions

In conclusion, the possibility of utilizing NTX DIC codrugs for systemic delivery of NTX across MN treated skin was explored. The DIC is used as an active pharmacological moiety to enhance the drug delivery window. The results indicated that the codrug approach can be used for the development of a seven day transdermal system. Drug products with two actives are routinely approved by the US FDA, thus this project is not limited from a regulatory perspective. The 3-O-ester codrug used in the current study bioconverted back to the parent drugs in the skin and the local concentration of DIC regenerated was high enough to keep the pores open, as evidenced by pore visualization studies. Stability and solubility enhancement techniques will be used to develop molecules that can deliver NTX in therapeutically relevant concentrations.

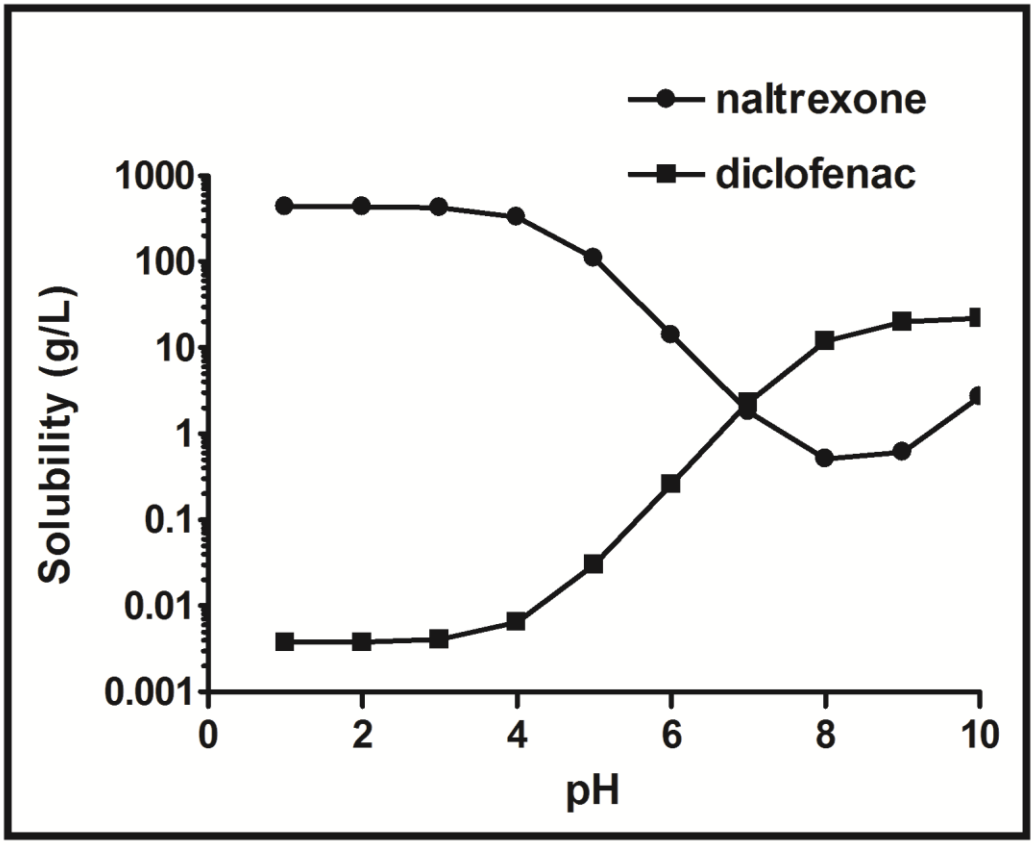

Figure 6.1 Solubility profile of NTX and DIC generated using predicted chemical property values from Scifinder® [19]

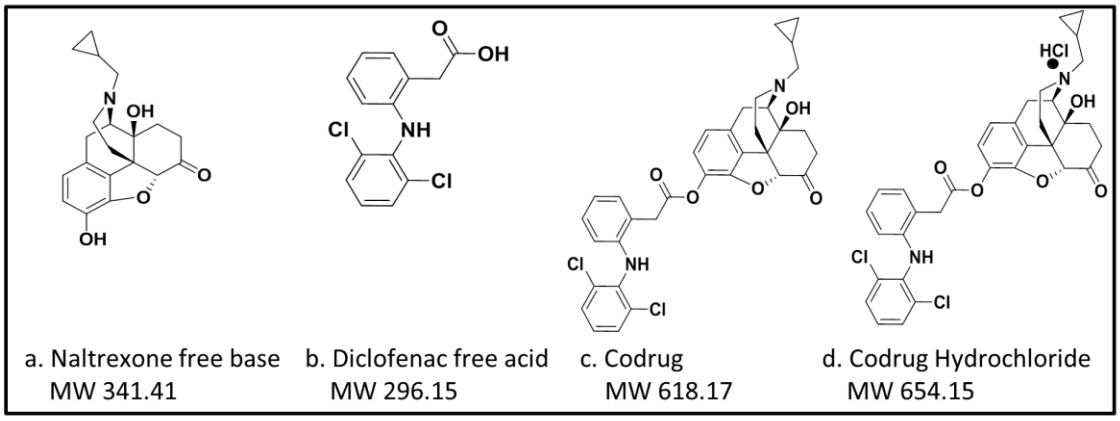

Figure 6.2 Structure of parent drugs, (a) NTX, (b) DIC (c) 3-O-ester codrug and (d) hydrochloride salt form of 3-O-ester codrug

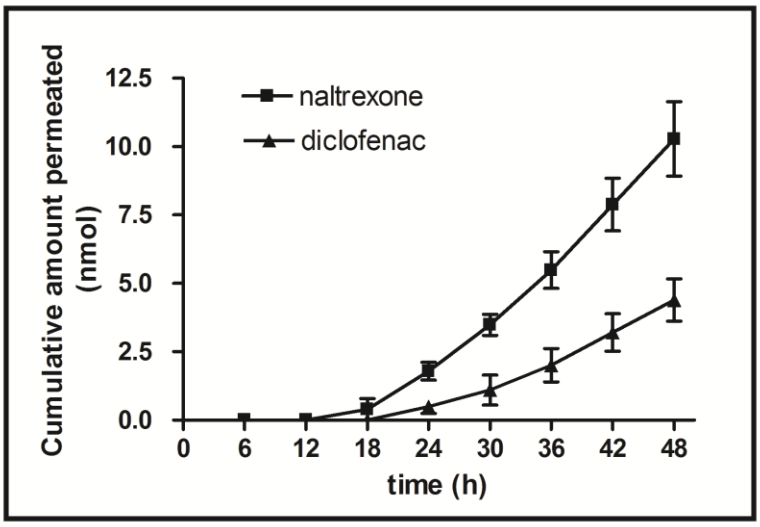

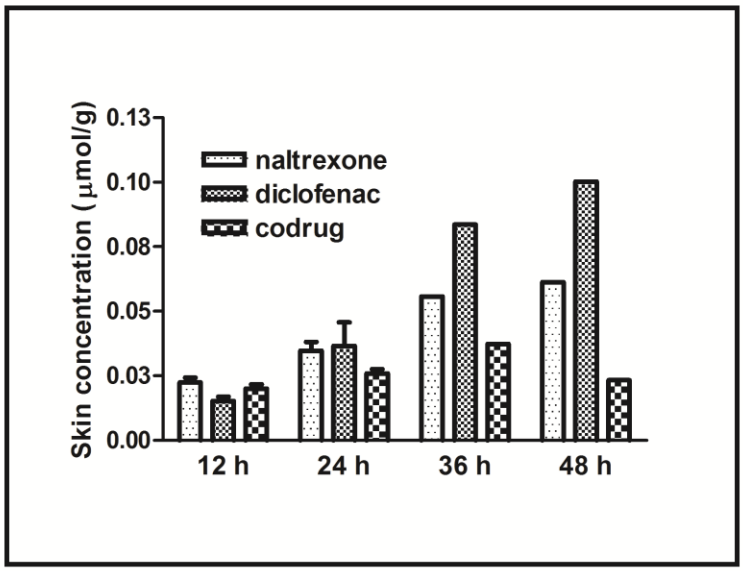

Figure 6.3 *In vitro* diffusion studies across full thickness Yucatan miniature pig skin of the base form of codrug (a) Permeation vs. time profile of NTX and DIC from the codrug at 48 hours post MN treatment. (n=3) (b) Skin concentration over time from the base form of the codrug. Both NTX and DIC concentration could be observed in the skin indicating the regeneration of the parent molecules. n=3 for 12h, 24h and n=2 for 36h and 48h

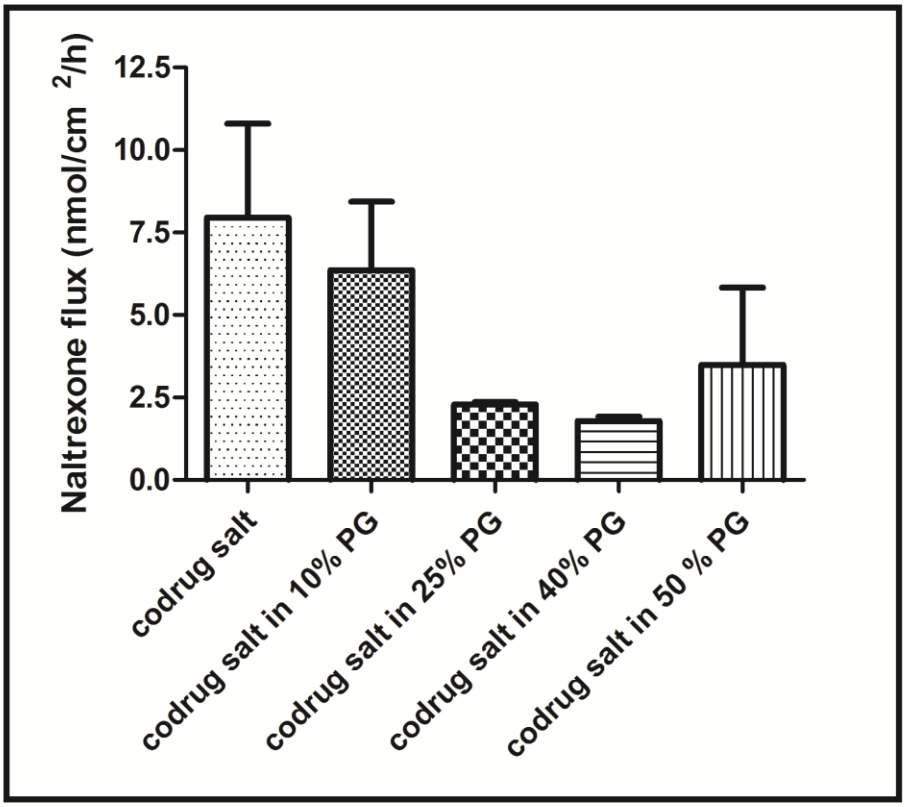

Figure 6.4 *In vitro* diffusion studies across full thickness Yucatan miniature pig skin comparing the flux of NTX at steady state from different donor formulations. Propylene glycol (PG) was used in different concentrations to optimize formulation for *in vivo* studies (n≥3)

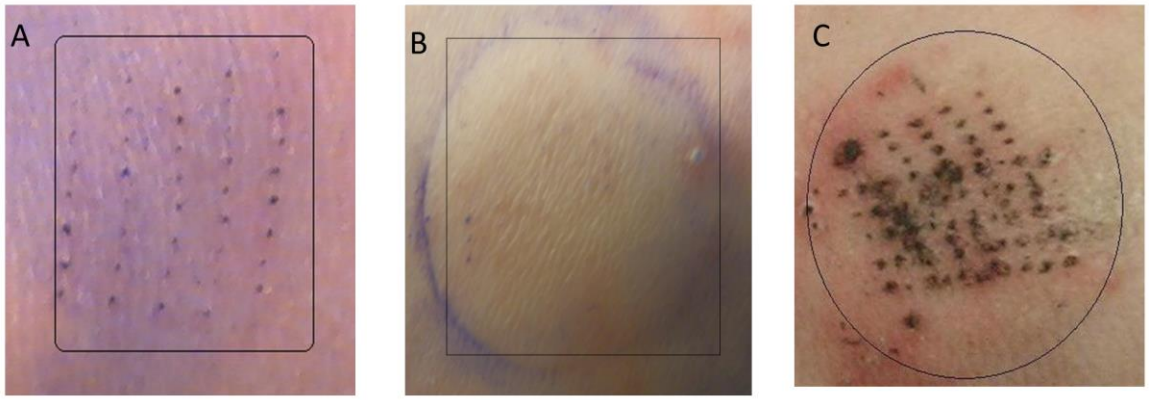

Figure 6.5 *In vivo* micropore visualization with different staining techniques. (A) Shows presence of micropores immediately following MN treatment, (B) shows absence of micropores with India Ink staining at 96h following treatment with NTX alone (C) shows presence of micropores with India Ink staining at 7 days following treatment with codrug

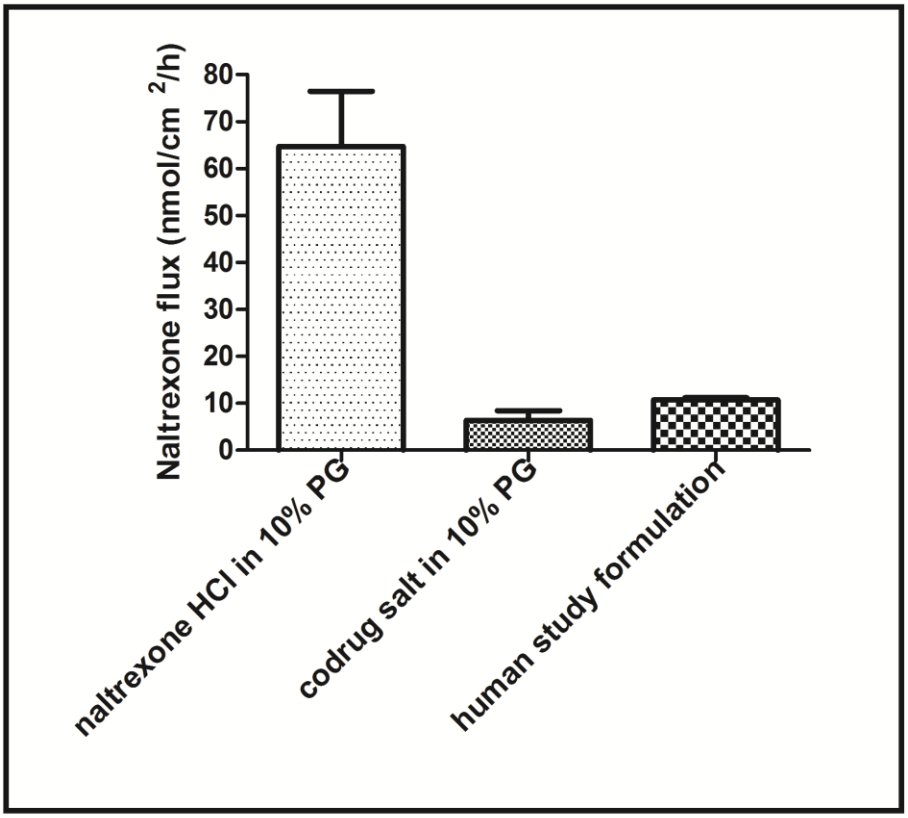

Figure 6.6 *In vitro* diffusion study across full thickness Yucatan miniature pig skin comparing the flux of NTX at steady state from NTX HCl, salt form of the codrug and previously studied formulation for *in vivo* human pharmacokinetic studies (n≥3)

Chapter 7

Optimization of naltrexone diclofenac codrugs for sustained drug delivery across microneedle treated skin

7.1 Introduction

The contents of this chapter have been submitted for publication in Pharmaceutical Research. (Revisions submitted May 2013) Codrugs or mutual prodrugs are two active pharmaceutical ingredients (API) linked via a covalent linkage to form a single chemical moiety. [23] They are primarily synthesized to solve drug delivery issues like stability and solubility of the parent compounds or to enhance permeation of one or both active moieties across biological barriers by modification of the chemical structure.[79] Codrugs and prodrugs are pharmacologically inactive in their modified form; however they are bioconverted back to parent drugs either by chemical or enzymatic hydrolysis in formulation, when crossing biological barriers, or in the plasma.[23, 79]

The overall goal of the current project was to optimize codrug structures in order to develop a sustained release transdermal drug delivery system for alcohol addiction. Naltrexone (NTX), the model compound (MW-341.4, log P-2.0) is a μ-opioid receptor antagonist approved for alcohol and opioid addiction treatment. [19] 6β-Naltrexol (NTXol) (MW-343.4, log P-0.68), the active metabolite of NTX, has also been shown to have therapeutic efficacy for alcohol addiction. [15, 128] The current available dosage forms for NTX are oral and an extended release intramuscular injection. Both forms have their own drawbacks. The oral dosage form has compliance issues in an addict population due to daily dosing and gastrointestinal side effects. [15, 155] The extended release intramuscular dosage form has been associated with serious injection site reactions and difficulty with removal in case of emergency opiate requirements. [17, 126]

NTX can potentially benefit from an alternative delivery route like transdermal drug delivery. This noninvasive technique allows delivery of drugs directly into the systemic circulation and bypasses gastrointestinal side effects. The transdermal route is also known to be patient-friendly and comparatively more effective in an addict population with compliance issues. [28] However, NTX doesn't cross the stratum corneum (SC) barrier at a therapeutically relevant rate by passive diffusion alone.[4] The SC, the topmost layer of the skin is formed of dead keratinized epidermal cells and a lipid matrix, and forms the most important barrier to transport of xenobiotics across the skin. [1]

Previous work, in both animal models and humans, has shown that by using small micron-scale needles or microneedles (MN), it is possible to deliver NTX at a rate that provides plasma concentrations in the lower end of the therapeutic range. [4] MNs are a physical enhancement technique used to permeablize the skin by creating micropores. The effectiveness of this technique for enhancement of transdermal drug delivery has been established in the literature over the past decade and a half. [42, 43] Using the 'poke (press) and patch' approach for MN treatment drug can be delivered across treated skin for 48-72h under occlusion. The drug delivery window can be further enhanced by local application of a non-steroidal anti-inflammatory drug, diclofenac sodium (DIC) (MW-296.1, log P-4.5). [8, 9, 19] Due to physicochemical incompatibility of the two molecules in formulation, daily or alternate day application of DIC was required to keep micropores open for a 7 day period. [14, 163] The incompatibility in formulation also leads to a significant decrease in flux of NTX across micropores in the presence of DIC, as compared to NTX alone, due to precipitation issues upon co-administration. [14]

The codrug approach was thereafter used to combine NTX and DIC into a single chemical moiety with the goal of solving the formulation issue. The bioconversion of the properly designed new chemical entities in the skin or plasma should not be a problem since it has been previously shown that prodrugs/codrugs are bioconverted in the skin,

both during passive delivery and MN enhanced delivery. [21, 82, 85, 86] The hypothesis was that following bioconversion in the skin, DIC would act locally and keep the pores open facilitating systemic delivery of NTX. A proof of concept study was conducted using a NTX-DIC 3-O-ester linked codrug to look at stability, solubility, transdermal flux and local skin concentration of the codrugs and the parent drugs. [147] Although pharmacokinetic profiles were not obtained from the study, pore visualization techniques were used to verify the presence of micropores in the skin at the end of 7 days, using the codrug formulation compared to absence of micropores for the NTX control. These studies confirmed that the codrug approach was useful for development of a 7 day system, however further optimization was required. The codrug also had a formulation half-life of around 4-5 days, and the solubility and transdermal flux were an order of magnitude lower compared to the most optimized formulation for NTX delivery across MN treated skin. [22, 139]

In the current study, four codrugs of NTX/ NTXol and DIC have been compared to look at structure vs. stability, solubility, transdermal flux and bioconversion in the skin. The study was carried out to satisfy research goal 3.4. The codrugs for this part of the research were synthesized by DoMin Lee from Dr. Kyung Bo Kim's laboratory at the University of Kentucky. 3-OH (phenol position) on NTX or the 6-OH (secondary alcohol) position on NTXol were used for the synthesis along with the –COOH group on diclofenac. Ester, carbamate or amide linkers were used to join the two molecules either directly, or with the help of a polyethylene glycol (PEG) linker. Furthermore, hydrochloride salts of promising codrugs were synthesized and tested to develop a formulation for *in vivo* pharmacokinetic studies.

7.2 Materials and Methods

7.2.1 Chemicals

NTX HCl and NTX base were purchased from Mallinckrodt (St. Louis, MO), DIC acid from AK Scientific, Inc. (Mountain view, CA) and DIC sodium salt from TCI America (Portland, OR). Water was purified using a NANOpure Diamond^{TM}, Barnstead water filtration system. Propylene glycol was purchased from Sigma (St. Louis, MO). Sodium acetate and acetic acid were obtained from Fisher Scientific (Fairlawn, NJ). 1-Octanesulfonate, sodium salt was obtained from Regis Technologies, Inc (Morton Grove, IL). Trifluroacetic acid (TFA), triethylamine (TEA) and acetonitrile (ACN) were obtained from EMD chemicals (Gibbstown, NJ). Unless otherwise noted, all other reagents for codrug synthesis were obtained from Sigma Aldrich (St. Louis, MO).

7.2.2 Synthesis of the codrugs

Codrug I and hydrochloride salt of codrug I were synthesized following previously reported procedures. [147] Codrugs II, III and IV were synthesized by DoMin Lee in Dr. Kyung Bo Kim's laboratory at the University of Kentucky.

Codrug II: Benzyl bromide (0.522 mL, 4.375 mmol) was added to a suspension of 6β-NTXol (500 mg, 1.458 mmol) and potassium carbonate (1 g, 7.3 mmol) in acetone (10 mL). The reaction mixture was then refluxed for 2 h before it was concentrated under reduced pressure. The resulting crude product was further purified by column chromatography on silica gel using dichloromethane-methanol mixture to obtain compound **1** as a white solid (500 mg, 79%). A mixture of compound **1** (500 mg, 1.153 mmol), DIC acid (685 mg, 2.306 mmol), and DMAP (7 mg, 0.06 mmol) were dissolved in dichloromethane (50 mL) and cooled to -78^{o}C in an acetone/ dry ice bath under N_2. To the reaction mixture, *N,N'*-dicyclohexylcarbodiimide (685 mg, 2.306 mmol) in dichloromethane (20 mL) was then added with vigorous stirring. After 1h, the reaction

mixture was allowed to warm up to room temperature and concentrated under reduced pressure. The resulting crude product was purified by column chromatography on silica gel using hexane-ethyl acetate mixture to yield compound **2** as a white solid (260 mg, 32%). Catalytic hydrogenation of compound 2 (100 mg, 0.140 mmol) over a Pd/C catalyst provided Codrug II as a solid (80 mg, 92 %).

Codrug III: Triethylamine (0.123 mL, 0.879 mmol) was added to a suspension of NTX·HCl (200 mg, 0.586 mmol) and 4-Nitrophenyl chloroformate (130 mg, 0.644 mmol) in dichloromethane (5 mL). The resulting solution was stirred for 4h at room temperature, and then concentrated under reduced pressure to yield an oilic crude product. The crude product was purified by column chromatography on silica gel using dichloromethane-methanol mixture to provide compound **3** as a light yellow solid (292 mg, 66%). To a dichloromethane solution containing compound **3** (61 mg, 0.143 mmol) and DIC-EBE (73 mg, 0.143 mmol) was added DMAP (35 mg, 0.286 mmol). The reaction mixture was then stirred for 1h at room temperature and then concentrated under reduced pressure. The resulting crude product was purified by column chromatography on silica gel using dichloromethane/methanol solvent systems to obtain codrug III as a light yellow solid (78 mg, 69%).

Codrug III hydrochloride salt: To a dichloromethane solution of codrug III (100 mg, 0.126 mmol), 1M HCl was slowly added and continuously stirred for 10 min. The resulting codrug III salt was filtered and dried to yield codrug III·HCl as a white solid (95 mg, 91%).

Codrug IV: To a suspension of 6β-NTXol (300 mg, 0.875 mmol) and di-tert-butyl dicarbonate (210 g, 0.962 mmol) in acetone (20 mL) was added potassium carbonate (604 mg, 4.373 mmol) with vigorous stirring. The reaction mixture was then refluxed for 1 h and concentrated under reduced pressure. The resulting crude product was further purified by column chromatography on silica gel using dichloromethane-methanol solvent systems to provide compound **4** as a white solid (340 mg, 88%). To a suspension of

compound **4** (340 mg, 0.766 mmol) and 4-Nitrophenyl chloroformate (232 mg, 1.149 mmol) in dichloromethane (10 mL) was added DMAP (280 mg, 2.298 mmol). The resulting mixture was stirred for 1h at room temperature and subsequently concentrated under reduced pressure to yield the crude product, which was further purified by column chromatography on silica gel using dichloromethane/methanol solvent systems to obtain compound **5** as a light yellow solid (445 mg, 95%). Next, *N, N*-Diisopropylethylamine (0.623 mL, 3.58 mmol) was added to a suspension of compound **5** (436 mg, 0.716 mmol) and DIC-EBE (458 mg, 1.074 mmol) in dichloromethane (10 mL) and stirred for 1h at room temperature. After the reaction mixture was concentrated under reduced pressure, the resulting crude product was further purified by column chromatography on silica gel using dichloromethane/methanol solvent systems to obtain compound **6** as a white solid (455 mg, 71%). %). Trifluoroacetic acid (1 mL) was added to a solution of compound **6** (300 mg, 0.334 mmol) in dichloromethane (10 mL). The resulting solution was stirred at room temperature for 1h. The reaction mixture was concentrated under reduced pressure. The crude product was purified by column chromatography on silica gel using dichloromethane-methanol mixture to afford Codrug IV as a semi solid (120 mg, 45%).

7.2.3 HPLC assay

All codrugs and parent drugs were quantified using HPLC. The HPLC instrument used consisted of a Waters™ e2695 separation module, a 2489 UV/Visible detector and Empower™3 software. A Perkin Elmer Spheri5 VL C18 column (5µ, 220 x 4.6mm) and a C18 guard column (15 x 3.2mm) were used with the UV detector set at a wavelength of 280nm/215nm. The mobile phase consisted of 70:30(v/v) ACN: (0.1% TFA with 0.065% 1-octane sulfonic acid sodium salt, adjusted to pH 3.0 with TEA aqueous phase). Samples were run at a flow rate of 1.5 ml/min. All codrugs and parent drugs were quantified using standard curves in the range of 100-10,000 ng/ml.

7.2.4 Stability studies

The stabilities of all codrugs were determined in 0.3M acetate buffer pH 5.0 at 32ºC. For stability studies drug was presolubilized in ACN. The solution was then used to spike prewarmed buffer at 32ºC (100µl in 10ml of buffer, <1% total ACN concentration). One hundred µl samples were obtained at regular time intervals and the reaction was terminated using 900µl of ACN. All samples were stored at -80ºC until analysis using HPLC. Samples were stable in -80ºC verified using quality control standards (data not shown). Data for all stability studies were analyzed using pseudo first-order kinetics. All studies were run in triplicate.

7.2.5 Donor solution preparation and solubility determination

Donor solution was prepared for all codrugs in 0.3M acetate buffer pH 5.0 containing 10% propylene glycol (PG). Excess drug was added to the above mixture, vortexed, sonicated for 10 min and left overnight at 32ºC (The only exception, codrug I was incubated in donor solution for an hour before dosing due to stability issues). The choice of the donor was based on previous studies using codrugs and flux of model compounds across MN treated skin.[21, 147] For solubility determination, codrug solution was removed from the donor, filtered using a 0.2µm, 500µl centrifugal filter and injected onto the HPLC after suitable dilution with ACN. Saturation solubility was determined for all codrugs except hydrochloride salt of codrug III due to limited availability of codrug. All solubility determinations were carried out in triplicate.

7.2.6 Melting point determination of codrugs

Differential scanning calorimetry (DSC) was used to estimate melting point of parent drugs and codrugs in the range of 50-300ºC. The apparatus used was a DSC 2920 with a DSC refrigerated cooling system from Texas Instruments (TA Instruments, New Castle, DE). Two to five mg of drug was weighed into hermetic aluminum pans and

sealed with a lid. Drug was heated @10ºC/min from 50-300ºC. Data was collected using Thermal Advantage and analyzed using Universal Analysis 2000 softwares from TA Instruments. Melting point was determined from the inflection point of the melting curve.

7.2.7 Diffusion studies

All diffusion studies were carried out using full thickness Yucatan miniature pig skin. Studies were approved by the IACUC protocols at University of Kentucky and University of Maryland, Baltimore. The skin was obtained from euthanized animals, dermatomed to a thickness of 1.4-1.8mm and stored at -20ºC until the day of the experiment. MN's for this study were obtained from Dr. Mark Prausnitz's laboratory at the Georgia Institute of Technology. A 5 MN in plane array was used for *in vitro* studies. Each MN was 750 µm long, 200µm wide and 75 µm thick and the interneedle spacing was 1.35µm. For all experiments skin was cut into small rectangular pieces. They were then placed on a wafer of Sylguard® 184 silicone elastomer to mimic the underlying tissue and treated with a 5 MN array, 20 times to generate a total of 100 MN pores per diffusion cell (within the 0.95cm^2 active area). The permeation experiments were carried out using a PermeGear® flow through system (In-line, Riegelsville, PA). The receiver solution used was water alkalified to pH 7.4 containing 20% ethanol at 37ºC. The flow rate was set at 1.5ml/h and the temperature of the diffusion cells was maintained at 32ºC to mimic physiological skin surface conditions. Each cell was charged with 250µl of the relevant codrug or parent drug for control cells and receiver solution was collected in 6h increments for a total of 48h. At the end of the study the cells were removed and drug was quantified both in the receiver solution and skin samples using HPLC. For the receiver solution, steady state flux values were determined for NTX/NTXol from the codrugs using Fick's first law of diffusion. The cumulative amount permeated was plotted as a function of time and the slope of the steady state portion of the curve was used to

determine flux. Permeation profiles did not reach steady state in the 48h timeframe for DIC and codrug, so cumulative amount of drug permeated was quantified, where applicable. Receiver samples were concentrated, if required by evaporating 1ml of the receiver solution under nitrogen at 37°C followed by reconstitution in 100µl of ACN. For quantification of the drug concentration in the skin samples, the active permeation area was dissected out and cut into small pieces. The concentration of parent drugs and codrug in the skin was determined by incubating the skin in 10ml of ACN overnight at 32ºC and analyzing the solution by HPLC after appropriate dilutions. All permeation studies were carried out in triplicate, at a minimum.

7.2.8 Statistical analysis

Data for all experiments were reported as mean ± standard deviation. Statistical analysis of data was carried out with Students't-test and one way ANOVA with post hoc Tukey's pairwise tests, if required, using GraphPad Prism® software, and version 5.04 software. $P<0.05$ was considered to be statistically significant.

7.3 Results

7.3.1 Synthesis of codrugs

Structures of all codrugs are provided in Figure 7.2. The synthesis of codrug I, base and salt form has been previously reported. [147] Codrugs II, III and IV and hydrochloride salt form of codrug III were synthesized successfully. The structures were verified using ^{1}HNMR and HRMS

Codrug II: ^{1}H NMR ($CDCl_3$, 500 MHz) δ 7.41-7.24 (m, 10 H),7.09 (m, 1H), 6.96-6.92 (m, 3H), 6.72 (m, 1H), 6.57-6.54 (m, 2H), 5.31 (2H, s), 5.12-5.07 (m, 3H), 4.79-4.71 (m, 2H), 4.04 (m, 2H), 3.86 (s, 2H), 3.49 (m, 2H), 3.08-2.99 (m, 2H), 2.64-2.56 (m, 2H), 2.39-2.18

(m, 4H), 2.09-1.95 (m, 7H), 1.81 (m, 1H), 1.71-1.60 (m, 12H), 1.49-1.43 (m, 2H), 1.37-1.27 (m, 6H), 1.17-1.11 (m, 7H), 0.84 (m, 1H), 0.52 (m, 2H), 0.12 (m, 2H)

Codrug III: ^{1}H NMR ($CDCl_3$, 500 MHz) δ 7.78 (s, 1H), 7.32 (m, 2H), 7.12-7.07 (m, 2H), 6.97-6.93 (m, 2H), 6.86 (t, 1H, *J* = 8.5 Hz), 6.71-6.66 (m, 3H), 6.60 (m, 1H), 6.49 (d, 1H, *J* = 8.5 Hz), 5.98 (m, 1H), 4.69 (m, 2H), 3.64-3.44 (m, 13H), 3.19 (s, 2H), 3.10-3.00 (m, 4H), 2.72-2.56 (m, 4H), 2.44-2.31 (m, 8H), 2.17-2.12 (m, 3H), 1.90-1.26 (m, 8H), 0.86 (m, 2H), 0.56 (m, 4H), 0.15 (m, 4H)

Codrug III HCl salt: ^{1}H NMR (DMSO-d_6, 500 MHz) δ 8.66-8.58 (m, 2H), 8.08 (s, 1H), 7.96 (s, 1H), 7.47 (s, 1H), 7.08 (m, 2H), 6.77-6.74 (m, 2H), 6.61 (m, 1H), 6.63 (d, 1H, *J* = 7.0 Hz), 6.41-6.36 (m, 2H), 6.28-6.22 (m, 2H), 5.85 (m, 1H), 4.70 (s, 1H), 4.58 (s, 1H), 3.61-3.56 (m, 2H), 2.82-2.79 (m, 6H), 2.71-2.50 (m, 11H), 2.30-2.23 (m, 3H), 2.09 (m, 12H), 1.74-1.59 (m, 4H), 1.09-1.07 (m, 4H), 0.67-0.64 (m, 6H), 0.27 (m, 2H), 0.20 (m, 2H), 0.10 (m, 2H), 0.00 (m, 2H)

Codrug IV: ^{1}H NMR ($CDCl_3$, 500 MHz) δ 7.62 (s, 1H), 7.33-7.31 (m, 2H), 7.17-7.15 (m, 1H), 7.09-7.08 (m, 1H), 6.96 (t, 1H, *J* = 8.0 Hz), 6.88-6.86 (m, 1H), 6.76-6.69 (m, 2H), 6.65 (d, 1H, *J* = 8.0 Hz), 6.49 (d, 1H, *J* = 8.0 Hz), 5.28 (m, 1H), 4.51 (m, 2H), 3.76-3.47 (m, 18H), 3.08-2.97 (m, 3H), 2.59-2.57 (m, 2H), 2.35 (m, 2H), 2.18-1.88 (m, 8H), 1.60-1.58 (m, 1H), 1.46-1.25 (m, 9H), 0.82 (m, 1H), 0.51 (m, 2H), 0.11 (m, 2H)

7.3.2 HPLC assay development

The first step towards analysis of codrugs and parent drugs was development of a HPLC method. The same column, mobile phase composition and wavelength (280nm) were used for all compounds. All codrugs and parent drugs had baseline resolution on the assay. The retention times (±0.1 min) for all compounds from the HPLC assay are reported in table I. Standard curves for both codrugs and parent drugs were prepared in

the range of 100-10,000 ng/ml for ACN samples and 100-5000 ng/ml for extracted receiver samples. All standard curves were linear (r^2>0.999).

7.3.3 Stability and solubility studies

Formulation stability was carried out for all codrugs to determine the relative rate of conversion due to chemical hydrolysis. The results indicated that stability was significantly enhanced by using the 6-O-secondary alcohol linkage over the 3-O-phenol linkage for both codrugs I and II, and codrugs III and IV. Stability was also significantly enhanced by using the PEG covalent link and carbamate/ amide linkage compared to the ester linkage, both for codrug I and III, and codrug II and IV. (Figure 7.4)

The solubility studies were carried out to quantify saturation solubility of codrugs in donor formulation and evaluate its effect on flux. The studies indicated that solubility of the NTX-DIC codrugs were significantly higher compared to NTXol-DIC codrugs with similar linkage. The PEG linkage enhanced solubility for codrug III and IV, as compared to codrug I and II. Solubilities of codrugs were also enhanced by using a hydrochloride salt form of the drug compared to a free base form.

7.3.4 Diffusion studies

The diffusion studies were carried out to quantify the permeation of NTX/NTXol across the skin and concentration of codrugs and parent drugs in the skin. The diffusion studies indicated that flux of NTX from codrugs I salt and III were significantly higher compared to flux of NTXol from codrugs II and IV ($p < 0.05$). The flux of NTX from codrug I salt and codrug III, and NTXol from codrug II and codrug IV were not significantly different from each other ($p > 0.05$). (Figure 7.5) Permeation of DIC and intact codrug was also observed for codrug III from the 10% PG containing formulation. Cumulative amount of DIC and codrug present in the receiver solution were 1.09 ± 0.36 nmol and

2.89 ± 1.0 nmol, respectively, at the end of the 48hr experiment. NTX flux was further enhanced by 2.5 fold on using the salt form of codrug III, over free base form. (Figure 7.6) Significantly higher permeation of DIC and intact codrug were also observed using the salt form of codrug III, they were 3.1±0.86nmol and 24.3 ± 8.8 nmol, respectively.

Skin concentration of codrugs and parent drugs were quantified at the end of the experiment to evaluate the effect of codrug structure on bioconversion in the skin. The skin concentration data indicated that bioconversion was more complete for NTX-DIC codrugs compared to the NTXol-DIC codrugs. Intact codrug was present in the skin for all codrugs, whereas NTX and DIC were only quantifiable for codrugs I and III. Skin concentrations of codrugs were not significantly different among the 4 codrugs. Skin concentration of NTX was not significantly different between codrugs I and III ($p>0.05$). Skin concentration of DIC was significantly different between codrugs I and III ($p<0.05$). Skin concentration was also determined for codrug III salt to evaluate the effect of salt form on skin concentration. No significant differences were observed for NTX or DIC concentration using codrug III base or salt form ($p>0.05$).

Flux data from codrug I has been previously reported. [147]The salt form of codrug I has been used for all comparisons for diffusion experiments in this study since the limited solubility of the free base form in 10% PG containing formulation prevented direct comparison of results.

7.4 Discussion

Prodrugs and codrugs have been explored for drug delivery via different routes over the last few decades. The approach is mostly used to solve a drug delivery issue and the major advantage lies in the fact that chemical modification renders the new chemical entity pharmacologically inactive thus decreasing potential side effects and the need for additional pharmacological evaluation. Compared to all other routes of drug

delivery, the topical/transdermal field has seen slower progress in terms of the number of new API's approved and on the market over the years. [29] The most important reason being the extreme barrier property of the skin/SC. Chemical modification of the API itself to form codrugs/prodrugs provides a new approach for flux enhancement, decreasing some of the need for excess permeation enhancer supplementation. Additionally, two API can be delivered at the same time in a codrug to have a synergistic effect. A few examples of topical/transdermal codrugs that have been evaluated include NTX and bupropion for smoking cessation and alcohol addiction, retinyl ascorbate and ascorbic acid for oxidative stress, and 5 fluorouracil with triamcinolone acetonide for actinic keratosis. [87, 88]

The current study evaluated codrugs for pore lifetime enhancement following MN treatment. Unlike previous codrug examples in the literature where both drugs were targeted either for systemic delivery or for topical application, the NTX/NTXol codrugs are designed for systemic delivery of NTX/NTXol while DIC acts locally in the SC/epidermal layer of the skin to enhance micropore lifetime. The physicochemical properties of NTX allow systemic permeation, and a higher log P and negative charge facilitates retention of DIC in the skin. [147]

Purity and structure of all codrugs were confirmed using NMR and HRMS. Quantitative analysis is an important step in the development of any drug delivery system. HPLC was used for quantification of codrug and parent drugs in stability, solubility and permeation studies. Since all compounds were evaluated using reverse phase chromatography and the same assay parameters, retention time on the HPLC can be used as a comparative estimate of hydrophobicity or log P of the molecules. [164] NTX and NTXol were comparable in hydrophobicity with NTXol being slightly more hydrophilic due to the presence of an additional hydroxyl group at the 6 position

compared to the ketone of NTX. DIC was the most hydrophobic of the parent molecules, which is expected from the reported log P values from Scifinder®. Comparing codrugs I and II, codrug I with a retention time of 4.9 min was more hydrophobic compared to codrug II at 4.4 min. The difference in hydrophobicity can be attributed to more significant hydrophilic interactions of a phenolic hydroxyl as compared to a ketone functional group substitution. Comparison of codrug III and IV followed the same pattern, where the retention time shifted from 3.8 min for codrug III to 3.7 min for codrug IV. Although in both cases the codrugs with the free phenolic hydroxyl had less retention on the column, the shift was much less significant for the PEG linked codrugs. This can be attributed to significant hydrophilic interactions of the PEG chain itself. Effect of PEG chain on enhancement of hydrophillicity is also confirmed by the fact that both codrug III and IV are eluted significantly earlier than codrug I and II. Since hydrophobicity/hydrophilicity plays an important role in permeation of molecules across intact and MN treated skin, the comparative analysis provides an estimate of solubility and transport. For MN treated skin, it has been shown that lower viscosity aqueous formulations lead to higher flux. Higher hydrophillicity would translate into enhanced solubility in an aqueous medium; a molecule with lower log P will be beneficial for the current delivery system in terms of higher solubility.

Codrugs/prodrugs are primarily designed to solve a drug delivery problem, but since these molecules are pharmacologically inactive chemical/enzymatic hydrolysis is imperative for bioconversion and function of these molecules. In the current project, codrugs were designed to formulate NTX and DIC in a single formulation so that precipitation of one drug on application of the other didn't lead to reduced NTX flux across the micropores. Thus, stability in formulation is a very important criterion for these codrugs. The results from the stability studies indicated that codrugs I and III (phenol

linked codrugs) were less stable in formulation compared to codrugs II and IV (secondary alcohol linked codrugs). This was expected since the resonance stabilization of a phenol makes it a better leaving group compared to a secondary alcohol. Codrug III was more stable compared to codrug I, and codrug IV was more stable compared to codrug II. This can be attributed to the carbamate/amide linkage in place of the ester linkage. It has been shown in the literature that ester linked prodrugs are more susceptible to chemical hydrolysis as compared to carbamate prodrugs at a formulation pH of 5.0. [21] On the other hand, carbamate linked prodrugs are less stable at physiological pH 7.4 at similar buffer concentrations. [21] The change in the rate of chemical degradation within the pH range indicates that the primary mechanism for hydrolysis of a monosubstituted carbamate in an aqueous formulation is probably via proton elimination and not nucleophile attack of hydroxyl groups. [165] Thus employing carbamate codrugs enhances formulation stability and could be beneficial because they are known to degrade faster under physiological conditions. Since NTX/ NTXol and DIC codrugs could not be linked directly with a carbamate linkage, a PEG link was used to serve the dual role of linking the molecules and enhancing solubility. PEG is one of the most commonly used topical/transdermal excipients, thus irritation, toxicity and side effects related to incorporation of PEG in the formulation should be limited or non-existent. Once inside the body, PEG is metabolized into a series of phase I and II metabolites, with no toxicological concern. Molecular weight of the PEG subunit does play a role in its metabolism, with PEG's >5000 showing little or no metabolism. [166] Thus from the stability studies it can be concluded that codrugs II, III and IV with more than 85% intact codrug in formulation at 7 days could be used for the development of a drug delivery system. Since the stability studies were conducted in aqueous buffers, the codrugs will be expected to be more stable in a 10% PG containing formulation since hydrolysis is the primary mechanism for degradation. Once inside the body, the codrugs

will be degraded by enzymatic hydrolysis in the skin, in addition to chemical hydrolysis for much faster regeneration of parent drugs. Presence of esterase, amidase, and protease, in addition to the normal phase I and II enzymes are well documented in the skin. [32, 159]

Solubility of drug in the donor is important for transdermal drug delivery. The drug concentration in formulation is the main driving force for transport across the skin. As stated before, MN-enhanced drug delivery with lower viscosity aqueous formulations has demonstrated significantly higher flux compared to viscous PG-rich formulations. Ten percent PG containing 0.3M acetate buffer at pH 5.0 was chosen as the formulation based on previous studies. [29, 147] The solubility data indicated that the PEG link significantly enhanced solubility for both codrug III and IV, compared to codrug I and II. Solubility of codrug I and III was higher compared to II and IV, indicating that phenol linked codrugs are more soluble compared to secondary alcohol linked codrugs. This can be further explained in terms of the melting point (MP) estimates where codrug I has a lower melting point compared to codrug II. Lower MP translates into higher aqueous solubility for the unionized form of the drug. [167]

Stability and solubility studies provide important information about how well drug transport might proceed, however skin permeation studies are required for estimation of flux and bioconversion in the skin. Diffusion studies were carried out using dermatomed Yucatan miniature pig skin. The choice of the animal model was based on previous studies with MN and transdermal drug delivery. [46, 146] The diffusion studies indicated that the flux of NTX from codrug I and III was significantly higher compared to NTXol flux from codrug II and IV. This can be attributed to the higher formulation stability of the NTXol codrugs; significant amounts of intact codrug were found in the skin, and no parent drugs were quantified at the end of the study suggesting that NTXol was not

released efficiently from the codrug to generate transdermal flux. The difference in physicochemical properties of NTX and NTXol could also be responsible for reduced flux of NTXol. Since NTXol has an additional hydroxyl group following conversion, H-bonding potential of NTXol is higher. It has been shown in the literature that the higher the number of hydrogen bonds, the lower the transdermal flux across intact skin. [53] The skin concentration study also showed that DIC was only present in the skin for the NTX codrugs. Since the presence of DIC in the skin is imperative for its local effect on pore lifetime enhancement, the NTXol codrugs would not be able to keep micropores open beyond 48-72h in the absence of DIC. Also, significantly lower flux from these codrugs as compared to the NTX codrugs is a disadvantage. The skin concentration of DIC is significantly different between codrug I and III. This can be explained with the help of mass spectrometry data (not shown) which indicates that DIC is not completely bioconverted in the skin from codrug III. A mixture of DIC (MW: 296) and DIC + PEG linker conjugate (MW: 452) was found in the receiver and skin samples by mass scan and ESI-/ ESI+ ionization. Since an accurate estimate of local skin concentration of DIC required for pore lifetime enhancement is not available, it would be beneficial to test codrug III *in vivo* to see if it is efficacious. If not, the linker at the DIC end of the molecule will have to be optimized further for faster release of DIC.

The hydrochloride salt form of codrug I led to a 13-fold enhancement in solubility and transdermal flux [147], but direct comparison of the effect of the salt formulation could not be evaluated due to changes in donor composition. A hydrochloride salt form of codrug III was synthesized and evaluated for further solubility and flux enhancement *in vitro*. Codrug III was chosen because formulation stability and solubility was higher as compared to codrug I. Codrugs II and IV were comparatively more stable but bioconversion, transdermal flux of NTXol, and skin concentrations of DIC were much

lower. The permeation studies indicated that flux of NTX can be further enhanced using a salt form of the codrug over the free base form. A 2.5 fold enhancement in NTX flux was obtained using a sub-saturated codrug III salt as donor compared to free base. (Saturated donor could not be used due to limited availability of codrug III salt.) The permeabilities of NTX from codrug and codrug salt were not significantly different from each other, indicating that the flux enhancement was due to enhanced solubility. Skin concentrations of codrug or parent drugs were not significantly different between salt and free base. Thus salt form has no significant effect on skin concentration of the parent drugs or the codrug, when comparing data from the same donor condition, irrespective of the physicochemical properties of the molecule. This will be useful if alternate salt forms are used to further enhance solubility, [139] and additional studies for determination of local skin concentration of DIC will not be necessary. The salt form also led to higher cumulative amounts of DIC and codrug permeation compared to the base. Intact codrug diffusing through the skin will convert under physiological conditions to regenerate parent drugs, thus further contributing to plasma concentrations of NTX. The amount of DIC permeated through the skin is well below therapeutic systemic concentrations and thus should not be of any concern.

Therefore, from the structure permeability evaluation it can be concluded that NTX-DIC PEG linked codrug (codrug III) is the best choice for the current project in terms of stability, solubility, bioconversion and NTX flux. NTX requires a flux of 12-90nmol/cm^2/h from a 25cm^2 patch for therapeutic efficacy, based on current oral dosing and clearance. Codrug III hydrochloride salt has a flux of 10.8 ± 2.1 nmol/cm^2/h from the currently tested sub-saturated solution; therefore further flux enhancement is expected using a saturated solution. From stability data, 85% of codrug III will be intact in

formulation over a 7 day patch application period, rendering it to be a suitable molecule for in vivo evaluation of the codrug concept via pharmacokinetic studies.

7.5 Conclusion

NTX/NTXol and DIC codrugs were designed and evaluated for development of a 7 day drug delivery system for alcohol addiction treatment. Stability, solubility, transdermal flux of NTX and local skin concentration of DIC were determined to develop a structure permeability relationship for the codrugs. A secondary alcohol linker enhanced stability of codrug molecules, however solubility, bioconversion, flux of NTX and local skin concentration of DIC were higher using phenol linked codrugs. Transport was further enhanced by utilizing a hydrochloride salt form of the PEG linked NTX-DIC codrug making it the most suitable candidate for further *in vivo* pharmacokinetic studies.

Table 7.1 Physical properties of parent drugs and codrugs

	Molecular weight (MW)	Color/Consistency	Retention time (min)	Melting point (ºC)
Naltrexone	341.4	White/Solid	2.1	178
Naltrexol	343.4	Yellowish white/Solid	2.0	191.5
Diclofenac	296.15	White/Solid	2.9	184
Codrug I **(hydrochloride salt)**	619.53 656.0	White/Solid White/Solid	4.9	--- 152.5
Codrug II	621.55	Slightly yellow/Solid	4.4	202
Codrug III **(hydrochloride salt)**	793.73 830.19	Yellow/Solid Yellow/Solid	3.8	---
Codrug IV	795.75	Cream/Solid	3.7	----

Table 7.2 Physicochemical characterization of codrugs

	Solubility (mM)	Pseudo first order rate constant (k) (days $^{-1}$)	Stability (Approx. half-life) (days)
Codrug I (hydrochloride salt)	7.23* 83.8 ± 15.4	0.0803	8.72 ± 1.05
Codrug II	-----	0.0052	130.88 ± 4.94
Codrug III (hydrochloride salt)	27.16 ± 0.5 87.67 ± 1.5†	0.0238	29.14 ± 1.04
Codrug IV	6.8 ± 0.2	0.0035	187.56 ± 8.55

n≥3 for all estimates except melting point determination

*Codrug I solubility was determined in 43% PG, 43% ethanol containing solution (data previously reported in [147]

†Saturation solubility could not be reported due to limited codrug

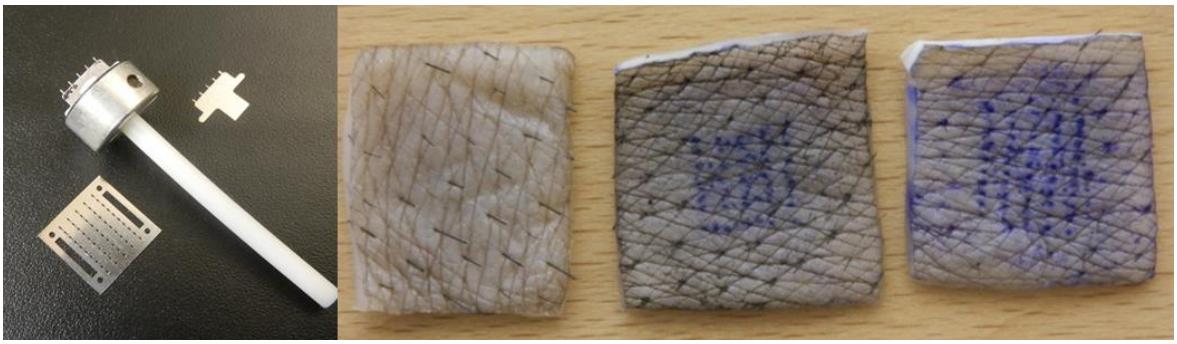

Figure 7.1 Microneedle array with 5 MN array for in vitro studies and 50 MN array for in vivo studies and applicator for 5 MN array(left panel), Yucatan miniature pig skin before treatment and following treatment with gentian violet for visualization (right panel)

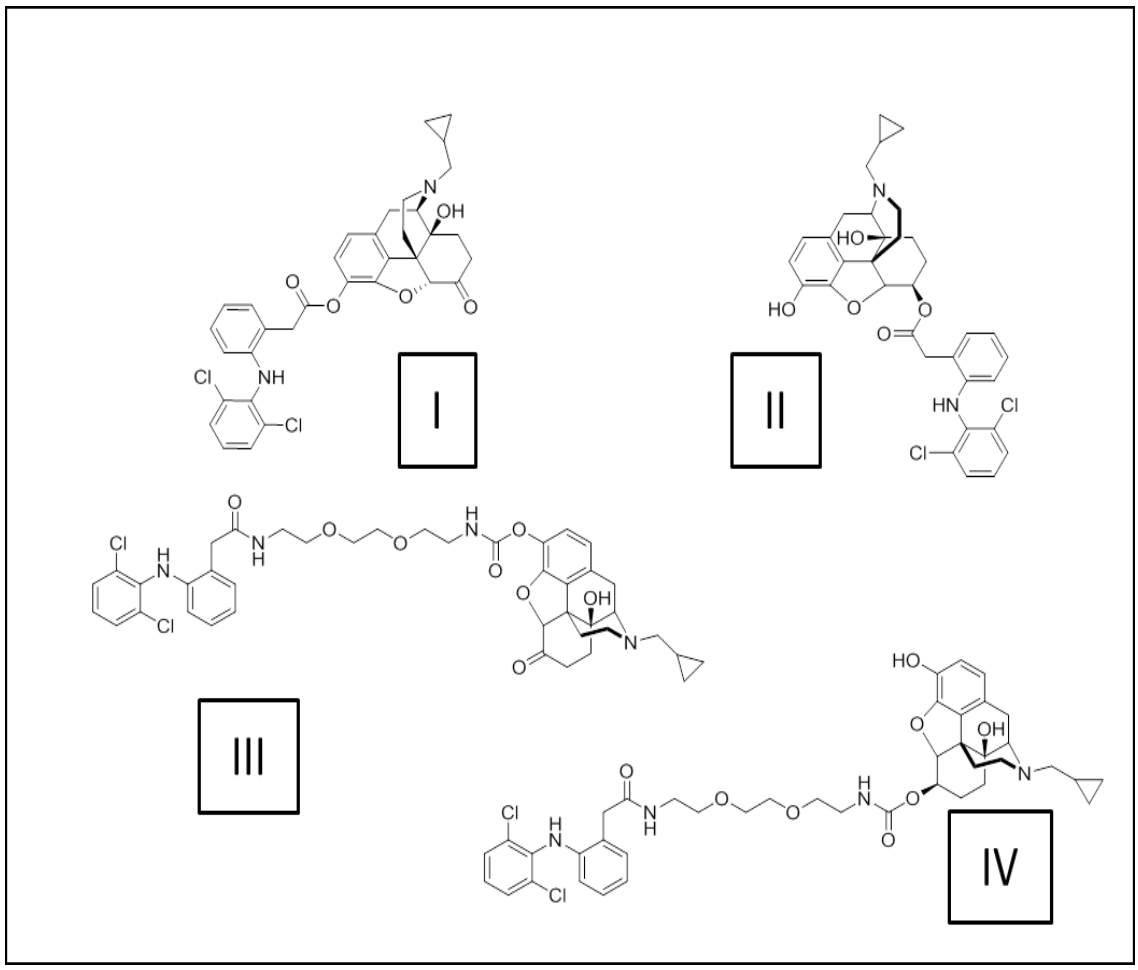

Figure 7.2 Structures of NTX/NTXol and DIC codrugs

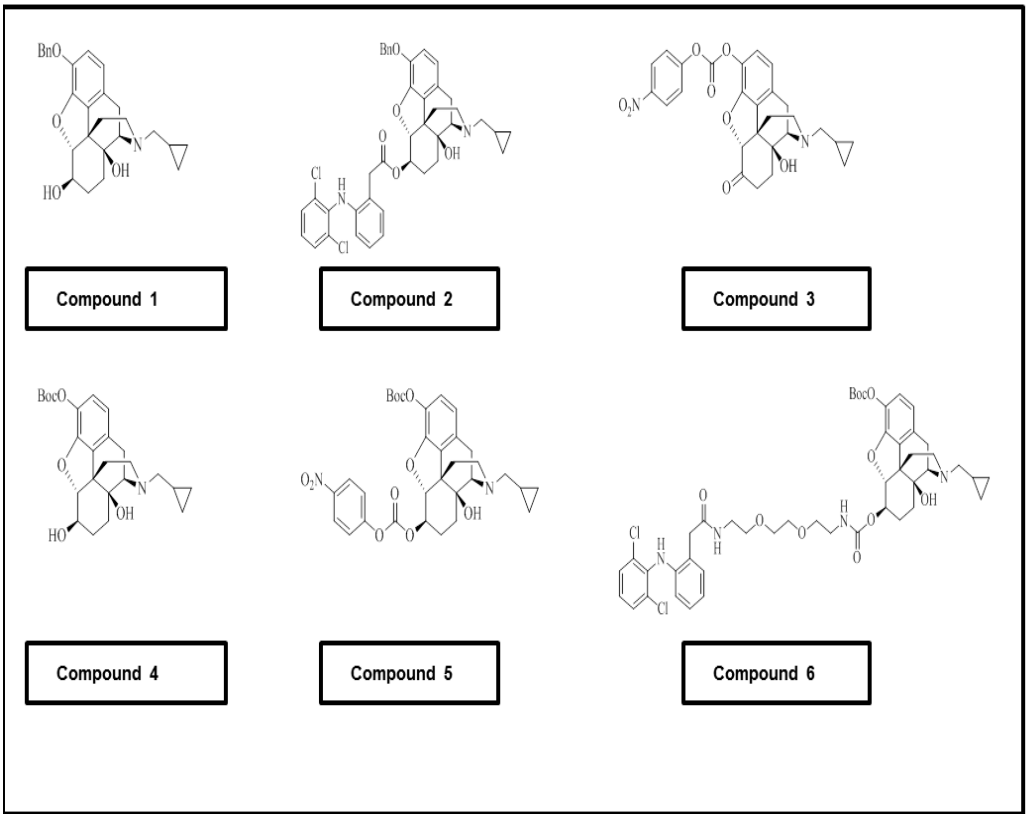

Figure 7.3 Structures of intermediates for codrug synthesis

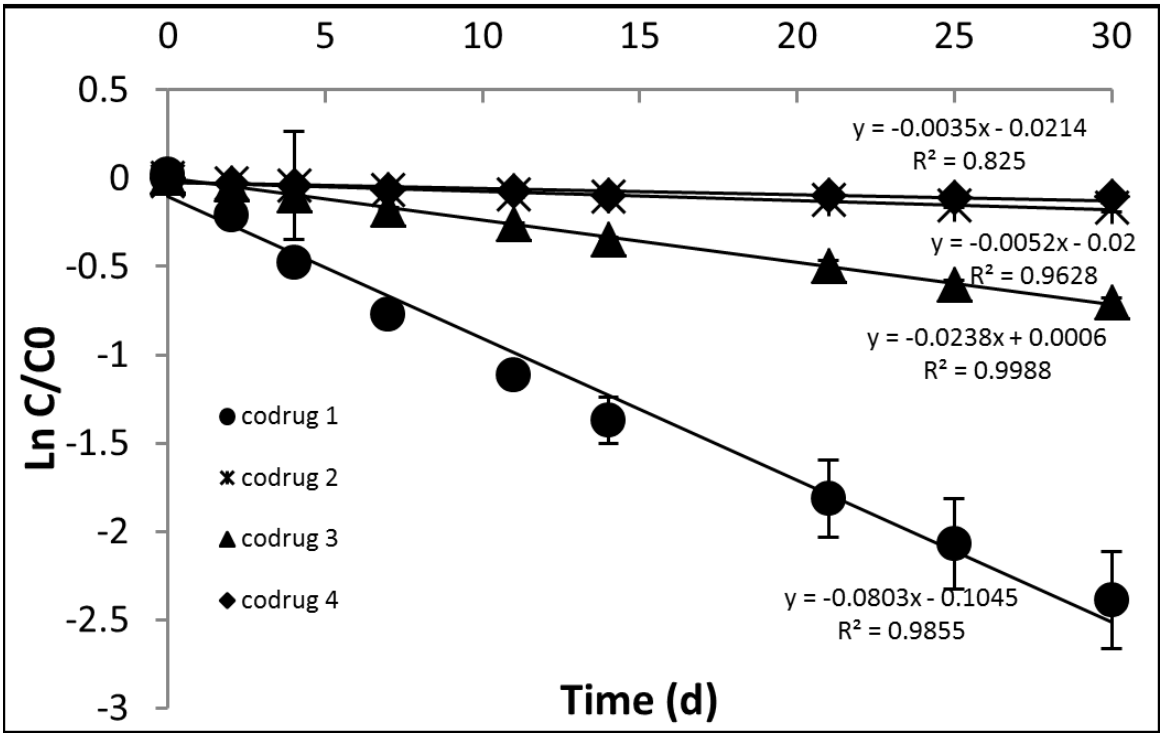

Figure 7.4 Stability of NTX/DIC codrugs in 0.3M acetate buffer pH 5.0. Data analyzed using pseudo first-order kinetics. n=3 for all codrugs

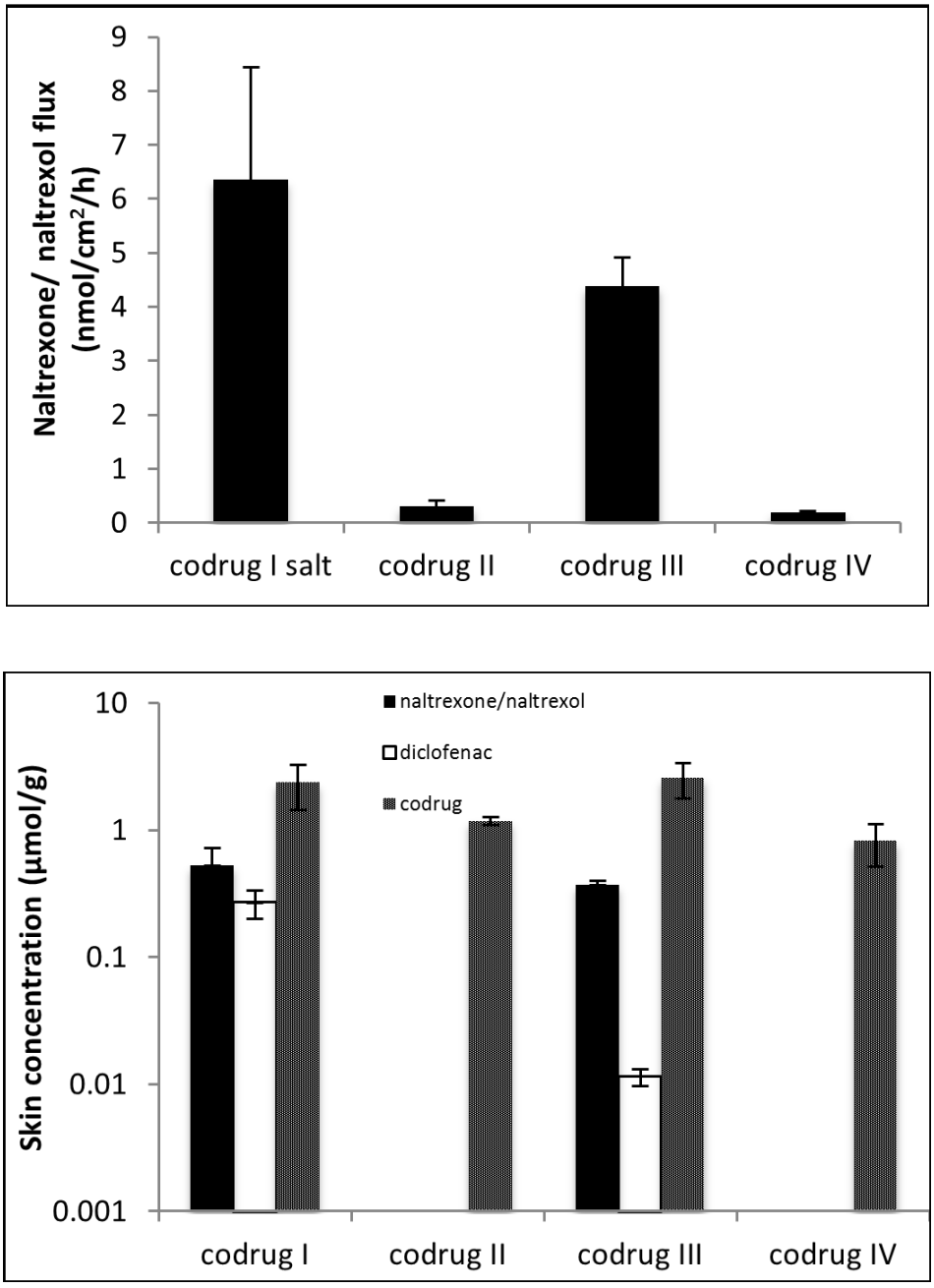

Figure 7.5 Flux of NTX/NTXol and skin concentration of parent drugs and codrugs. n≥3 for all studies. Flux of NTX from codrug I and codrug III are not significantly different ($p>0.05$) and they are higher than NTXol flux from codrug II and codrug IV ($p<0.05$). Skin concentration of NTX and codrug are not significantly different for I and III ($p>0.05$). Skin concentration of DIC is significantly different ($p<0.05$)

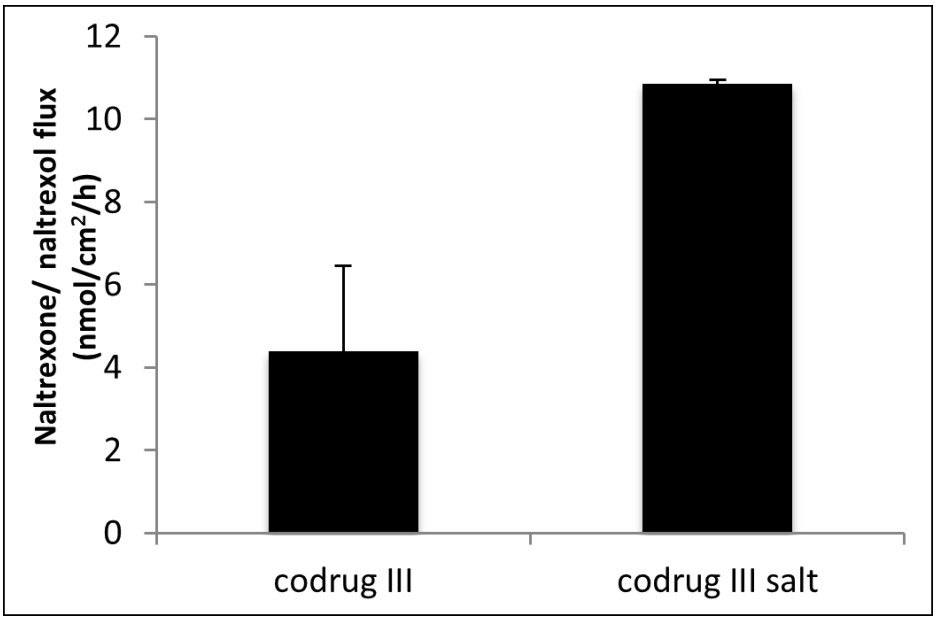

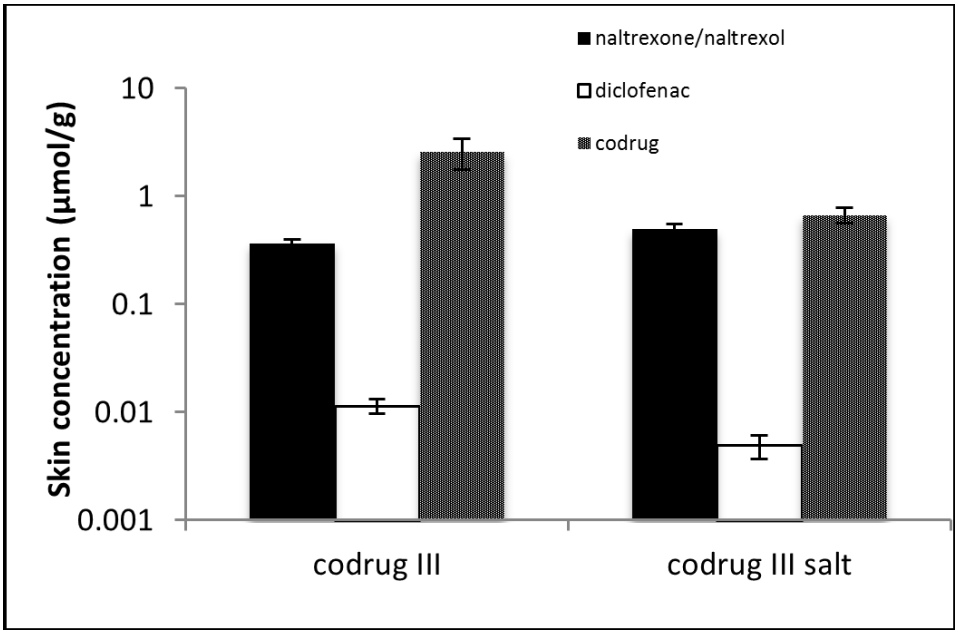

Figure 7.6 Flux and skin concentration from codrug III and codrug III salt. n≥3 for all studies. Flux of NTX was significantly higher ($p<0.05$). No significant difference in skin concentration except for codrug ($p>0.05$)

Chapter 8

Fluvastatin as a micropore lifetime enhancer for sustained delivery across microneedle treated skin

8.1 Introduction

Transdermal drug delivery allows delivery of drugs across the skin. The skin is best described as a three layer model for drug delivery purposes. From top down these layers are stratum corneum (SC), the epidermis and the dermis. Among these, the SC is the major rate limiting step to delivery of most drugs across the skin, due to its rigid structure and high lipophilicity. [1] A very small subset of molecules can effectively cross the SC barrier in therapeutically relevant amounts[29]. The structure of the SC is composed of dead keratinized remains of once rapidly dividing epidermal cells bound tightly by a lipid matrix. [29] The intercellular domain of the SC is composed of three different lipid molecules, namely cholesterol, free fatty acids and ceramide in equimolar ratio. [73, 75] There is a plethora of literature on the proposed mechanisms of recovery after SC disruption using different methods like tape stripping, acetone treatment, surfactants, etc. Formation and release of lamellar body contents is a major process in regeneration of the SC barrier following disruption or normal wear and tear. There is an initial burst (0-30 minutes) release of preformed lamellar body contents followed by the up regulation of lamellar body synthesis, which includes both lipid precursors and hydrolytic enzymes. [74, 92] Following release at the interface of the SC and epidermis, the lamellar body contents undergo extracellular processing to form comparatively nonpolar SC lipids from their polar precursors. Thus a host of enzymes and biochemical pathways are involved in proper functioning of the SC barrier. Modulation of a number of the precursors and the enzymes involved lead to malformation of the SC barrier following insult. [73, 75] A constant molar ratio of the lipids is one of the most important parameters in barrier

recovery and a decrease in synthesis of any of the three lipids or their precursors leads to a delay due to malformation of lamellar bodies. [24]

Microneedles (MN) are an alternative technique used to permeablize the SC barrier and increase the number of drugs that can be delivered transdermally. It is a physical enhancement technique. [42] There are a number of different types of MN and application techniques. Solid MN's are used to permeablize the skin followed by application of drug over treated skin, or drug coated onto the MN itself. Polymer MN's are used to load drug into the polymer itself for delivery. Hollow MN's are used in conjunction with an infusion pump to facilitate delivery of hormones and vaccines over short periods of time. [2, 27, 42] The effectiveness of MN as a drug delivery vehicle has been established in the literature over the past decade. [4, 43, 44, 47, 168] The MN delivery system is very useful for short term delivery, over a few hours. [5, 30, 57] However, the efficacy of the technique is severely limited due to normal healing processes of the skin which lead to re-sealing of the micropores anywhere between a 48-72h timeframe under occlusion. [10-12] Thus, drug can only be delivered across MN treated skin for a maximum of 3 days under occlusion. [4, 14] Lifetime of the micropore when exposed to air is much shorter and ranges from 15 minutes to a few hours depending on the MN geometry, animal model and detection method used. [10-12] The shorter timeframe of micropore resealing can be explained in terms of enhanced transepidermal water loss (TEWL) in absence of occlusion. TEWL is the most important signal for barrier recovery and lamellar body secretion following insult to the skin. [94]

Biochemical enhancers/lipid biosynthesis inhibitors prevent the synthesis of the essential lipids required for lamellar body synthesis and thus the proper formation of the SC. Local concentrations of specific inhibitors of the three lipid synthesis pathways namely cholesterol, fatty acids and ceramides can be used to alter the molar ratio and

thus delay barrier recovery . [75] The inhibitors can be used either as a pretreatment or in formulation. Some of the inhibitors that can be used for the above mechanism are 5-(tetradecycloxy)-2-furancarboxylic acid (TOFA) for fatty acid synthesis, fluvastatin (FLU) for cholesterol synthesis, and β-chloroalanine (BCA) for ceramide synthesis. [75]

The goal of the current study was to evaluate the effectiveness of FLU, an HMGCoA reductase inhibitor and the most important enzyme of the cholesterol synthesis pathway, as a pore lifetime enhancement agent for sustained drug delivery across MN treated skin. Solid stainless steel MN's were used to permeablize the skin. This technique is also known as the "poke (press) and patch" approach and is advantageous for sustained delivery because the MN is only used to permeablize the skin and does not remain in contact with skin thereafter. [42] The current efforts are directed towards enhancing the drug delivery window to 7 days, the ideal transdermal patch wear time, by using a biochemical enhancement technique in addition to MN. The study fulfills research goals 3.5, 3.6 and 3.7.

The model compound for the drug delivery project was naltrexone (NTX). It is a μ-opioid receptor antagonist used for alcohol and opioid addiction. The currently approved dosage forms include oral and an extended release intramuscular injection. [16, 17] The oral dosage form has issues with variable bioavaibility and compliance in its treatment population due to daily dosing and side effects. [16, 124] The extended release intramuscular injection is difficult to remove if there is a need for emergency opiate treatment, and also leads to injection site reactions.[17, 126] Thus NTX is a suitable candidate for transdermal patch development and an active delivery system in the form of MN is used in this project since the drug cannot be delivered in therapeutic concentrations via passive delivery. [4] It has been previously shown that by using MN, NTX can be delivered at therapeutic levels for 2-3 days in humans.[4]

8.2 Experimental section

8.2.1 Materials

Naltrexone HCl was purchased from Mallinckrodt (St. Louis, MO), and fluvastatin sodium from Cayman chemical (Ann Arbor, MI). Propylene glycol and ethanol (200 proof) were purchased from Sigma (St. Louis, MO). Acetic acid, ammonium acetate and benzyl alcohol were obtained from Fisher Scientific (Fair Lawn, NJ). 1-Octanesulfonate, sodium salt was obtained from Regis Technologies, Inc (Morton Grove, IL). Trifluroacetic acid (TFA), triethylamine (TEA), methanol, ethyl acetate and acetonitrile (ACN) were obtained from EMD chemicals (Gibbstown, NJ). Natrosol® (hydroxyethlycellulose) was obtained from Ashland (Wilmington, DE). Ethanol (70%) was obtained from Ricca chemical (Arlington, TX). Sterile water for injection was from Hospira (Lake Forest, IL) and water was purified using a NANOpure DIamond™, Barnstead water filtration system for all in vitro experiments.

8.2.2 HPLC methods

NTX and FLU were quantified using high pressure liquid chromatography (HPLC). The HPLC system consisted of a Waters 717 plus auto-sampler, a Waters 600 quaternary pump, and a Waters 2487 dual wavelength absorbance detector with Waters Empower™ software. A Perkin Elmer Brownlee™ Spheri 5 VL C18 column (5 µ, 220 x 4.6 mm) and a C18 guard column (15 x 3.2 mm) were used with the UV detector set at a wavelength of 280 nm for NTX and 305nm for FLU. The mobile phase consisted of 65:35 (v/v) ACN: (0.1% TFA with 0.065% 1-octane sulfonic acid sodium salt, adjusted to pH 3.0 with TEA aqueous phase). Samples were run at a flow rate of 1.5 ml/min. The injection volume used was 100µl for all samples.

8.2.3 *In vitro* experiments

The in vitro studies were carried out to look at the flux across MN treated skin and the skin concentrations of NTX and FLU in the skin. Full thickness Yucatan miniature pig skin was used for all in vitro experiments. All pig tissue harvesting experiments were done under IACUC approved protocols at the University of Kentucky. Fresh skin was cleaned to remove excess subcutaneous fat, dermatomed and stored at -20°C. Skin was thawed and cut into small square pieces on the day of the diffusion experiment. The thickness was measured for each individual piece of skin and the average thickness of all treatment groups was maintained between 1.4-1.8mm. Skin was next treated with a 5 MN in-plane array, 10 times in one direction and 10 times in a mutually perpendicular direction to generate a total of 100 MN insertions within the active treatment area of 0.95$cm^{2.}$ Five treatment groups were used based on the 4 different vehicles used for FLU and a control for NTX only; all studies were done in triplicate. Saturated NTX gel was prepared by mixing 90mg/ml of NTX HCl (saturated solution) with propylene glycol (PG) (10%). A 3% HEC gel of the NTX solution was used for the *in vitro* studies. The 4 different FLU treatments were FLU in 200 proof ethanol, acetone, PG: ethanol=7:3 and PG: ethanol: water=1:2:1. All the vehicles for FLU were based on previous studies looking at recovery of the skin or commonly used drug deposition methods. [72, 75] The concentration of FLU was 1.5% for all the formulations and 40µl of the formulation was applied to each cell. The receiver solution was water alkalified to pH 7.4 containing 20% ethanol at 37ºC to mimic physiological conditions. The temperature of the diffusion cell skin surface was maintained at 32ºC. Samples were collected every 6h for 48h. All samples were analyzed using HPLC. The steady state flux of NTX was calculated using the steady state portion of the cumulative amount permeated vs. time plot. The skin concentrations of both drugs were also determined at

the end of the study by extracting the drug overnight into 10ml of ACN, and injecting the extracted sample onto the HPLC column after appropriate dilutions.

8.2.4 Pharmacokinetic studies

Pharmacokinetic (PK) studies were carried out in hairless guinea pigs (HGP) using FLU and NTX to evaluate the effectiveness of FLU as a pore lifetime enhancement technique. All animal studies were approved by the IACUC at University of Kentucky and University of Maryland. All animals used had jugular vein catheters. Catheters were either implanted in the laboratory or animals were purchased with catheters from Charles River. Three treatment groups were used for the PK studies. Treatment group: 300µl of NTX gel + 40µl of FLU in ethanol (200 proof), vehicle control group: 300µl of NTX gel + 40µl of ethanol (200 proof), MN control group: 200µl of NTX gel. For PK studies, preparation of the NTX gel was similar to the *in vitro* studies except 1% benzyl alcohol was added as an antibacterial agent. All sites were treated twice with a 50 MN array to generate a total of 100MN pores and there were 2 treatment sites per animal. FLU was deposited using the ethanol solution in the active treatment group; only ethanol was used in the vehicle control group followed by NTX gel for all three groups. All sites were occluded using patches [148] for 7 days following treatment. Two hundred µl blood samples were withdrawn from the catheter at regular intervals into collection tubes precoated with 500IU/ml heparin. The blood samples were immediately centrifuged at 10,000 x g for 3 min; plasma was separated and stored at −80°C until analysis. All *in vivo* studies were carried out at least in triplicate. Data for control studies were previously reported in Nicole Brogden's thesis at the University of Kentucky.[14]

8.2.5 LC/MS-MS analysis of plasma samples

All plasma samples were extracted using a previously validated method. [146] Five hundred µl of 1:1 ACN: ethyl acetate was added to 100 µl of plasma for protein

precipitation. The mixture was vortexed for 15 seconds and centrifuged for 20minutess at 12000 x g. The supernatant was removed carefully without disturbing the pellets and dried under nitrogen in a glass test tube. The extract was suspended in 100µl ACN, vortexed, sonicated for 10 minutes and transferred to HPLC vials with low-volume inserts for injection. For plasma standards, the 100µl of the blank plasma was spiked with 10µl of ACN standards and extracted following the same method as above.

The LC/MS-MS system consisted of HPLC Waters Alliance 2695 Separations Module, Waters Micromass® Quattro MicroTM API Tandem Mass Spectrometer and Masslynx Chromatography software with Waters Quanlynx (V. 4.1) analysis software. A Waters Atlantis Silica HILIC column (5µ, 150 x 2.1mm) and guard column (10 x 2.1mm) were used for LC separation. The mobile phase composition was methanol with 0.1% acetic acid: 20mM ammonium acetate =95:5, the flow rate was 0.5ml/min and positive mode atmospheric pressure chemical ionization was used for detection of NTX (APCI+). Multiple reaction monitoring (MRM) was carried out with the following parent to daughter ion transitions for NTX•HCl *m/z* 341.8→323.8. The corona voltage was 3.5 µA, cone voltage 25 V, extractor 2 V, RF lens 0.3 V, source temp 130 °C, APCI probe temperature 575 °C. The collision gas was 20 eV. Nitrogen gas was used as a nebulization and drying gas at flow rates of 50 and 350 l/h, respectively. Injection volume was 40µl.

8.2.6 Pharmacokinetic analysis

The plasma concentration vs. time data obtained using the MS were modeled by fitting data to a non-compartmental model with extravascular output (WinNonlin Professional, version 4.0, Pharsight Corporation, Mountain View, California) to obtain pharmacokinetic parameters like area under the curve (AUC), maximum concentration (C_{max}) and time to maximum concentration (T_{max}).

8.2.7 Reversibility/recovery of pores

The reversibility/recovery of the pores following removal of occlusion was studied using transepidermal water loss (TEWL) in a HGP model. Five different sites were chosen on the dorsal region of an animal. The treatment sites were site 1: MN+NTXgel+FLU (200 proof ethanol), site 2: MN+NTX gel+200 proof ethanol, site 3: MN+placebo gel, site 4: no MN treatment+ placebo gel and site 5: occlusion only. All sites were marked and cleaned on the day of the treatment. Sites 1,2 and 3 were treated twice, with 50 MN arrays (620µm), (the two treatments being mutually perpendicular to each other to give a total of 100 non overlapping insertions) and TEWL readings were obtained before and immediately following treatment at all sites using a TEWL evaporimeter (cyberDERM, Media, PA). The concentration and amount of NTX gel and FLU were consistent with the PK studies. A placebo gel was used for site 3 and site 4. The placebo gel was similar in composition to the NTX gel with 10% PG, 1% benzyl alcohol and 3% HEC as the gelling agent. Forty µl of the 1.5% FLU in ethanol or 200 proof ethanol was applied to the treated skin at site 1 and 2, respectively and 300µl of NTX/placebo was applied to sites 1-4. All sites were occluded using a transdermal patch [147] secured in place with Bioclusive™ tape. The occlusive patch was removed after 7 days and TEWL measurements were obtained for 30-45min at all sites or until values returned to baseline (pretreatment values). All experiments were conducted at least in triplicate.

8.2.8 Skin irritation

Local skin irritation can be one of the major drawbacks of topical/transdermal delivery, so irritation studies were conducted to look at the effect of local FLU treatment of the skin in HGP. The studies were conducted using the same treatment groups as the recovery studies. Colorimeter (Chroma Meter CR-400, Konica, Minolta, Japan) readings

were obtained, in triplicate, at each site before and immediately after the treatment. The data was used to record changes in the color of the skin from baseline based on 3 different color axes, the red-green axis (a*), the black-white axis (L*) and the yellow-blue axis (b*). The sites were then occluded for 7 days and readings were obtained after removal of occlusion. The degree of redness of the skin or the change in erythema of the skin was measured by the change in the red green axis (Δa*) values. Skin irritation studies were conducted in triplicate.

8.2.9 Staining/ pore visualization studies

Pore visualization studies were carried out to look at the pores on the skin following treatment with FLU. Two sites were used on the same animal for these studies. Site 1: MN + NTX gel +FLU (200 proof ethanol) and site 2: MN : NTX gel+ 200 proof ethanol. The amount and concentration of all gels were consistent with the other studies. The skin was occluded for 7 days following treatment. Gentian violet was used to stain the skin after removal of the occlusive patch. The dye stains viable epidermis and not SC, so a grid can be clearly visualized for MN treatment/ presence of micropores in the skin, whereas no staining can be observed on skin with intact SC.

8.2.10 Statistical analysis

Data for all experiments are reported as mean ± standard deviation. Statistical analysis of data was carried out with Students' t-test and one way ANOVA with post hoc Tukey's pairwise tests, if required, using GraphPad Prism® software, version 5.04 software. $P<0.05$ was considered to be statistically significant.

8.3 Results

8.3.1 HPLC assay

NTX and FLU were quantified in ACN for skin samples and receiver samples from diffusion using HPLC. The retention times were 2.2 minutes and 3.2 minutes for NTX and FLU, respectively. All retention times are reported ±0.1 minutes. All standard curves were linear in the range of 100-10,000ng/ml, r^2>0.99.

8.3.2 Diffusion studies

The *in vitro* diffusion studies were carried out to optimize the formulations for *in vivo* studies. All formulations for FLU were chosen based on previous publications on skin recovery following FLU treatment. The NTX was formulated in 10% PG containing formulation because concentrations higher than 10% of PG have been shown to decrease flux across MN treated skin significantly. [146] The *in vitro* results indicated that there was no significant difference in flux across MN treated skin among the 5 different treatment groups (p>0.05). The skin concentration data indicated that there was no significant difference in the concentration of NTX or FLU in the skin irrespective of the method of FLU deposition (p>0.05). Ethanol (200 proof) was chosen as the vehicle for FLU deposition from these studies.

8.3.3 Pharmacokinetic studies

The pharmacokinetic studies were carried out to evaluate the effect of FLU treatment on micropore closure *in vivo* in a HGP model. The three treatment groups were evaluated either for 168h for the treatment and vehicle control groups, or for 96h for MN control. The results indicated that detectable levels of NTX were present in the plasma for 72h for all study groups. The average plasma concentration for the MN only control was below 2 ng/ml beyond 58h. The plasma concentrations from vehicle control

treatments were below 2 ng/ml beyond 144h, and plasma concentrations for FLU treatment group were above 2 ng/ml throughout the range of the study. The WinNonlin parameters indicated that the areas under the curves (AUC) for plasma concentration vs. time plots were not significantly different from each other for the treatment group and the vehicle control group ($p>0.05$). There was no lag time observed with MN enhanced delivery in any of the three groups. There was no significant difference in maximum drug concentration (C_{max}) among the 3 groups ($p>0.05$). The average plasma concentration was 39.2 ± 15.4 ng/ml. T_{max} or time to maximum plasma concentration was reached between 15 minutes and 4 hours for all studies. The standard curves in ACN and plasma were linear in the range on 1-75 ng/ml, $r^2 \geq 0.98$.

8.3.4 Recovery studies

The recovery of the skin i.e. regeneration of the barrier function of the SC was studies using TEWL were carried out to look at the effect of the local concentration of FLU on the recovery/healing of the skin on removal of occlusion. The data (Figure 8.3) is represented as a ratio of the post treatment values to the pretreatment intact skin /baseline values. Values with an enhancement ratio of less than 1 were not used for the calculation since values below baseline indicates complete reversal of treatment. The recovery studies indicated that there were no significant differences among the 5 treatment groups used for the recovery studies ($p>0.05$)

8.3.5 Irritation studies

The irritation studies were carried out to look at the effect of local FLU treatment on the skin at 7 days. The data (Figure 8.4) indicated that there were no significant differences among the treatment groups immediately following treatment or following removal of the patches at 7 days following treatment ($p>0.05$). The established positive control treatment for irritation studies in HGP is 0.5% sodium lauryl sulfate solution and

the corresponding Δa* value is 12.3. [169] All the experimental values were significantly lower ($p<0.05$)

8.3.6 Staining studies

The staining studies indicated that pores were present in the FLU treated group at the end of the 7 day patch application period compared to the absence of pores in the ethanol treated vehicle control group. In some of the studies staining was observed in the region surrounding the micropores for the treatment group. FLU is a known inhibitor of the cholesterol synthesis pathway; therefore it can influence the normal turnover of the intact skin in addition to the healing of the micropores. This process can lead to staining of the regions around the micropores.

8.4 Discussion

MN enhanced transdermal delivery has been established as a safe, effective and pain free method for drug delivery over the last decade. However, the re-sealing of the micropores is a rate limiting step in effective delivery of drugs across MN treated skin for more than 48 hours. Pore lifetime enhancement methods have been explored in the literature to enhance the drug delivery window. One such method is topical application of Solaraze® (3% diclofenac sodium, 2.5% hyaluronic acid), a non-steroidal anti-inflammatory drug. The hypothesis was that inhibition of the cyclooxygenase pathway would lead to decreased local subclinical inflammation following MN treatment, thus enhancing the drug delivery window. The results from impedance spectroscopy, TEWL and PK studies in animal models and humans indicated that daily/alternate day application of diclofenac allowed drug delivery for a period of 7 days compared to 2-3 days in the absence of a pore lifetime enhancement agent in formulation, following MN treatment. [8, 9, 14] However, the studies required frequent application of diclofenac, which is not ideal for a 7 day transdermal patch system and formulating high concentrations of

diclofenac at the skin surface pH of around 5 was difficult due to the physicochemical properties of the molecule.

The current study was designed to evaluate the role of FLU, a lipid biosynthesis inhibitor, as a pore lifetime enhancement agent. Expression levels of mRNA of most enzymes of the lipid biosynthesis pathway are upregulated following insults to the SC barrier. [74] Inhibitors of these enzymes have been shown to delay barrier recovery following acetone or surfactant treatment. [75] Since the exact nature of barrier insult following MN treatment is not well established, the goal of the current study was to evaluate the effect of FLU as a one-time topical application on micropore healing and drug delivery using pharmacokinetics and TEWL for evaluation. It was believed that frequent reapplication or formulation issues would not arise with the FLU treatment as compared to diclofenac, since only very small concentrations of potent lipid biosynthesis inhibitors were required for previously published studies,. The hypothesis was that down regulation of cholesterol synthesis would lead to delay in barrier recovery and enhance the drug delivery window. FLU (M.W. 411.47, log P 4.6, pKa 4.27) was chosen over other lipid biosynthesis inhibitors because it is a well-known statin drug and the dosage, metabolism, pharmacokinetics and toxicity profile is well established in humans. [16, 19] The lowest therapeutically relevant oral daily dose is 20 mg and the oral bioavaibility is 9-50%. [16] Therefore, even if the bioavaibility is 100% from the topical formulation, the maximum delivered dose would be 1.2 mg over 7 days, which is significantly below the therapeutic dose. In comparison, TOFA and β-chloroalanine are investigational drugs with very limited data being available.

Optimization of formulation for *in vivo* studies was required in order to maximize FLU skin concentration and NTX flux. Four different methods were chosen for FLU deposition. The results indicated that there was no significant difference in NTX flux or

skin concentration of FLU using any of the deposition methods. Ethanol (200 proof) was chosen for *in vivo* studies because it is a frequently used topical excipient and most of the 40 µl ethanol used was allowed to evaporate before application of the drug gel. Acetone is similar in action to ethanol; however it caused irritation in the MN-treated animal models (data not shown) and thus was not used for *in vivo* studies. The other two formulations tested contained either 70% or 25% PG. PG has been shown to interact with the underlying dermis and microchannels in MN treated skin. [146] The high viscosity of PG rich formulations significantly decreased flux across MN treated skin, as compared to an aqueous formulation. [22] The formulations also contained large amounts of ethanol, a known permeation enhancer, and evaporation of the ethanol from these was not as efficient due to the presence of PG. Solubility of FLU was not an issue with any of the formulations. Therefore, 40 µl of 1.5% FLU in 200 proof ethanol was chosen as the vehicle for FLU deposition for all *in vivo* studies. Ethanol is a well-known chemical enhancer used in the topical/transdermal industry. It acts by replacing the water molecules in the lipid polar head groups as well as the protein regions of the SC, thus enhancing free volume and permeability of molecules across the skin. [69] Therefore, a control was used in PK, recovery and irritation studies to evaluate the effect of ethanol alone on micropore lifetime.

PK studies are the most direct measure of drug delivery and micropore closure. Three different groups were evaluated to look at the effect of FLU in ethanol and MN, ethanol only and MN, and MN only in HGP. A non-MN treated control was not evaluated for animal studies since it is known that permeation of ionized species like NTX HCl is limited across the intact SC. The PK data indicated that for the MN only control, plasma concentration dropped below 2 ng/ml beyond 58h. This data is in agreement with previously published pharmacokinetic data where the drug delivery window following one

time application of MN has been shown to be between 48-72 hours. [4, 8] The treatment group showed NTX levels above 2 ng/ml for the entire length of the study, as compared to the vehicle control group which showed levels above 2 ng/ml until 144hours. The AUC values for the treatment group and the vehicle control group were not significantly different from each other indicating that ethanol treatment alone also enhanced the drug delivery following MN treatment. As mentioned before, ethanol is a known permeation enhancer used in passive transdermal delivery. However, the role of ethanol has never been evaluated in MN enhanced delivery. Since an intact skin control with ethanol treatment was not evaluated in the current study, it is difficult to assess the exact mechanism via which the drug delivery window was enhanced. A direct comparison is difficult because evaluations of NTX plasma concentrations resulting from delivery of NTX HCl across intact skin are limited by the LLOQ of the LCMS-MS assay. The C_{max} and T_{max} values indicated that treatment of all animals were consistent across the treatment groups. Drug was quantified in plasma within 15 minutes of treatment indicating that there is no significant lag time associated with the patch system. Such profiles are commonly observed for MN treatment and immediate delivery in addition to sustained release is one of the advantages of such a delivery system. The shape of the plasma concentration time curve is consistent with reported profiles of MN enhanced delivery, where a peak is observed immediately following patch application followed by a decline in the plasma concentration due to re-sealing of the micropores. Such data can be modeled using a 3 compartment model for drug permeation across skin, pharmacokinetics of the drug in the body, and healing of the micropores. [146] Rate of micropore re-sealing in the presence of an active pore lifetime enhancement agent can then be estimated if permeation values are known from *in vitro* studies and PK estimates are obtained from *in vivo* studies. Thus from the PK studies it can be concluded that both

FLU and an ethanol vehicle can be used to enhance the drug delivery window, however the exact mechanism of ethanol action is not known.

Recovery of the skin i.e regeneration of barrier function and irritation of skin following local application of biochemical inhibitors and permeation enhancers are important aspects during development of transdermal delivery systems for chemical enhancement techniques. [66, 67] Therefore, recovery of the skin following removal of treatment at 7 days was monitored using TEWL. Five sites were compared for the recovery and irritation studies. In addition to the treatment group and vehicle control, site 3 was used to evaluate the role of the NTX gel, site 4 was used to evaluate the effect of MN treatment, and site 5 was only occlusion used to control for TEWL enhancement at all sites due to occlusion alone. There was no significant difference among the sites following removal of treatment or at any of the later time points indicating that recovery of the skin was not influenced by the presence of FLU or ethanol. Recovery of the skin was expected, since removal of occlusion leads to increased TEWL across disrupted SC, which in turn acts as one of the major signals for lamellar body release and skin healing. [94] Irritation data also indicated that there was no significant difference among the sites and Δa* values, and all sites were much lower compared to the positive control in HGP, the most sensitive model for skin irritation for transdermal and topical studies.

The staining studies were conducted to visualize the micropores at the end of the 7 day period. The studies were used as a visualization technique for presence of micropores for correlation with PK data. The studies indicated that micropores could be visualized in FLU treated groups; however they were not present for the ethanol control group at 7 days. NTX concentration in the plasma of the ethanol treated group was <2ng/ml at 7 days probably indicating that micropores had re-sealed by that time. A time dependent study for the ethanol treated group with time points on day 5 and 6 in addition

to day 7 would help with better correlation of pore visualization to the PK data. The FLU treated group showed additional staining in the regions between the micropores. Cholesterol is required for the normal turnover process of the SC in addition to healing. Thus it might be possible that local application of the inhibitors decreased cholesterol synthesis in the entire treated region leading to malformation of the barrier. However this should not be of additional concern for FLU treatment because both recovery and irritation studies indicated that there was no significant effect of the treatment following removal among the groups.

Thus overall the FLU in ethanol treatment was effective in enhancing the drug delivery window of NTX but the exact role of ethanol and FLU could not be evaluated in this study. Further, pretreatment with MN and FLU before application of the NTX gel is a three step process which is not practical outside a clinic setting. Therefore further optimization of formulation is required for incorporation of NTX and FLU into a single formulation. The other inhibitors of the lipid biosynthetic pathway in addition to FLU could be evaluated separately or in combination to understand their role in micropore lifetime enhancement. Synergistic effects of enhancement strategies and inhibitors have been reported previously.

8.5 Conclusion

The current study was conducted to evaluate the role of FLU as a pore lifetime enhancement agent. The data indicated that FLU pretreatment allowed delivery of therapeutically relevant NTX for 7 days while treatment with the ethanol vehicle allowed delivery upto 5 days. Recovery of the skin following removal of treatment and irritation issues due to local application of FLU were not significant with the current drug delivery system. Staining studies further confirmed the presence of micropores on the skin at 7 days for the FLU treatment. Thus in conclusion, FLU in ethanol was effective in

enhancing micropore lifetime, however the exact mechanism of enhancement could not be clearly evaluated from the current studies, and further evaluation is needed.

Table 1: WinNonlin parameters from pharmacokinetic studies

	Treatment group	Vehicle control	MN control
C_{max} (ng/ml)	38.1 ± 19.7	39.3 ± 19.2	39.4 ± 11.5
T_{max} (h)	2.7 ± 3.8	1.4 ± 1.7	2.8 ± 2.0
AUC (ng*h/ml) (time for AUC calculation)	1411.1 ± 1040.5 (146.7 ± 24.4)	1696.1 ± 1665.8 (151.0 ± 25.7)	613.5 ± 212.9 (80.0 ± 13.9)
C_{ss} (ng/ml)	9.3 ± 5.6	11.1 ± 9.7	7.5 ± 1.5
n	3	4	3

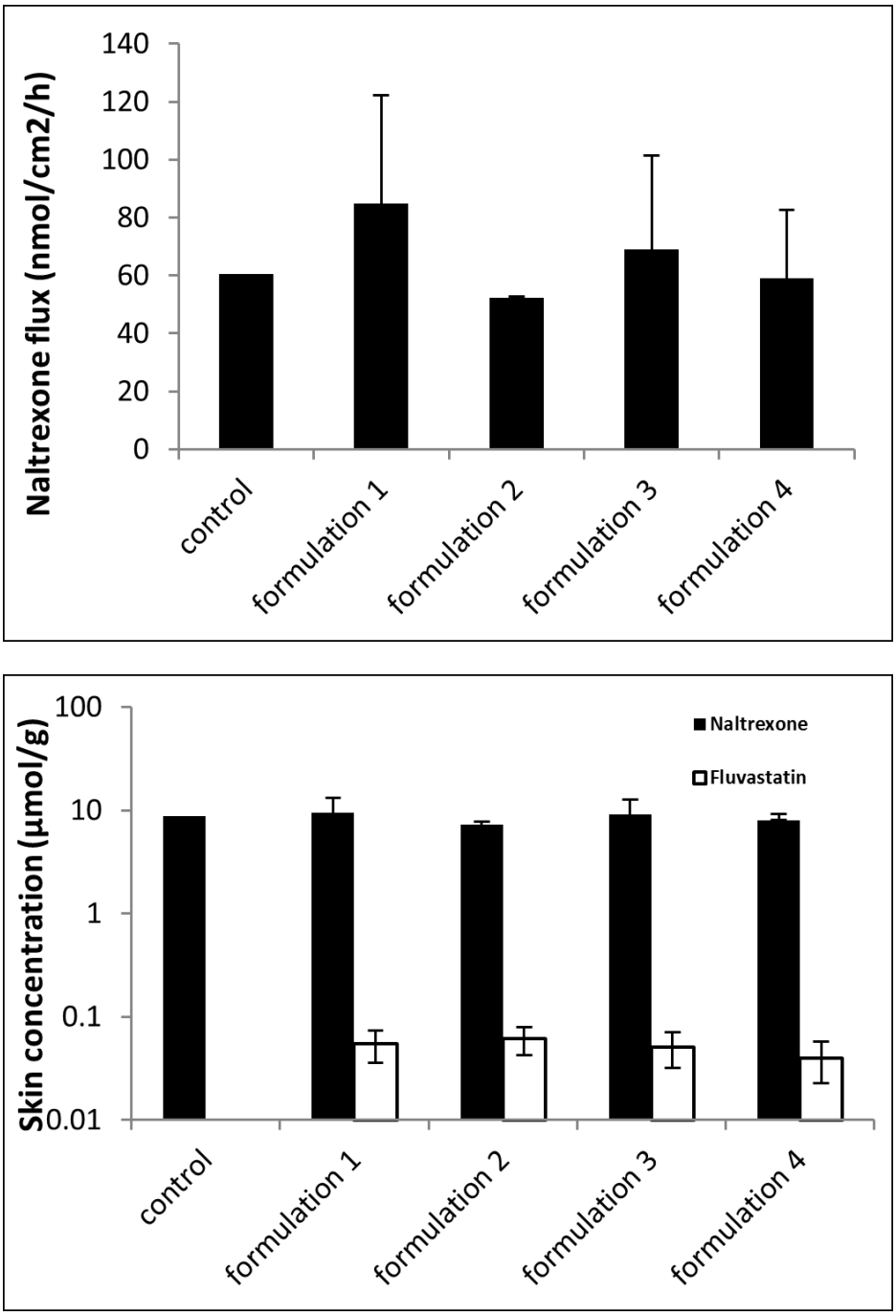

Figure 8.1 Formulation optimization for application of FLU along with NTX gel. Flux of NTX across MN treated skin (top panel), skin concentration of NTX and DIC across MN treated skin (bottom panel). n≥3 for all studies except control NTX. p>0.05 for flux and skin concentration data among all groups.

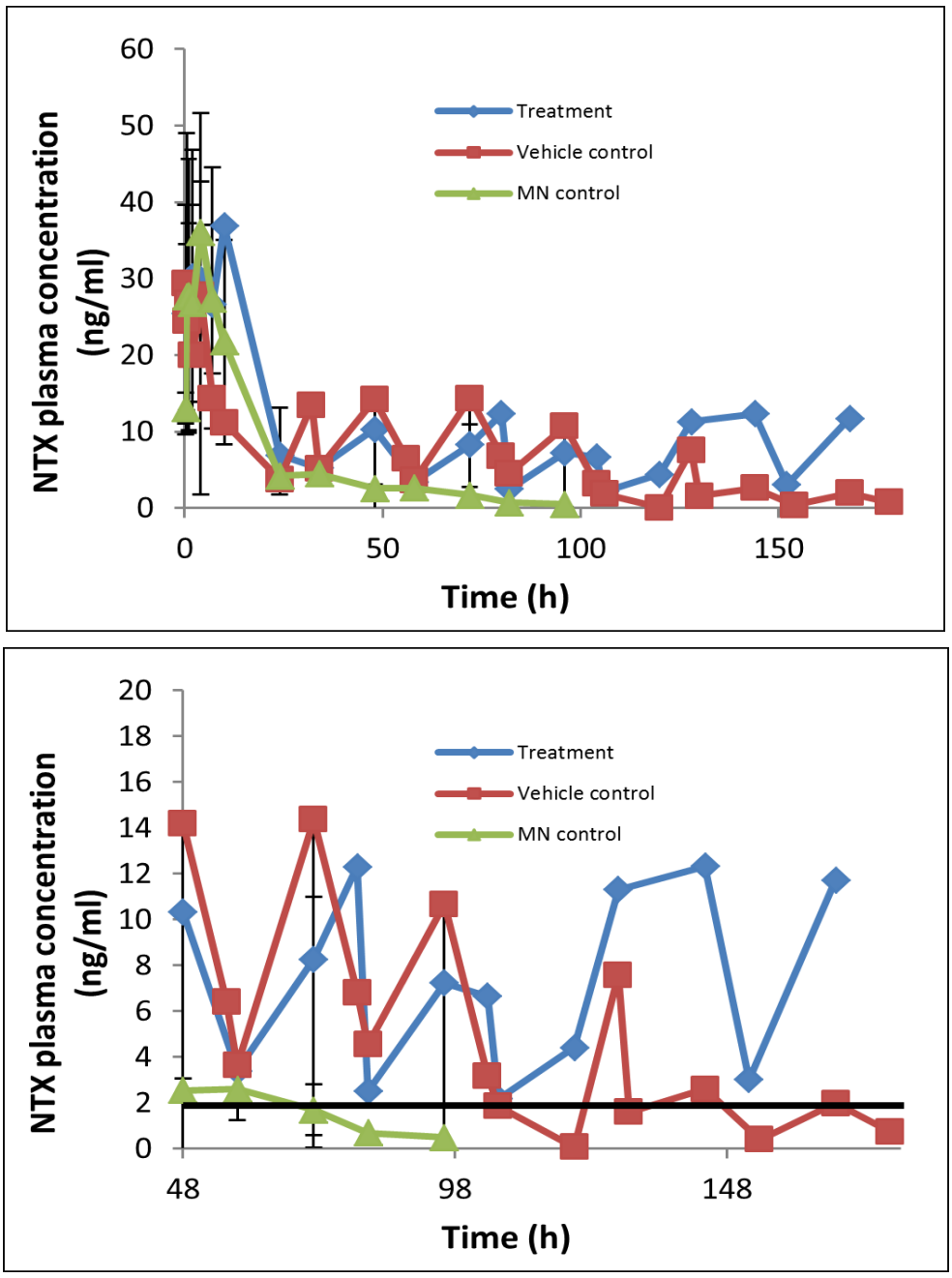

Figure 8.2 NTX plasma concentrations in HGP following application of MN and FLU, MN and vehicle control or MN only. Full profile (top panel) and later timepoints (bottom panel). n≥3 for all studies. The data indicated that there was no statistical difference in AUC between the FLU treated group and vehicle control group. Plasma concentration was below 2ng/ml for vehicle control group beyond 144 hours.

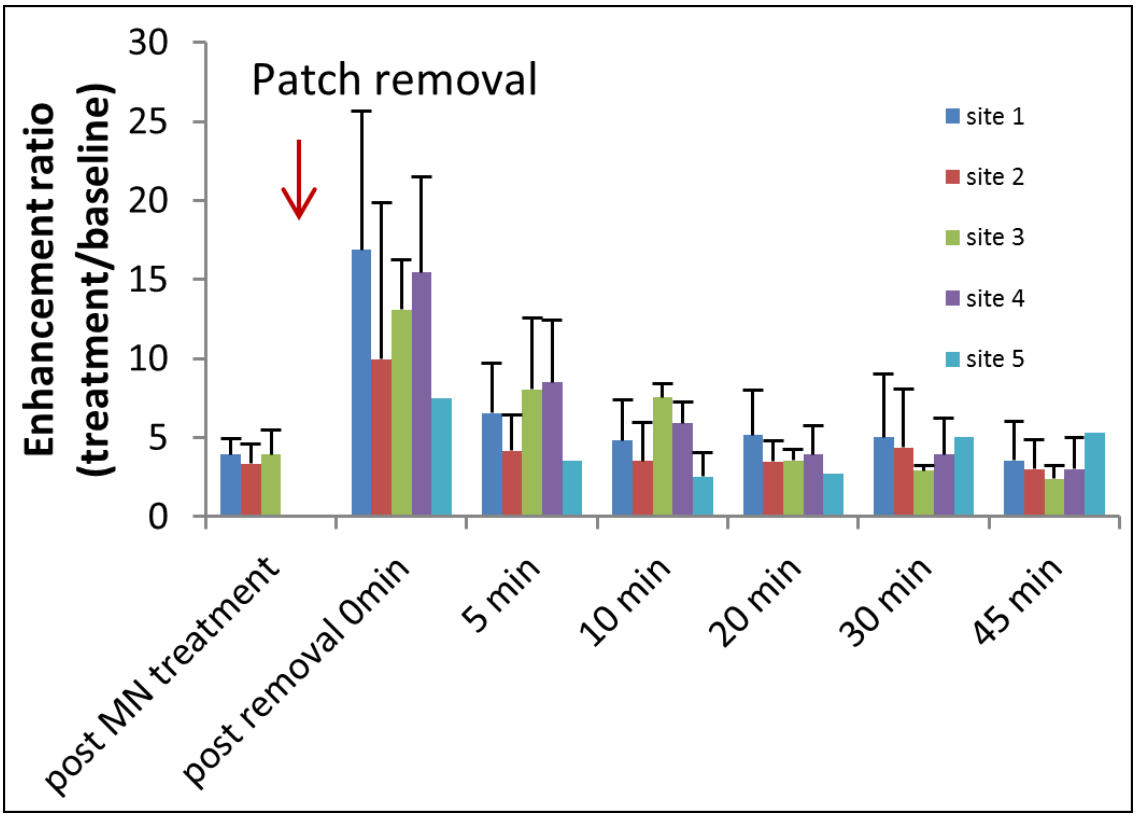

Figure 8.3 Recovery of skin following 7 day treatment with FLU using TEWL. Measurements were obtained before, immediately following treatment and after removal of patches at 7 days. n=3. Data is presented as a ratio of TEWL enhancement over baseline.p>0.05 among all sites

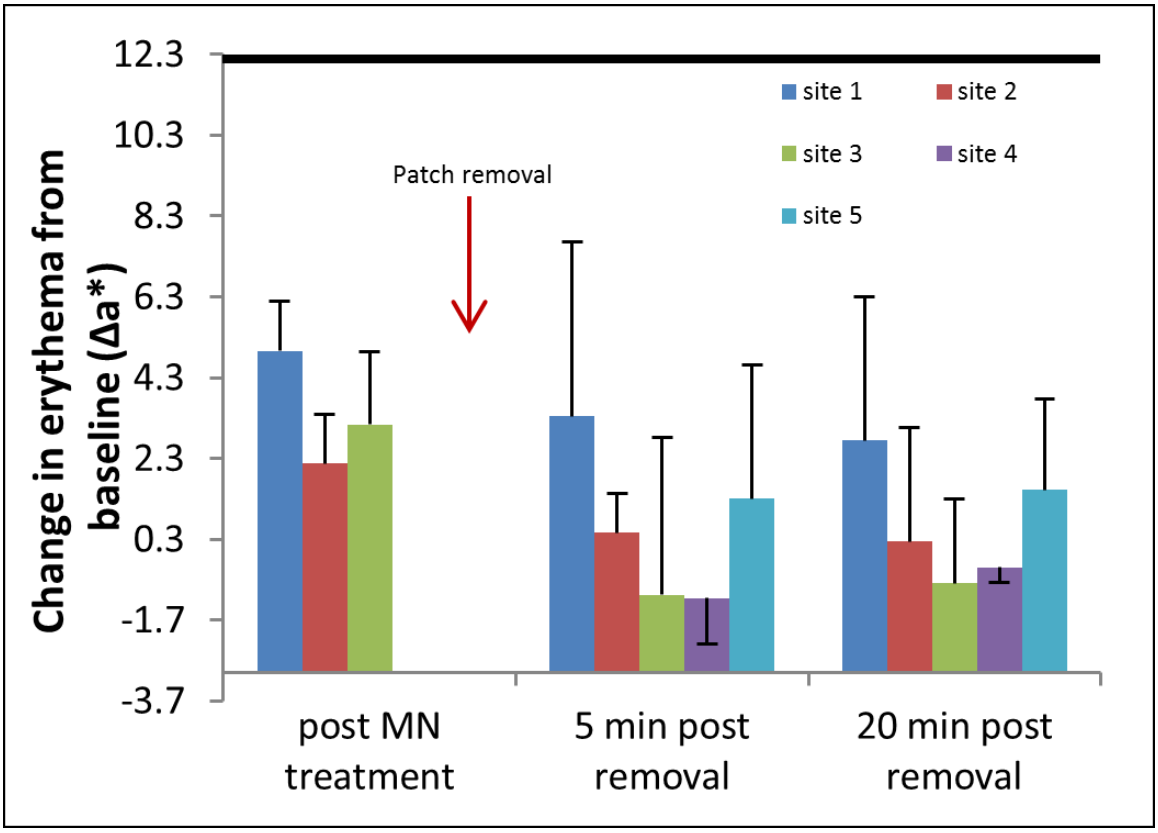

Figure 8.4 Change in erythema of the skin following 7 day treatment with FLU using colorimetry. Measurements were obtained before, immediately following treatment and following patch removal at 7 days. n=3, p> 0.05 among all sites. Positive control for skin irritation is from [169]

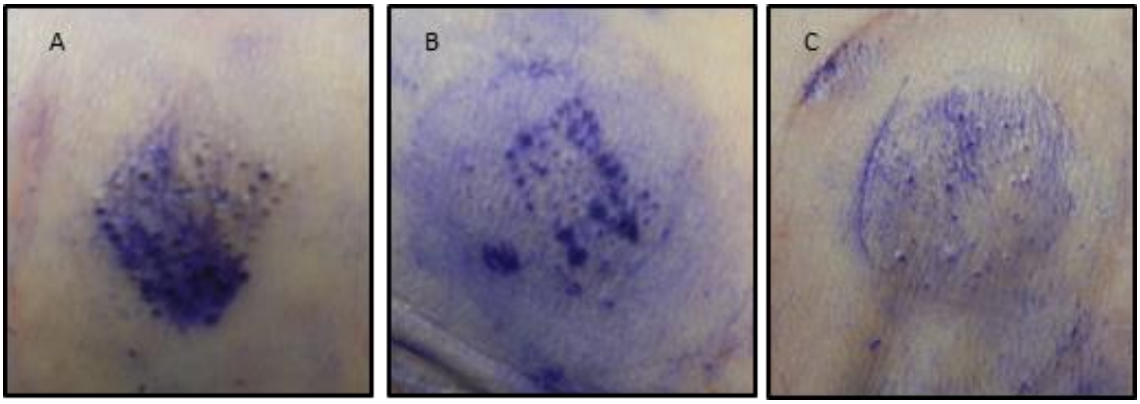

Figure 8.5 Gentian violet staining in HGP at 7 days following treatment with 1.5% FLU in 200 proof ethanol (A) and (B) or 200 proof ethanol only (C). The images show that pores can be visualized at 7 days following FLU treatment in HGP while staining of pores cannot be visualized in the ethanol control

Chapter 9

Conclusions and future directions

The overall goal of the project was to optimize formulation for sustained drug delivery across microneedle (MN) treated skin. Naltrexone (NTX) has been used as the model compound to optimize drug delivery following the “poke and patch” method of MN treatment. Currently, NTX can be delivered across MN treated skin for 48-72 hours under occlusion and up to 7 days using daily/alternate day topical application of Solaraze®. NTX is used for alcohol and opioid addiction and a 7 day transdermal patch system could be beneficial for such treatment. Since NTX doesn’t permeate at a therapeutic rate through intact skin, MN has been used as a physical enhancement technique. The project was focused on optimizing formulation for extending the micropore lifetime following one time application of MN.

Three different strategies were investigated in the current project. The first strategy was to utilize the pH of the formulation for extending micropore lifetime and enhancing transport across MN treated skin. The effect of pH on micropore healing was evaluated using impedance spectroscopy. Although, pharmacokinetic studies provide the most direct measurement of drug delivery/ micropore healing, such studies are time consuming and expensive. Impedance spectroscopy is an alternative technique where resistance drop across the skin or impedance of the skin is used as a surrogate marker for measurement of the barrier properties of the skin. Earlier studies have shown that when the “acid mantle” of the skin barrier is destroyed following insult, recovery of the skin is delayed at pH 7.4 compared to pH 5.5. [18] The results can be explained in terms of the reduced activity of β-glucocerebrosidase, an important enzyme of the ceramide biosynthetic pathway. However, the exact nature or depth of injury following treatment with MN (of the specific geometry) is not very well understood. Thus it is not known

whether the “acid mantle” is actually destroyed following MN treatment and the time frame associated with the process. Impedance measurements over a period of 100 hours following MN treatment indicated that there were no significant differences in the rate of micropore healing at pH 5.5, pH 6.5 and pH 7.4 after the initial 24 hours. Since the goal was to extend micropore lifetime for up to 7 days, formulation pH cannot be used to achieve the desired results. There could be several factors influencing the results of these studies. In previously reported studies in the literature, the nature of the skin insult was different. Tape stripping or acetone treatment was used to destroy the barrier properties of the skin, and measurements were obtained up to a maximum of 24 hours following insult. [18] Thus it is possible that for MN treatment, either the “acid mantle” is not destroyed or its properties are recovered within the first few hours due to rapid release of the lamellar body contents, and thus no long term effects of formulation pH are observed on healing of the micropores.

Formulation pH was also used to evaluate the role of ionization state of the molecule on transport across MN treated skin compared to intact skin. NTX is a weak base and the most acidic pKa of NTX is 7.5.. Flux of NTX base was compared from 6 different pH values (pH 5.76, pH 6.30, pH 6.43, pH 6.72, pH 7.56, pH 8.26) across MN treated skin. The results indicated that a lower pH formulation led to significantly higher flux values across MN treated skin; however there was no significant difference in flux across intact skin. Thus the rate limiting step for delivery of drugs in MN enhanced delivery is the drug concentration in the formulation and not the lower layers of the skin. This is different from intact skin delivery where the stratum corneum (SC) is the rate limiting step in delivery of most molecules, and the lower layers of the skin are rate limiting only for highly lipophilic molecules (generally log P>5). Further analysis of flux via the microchannel pathway and the intact skin pathway (skin surrounding the MN

pores for MN treatment) indicated that as the unionized component of the drug increased in formulation with increase in pH, the contribution of the MN pathway flux towards total flux also decreased. This indicates that when a completely ionized molecule is used for transport across MN treated skin; transport is mostly via the aqueous/porous pathway created in the skin due to MN treatment. However when a unionized molecule is used, transport takes place via the intact skin surrounding the MN treatment and there is no significant difference in the flux across MN treated skin vs. intact skin. This is important for formulation of molecules for MN enhanced drug delivery systems since the advantage of MN is only obtained when permeation takes place through the MN pathway, in addition to the intact skin pathway to generate the increased total flux. Permeability calculation indicated that there were no significant difference in permeability across the pH range for MN treated skin, permeability increases with increase in pH (decreased ionization) for NTX across intact skin. Thus the enhanced flux at lower pH values is due to enhanced solubility of the ionized drug in an aqueous formulation. Modeling of the permeability data using permeability of the ionized and unionized form of the drug across the microchannel pathway and intact skin pathway allows for better understanding of the transport, and contribution of each species towards total flux. The models can be further used to calculate permeability of a host of drug molecules across the pH range if the pKa, intrinsic solubility, and permeability of the ionized form across the MN pathway are known. This would help in reducing wet lab experiments and facilitate faster optimization of formulation for MN-enhanced and intact skin delivery.

The second approach was to use codrugs of NTX/naltrexol (NTXol) and diclofenac (DIC). Solaraze® (3% diclofenac sodium, 2.5% hyaluronic acid) has been used in previous studies to show that local application of Solaraze® can be used to

extend micropore lifetime for up to 7 days following MN treatment. However, DIC is an acid with a pKa of 4.2 and solubility of DIC is low around the formulation pH of 5 for NTX. Precipitation is observed on top of the skin on co-application of NTX and Solaraze®. Such precipitation reduces the permeation of NTX across micropores which in turn decreases the plasma concentration of the drug. Additionally, daily/alternate day application of Solaraze® was required for therapeutic efficacy which is not ideal for a 7 day transdermal patch system. In order to solve the drug delivery issue codrugs were designed and evaluated for therapeutic efficacy *in vitro* and *in vivo*. A NTX-DIC ester codrug (codrug I) was used for proof of concept studies to evaluate bioconversion of codrug in the skin, permeation of NTX and local skin concentration of DIC. The results indicated that the codrug bioconverted in the skin to regenerate parent drugs but the flux of NTX from the codrug was not high enough so a hydrochloride salt form was used to enhance flux, since it is known that ionized molecules with higher aqueous solubility lead to enhanced flux across MN treated skin. A proof of concept hairless guinea pig (HGP) staining study was used to show that micropores were present on the skin at the end of 7 days using the codrug, indicating that the codrug strategy could potentially be used for drug delivery. However, the codrug had a short half-life and significantly lower flux compared to the most optimized NTX formulation, so structure optimization was required for better stability and flux enhancement. 6-β NTXol, the active metabolite of NTX, was used along with NTX to design codrugs along with amide and carbamate linkages for better stability. A polyethylene glycol (PEG) chain was used to link the molecules where direct linkage was not possible, to further enhance solubility. The results from 4 codrugs synthesized indicated that all codrugs bioconverted in the skin, and the NTX codrugs were less stable due to the phenolic linker compared to the secondary alcohol linker used for the NTXol codrugs. However, permeation studies across Yucatan miniature pig (YP) skin showed that permeation of NTXol from codrugs was significantly lower

compared to NTX codrugs, and parent drugs were not quantified in the skin for the NTXol codrugs. Since the presence of diclofenac from the codrug in the epidermal region of the skin is imperative to the therapeutic efficacy of codrugs, only NTX codrugs from the current design can be used for development of a drug delivery system. Skin concentration of DIC was lower from codrug III (amide/carbamate PEG linked codrug) compared to codrug I, and subsequent investigation indicated that complete bioconversion of the amide linkage did not take place in the skin. Codrug III HCl salt was further evaluated to maximize flux and future studies for the project would include *in vivo* pharmacokinetic studies with codrug III HCL salt. Optimization of the linker at the DIC end of the codrug molecule might be necessary for faster release of DIC, if the current skin concentration is not optimum for keeping the micropores open for a 7 day period following one time application of MN. Further modification of formulation might also be necessary to retain DIC in the skin longer, since hyaluronic acid (HA), the excipient used in Solaraze®, facilitates retention of DIC in the upper layers of the skin. It has been shown that HA alone is not responsible for extending micropore lifetime, but the effect of HA in the DIC formulation is not clearly understood yet. [9]

The third strategy was development of a topical/transdermal system using small quantities of fluvastation (FLU), an inhibitor of the cholesterol synthesis pathway, as a topical application followed by transdermal delivery of NTX. A constant molar ratio of the essential SC lipids-cholesterol, fatty acid and ceramide is imperative to the proper formation of the SC barrier. Inhibitors of the metabolic pathways have been shown to decrease synthesis of the SC lipids or inhibit their extracellular processing, thus leading to malformation of the SC barrier following insult. [75] The main advantage of this strategy over DIC is the fact that very small concentrations (40 µl, 0.5-1.5%) of inhibitors have been used to show efficacy in previously reported studies using alternate methods of

barrier disruption. Different deposition methods were used to evaluate the effect of topical application of FLU on flux of NTX across MN treated skin. Ethanol (200 proof) was chosen as the vehicle for FLU deposition for *in vivo* pharmacokinetic studies, irritation and recovery studies. The choice of vehicle was based on ease of application of drug in an ethanol based vehicle, PG containing vehicles were not used due to effect of PG on flux across MN treated skin.The pharmacokinetic data indicated that local application of FLU allowed NTX delivery across MN treated skin for 7 days. Topical application of ethanol alone as a vehicle control also enhanced transport of NTX and extended micropore lifetime compared to NTX only control animals for up to 5 days, however it was not effective in delivery of NTX in therapeutically relevant concentration for 7 days. Ethanol is a known permeation enhancer thus increased permeation of NTX in presence of ethanol was expected, however the exact mechanism of action could not be elucidated from the current study. There was also no significant difference in area under the plasma concentration vs. time curve (AUC) between the treatment group and the vehicle control group. This can be attributed to the huge variability associated with the study and the limited animals per group. Recovery of the skin following removal of treatment was monitored to ensure that local application of inhibitors did not lead to a permanent effect on skin/micropore healing. The results indicated that there was no significant difference in recovery of the barrier function following removal of treatment between inhibitor treated sites and controls. Irritation due to inhibitor as well as ethanol application was also a concern. Colorimetric studies were used to evaluate the redness/irritation potential of the skin. Results indicated that there was no significant irritation due to topical application of the inhibitor. Staining studies were conducted to visualize micropores following 7 day patch application period. Gentian violet staining indicated that ethanol did not keep the pores open for 7 days; however micropores were visible for FLU treated sites. The skin around the micropores also exhibited nominal

staining in the FLU treated group indicating that presence of topical inhibitors influence the normal turnover process of the skin in the region between the micropores, in addition to the micropores. However this did not lead to any irritation in HGP, the most sensitive model, so should not be of concern for development of a drug delivery system.

Inhibitors of the other pathways of lipid synthesis can also be used to enhance micropore lifetime. Some examples include TOFA for fatty acid synthesis and β-chloroalanine for ceramide synthesis. Concentration of the inhibitors as well as the application method can be further optimized to enhance the effect. A three-step application process for a transdermal patch system is not patient friendly outside a clinic setting, thus further optimization of formulation is also required to incorporate NTX and the lipid biosynthesis inhibitors in a single formulation.

Thus, overall the current research investigated three different mechanisms for micropore lifetime enhancement and sustained NTX delivery. Formulation pH can be used to maximize NTX transport however a higher pH formulation was not useful for enhancement of micropore lifetime. The codrug approach can be used for NTX delivery across the MN treated skin for up to 7 days. Future pharmacokinetic studies with codrug III salt will further validate the efficacy of the drug delivery system. Topical application of lipid biosynthesis inhibitors, such as FLU, can also be used to deliver NTX for 7 days. Further optimization of the application process is required to decrease variability in the data.

The current research was conducted using NTX as the model compound. Although development of a 7 day transdermal system for NTX is important, one of the major areas where MN delivery can provide a huge advantage is delivery of macromolecules, like proteins and peptides. Protein and peptide therapeutics are quickly becoming the first line of treatment for a host of diseases. [170,171] One of the major issues in development of protein therapeutics is that oral delivery of these compounds is almost

impossible due to the fact that the gastrointestinal tract is designed for degradation of proteins. The chemical and biochemical challenges involved in oral delivery include acid hydrolysis in the stomach, enzymatic degradation in the intestine and bacterial fermentation in the colon. [172] The physicochemical characteristics of these protein/peptide drugs, including molecular weight and hydrophillicity, prevent effective transport across the intact skin by passive delivery. Therefore, several protein drugs have been evaluated for transdermal drug delivery using physical enhancement techniques like iontophoresis, ultrasound, etc. Some examples include calcitonin, vasopressin and insulin. [173,41] MN will thus be an excellent alternative method for delivery of macromolecules. Recent studies have evaluated short term macromolecule delivery using MN to establish efficacy. Parathyroid hormone (PTH) therapy using MN has been shown to be effective in phase 2 clinical trials. [57] Thus translating our current understanding of MN enhanced delivery of small molecules to macromolecules will be beneficial towards the development of the field. One unique aspect of MN enhanced transdermal delivery of the macromolecules is the spike in the plasma concentration profile. A steady state plasma profile is usually associated with passive delivery. The peak in the plasma concentration has been attributed to lymphatic uptake of macromolecules, compared to systemic uptake of small molecules. [56] It will be interesting to study the effect of micropore healing in addition to lymphatic uptake on plasma concentration for long term delivery of macromolecules across MN treated skin.

Appendix I

Synthetic schemes for codrugs

Synthetic scheme for codrug I

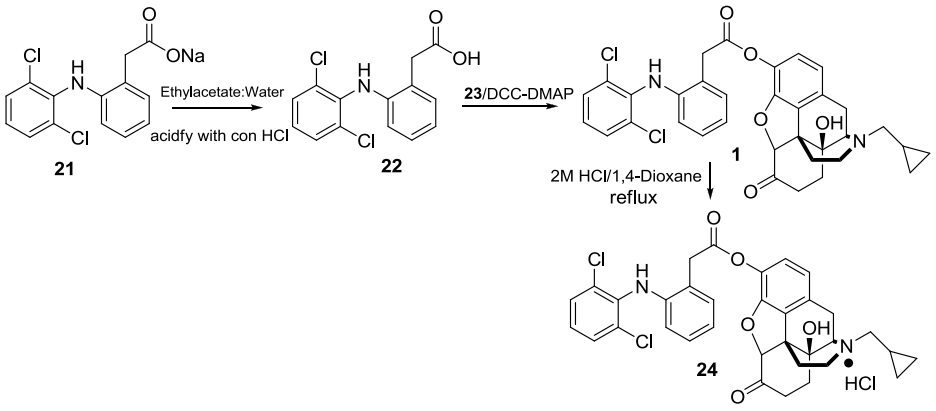

Synthetic scheme for codrug II

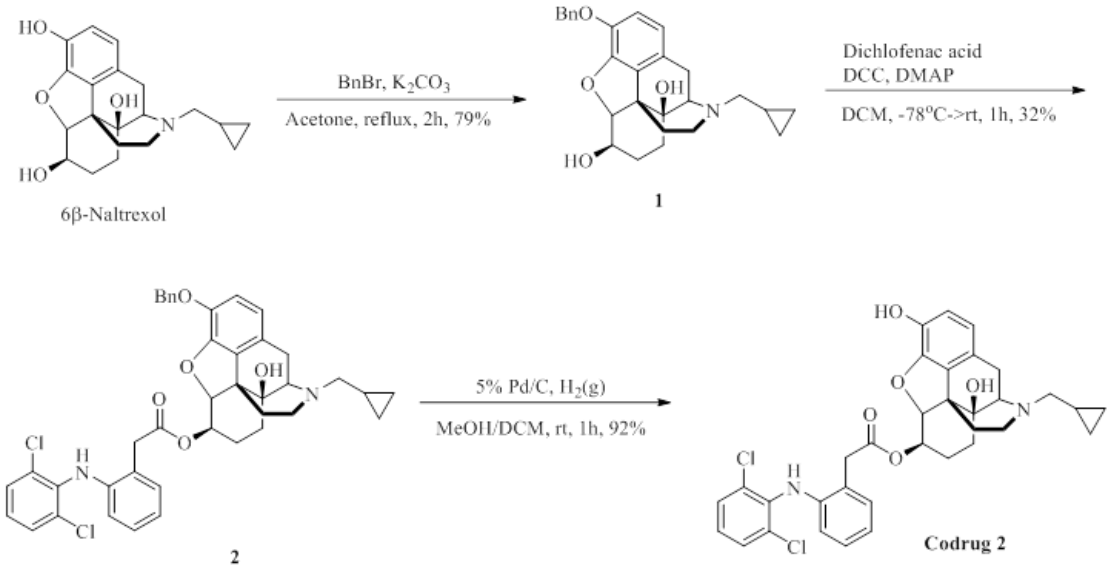

Synthetic scheme for codrug III and codrug III HCl salt

Scheme

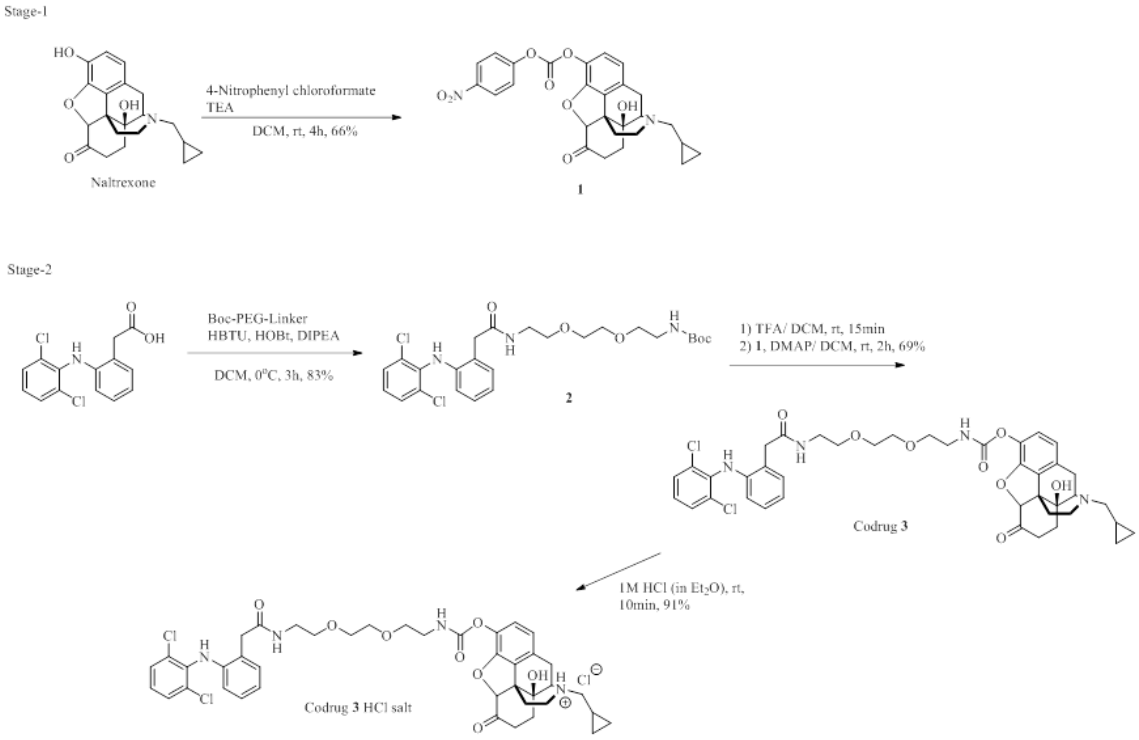

Synthetic scheme for codrug IV

Scheme

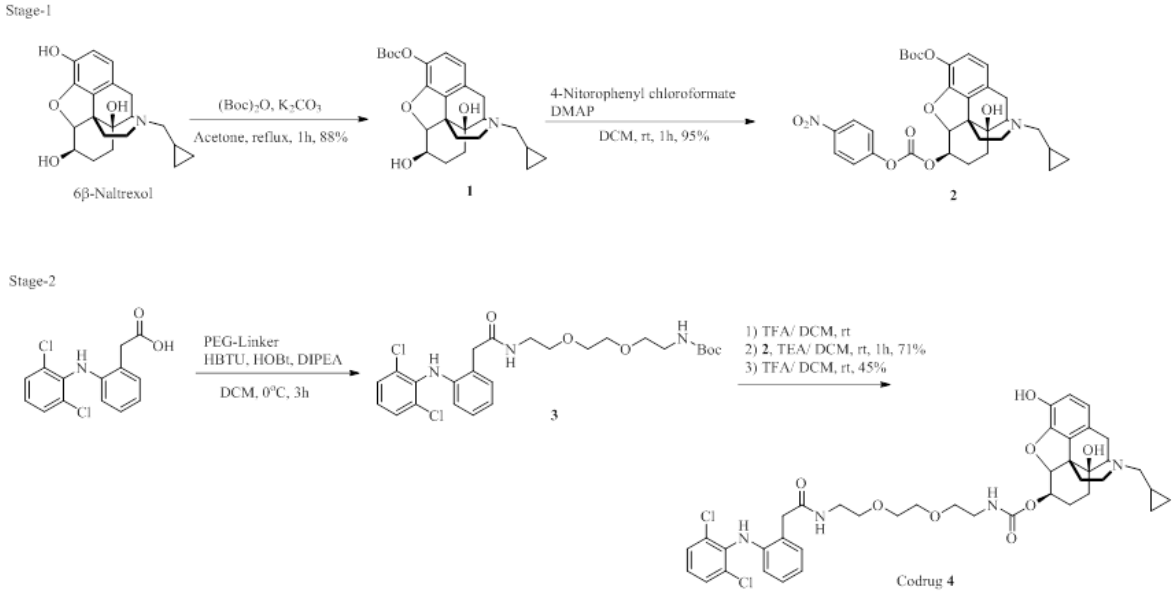

Appendix II

Assay development for HPLC and LCMS/MS

HPLC assay for naltrexone, diclofenac and codrugs

Naltrexone (NTX), diclofenac (DIC) and codrug concentrations in all samples were quantified using a high pressure liquid chromatography (HPLC) assay, using a modified version of the previously reported NTX assay. [22] The HPLC system consisted of a Waters 717 plus auto-sampler, a Waters 600 quaternary pump, and a Waters 2487 dual wavelength absorbance detector with Waters Empower™ software. A Perkin Elmer Brownlee™ Spheri 5 VL C18 column (5 µ, 220 x 4.6 mm) and a C18 guard column (15 x 3.2 mm) were used with the UV detector set at a wavelength of 280 nm. The mobile phase consisted of 70:30 (v/v) ACN: (0.1% TFA with 0.065% 1-octane sulfonic acid sodium salt, adjusted to pH 3.0 with TEA aqueous phase). Samples were run at a flow rate of 1.5 ml/min. The injection volume used was 25µl for receiver samples and 100µl for the skin disposition samples. The retention times for all compounds are reported in Table 7.1. All retention times reported are value ± 0.1 minute. Standard curves for both codrugs and parent drugs were prepared in the range of 100-10,000 ng/ml for ACN samples and 100-5000 ng/ml for extracted receiver samples. The standard solutions exhibited excellent linearity over the entire concentration range employed in the assays, r^2 >=0.99

LCMS/MS assay for NTX

Plasma samples were extracted using a previously validated method. [146] Five hundred µl of 1:1 ACN: ethyl acetate was added to 100 µl of plasma for protein precipitation. The mixture was vortexed for 15 seconds and centrifuged for 20 minutess at 12000 x g. The supernatant was removed carefully without disturbing the pellets and

dried under nitrogen in a glass test tube. The extract was suspended in 100µl ACN, vortexed, sonicated for 10 minutes and transferred to HPLC vials with low-volume inserts for injection. For plasma standards, the 100µl of the blank plasma was spiked with 10µl of ACN standards and extracted following the same method as above.

The LC/MS-MS system consisted of HPLC Waters Alliance 2695 Separations Module, Waters Micromass® Quattro MicroTM API Tandem Mass Spectrometer and Masslynx Chromatography software with Waters Quanlynx (V. 4.1) analysis software. A Waters Atlantis Silica HILIC column (5µ, 150 x 2.1mm) and guard column (10 x 2.1mm) were used for LC separation. The mobile phase composition was methanol with 0.1% acetic acid: 20mM ammonium acetate =95:5, the flow rate was 0.5ml/min and positive mode atmospheric pressure chemical ionization was used for detection of NTX (APCI+). Multiple reaction monitoring (MRM) was carried out with the following parent to daughter ion transitions for NTX•HCl *m/z* 341.8→323.8. The corona voltage was 3.5 µA, cone voltage 25 V, extractor 2 V, RF lens 0.3 V, source temp 130 °C, APCI probe temperature 575 °C. The collision gas was 20 eV. Nitrogen gas was used as a nebulization and drying gas at flow rates of 50 and 350 l/h, respectively. Injection volume was 40µl. Standard curves were prepared in the range of 1-50 ng/ml for ACN samples and extracted plasma samples. The standard solutions exhibited excellent linearity over the entire concentration range employed in the assays, r^2 >=0.98

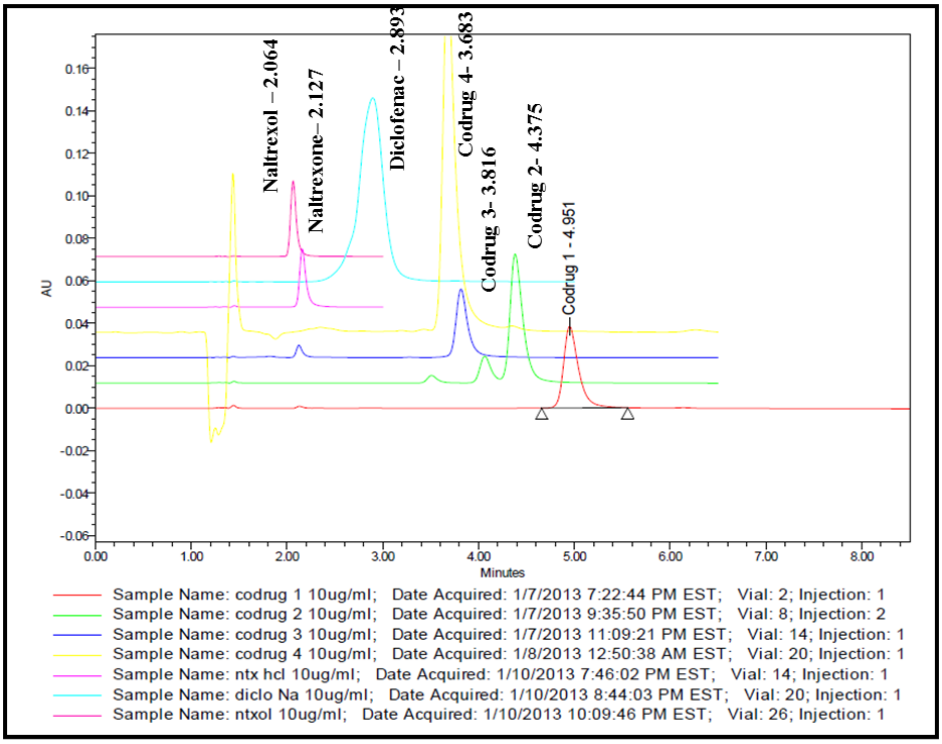

Figure II.1 Sample chromatograms for NTX, DIC and codrugs on HPLC

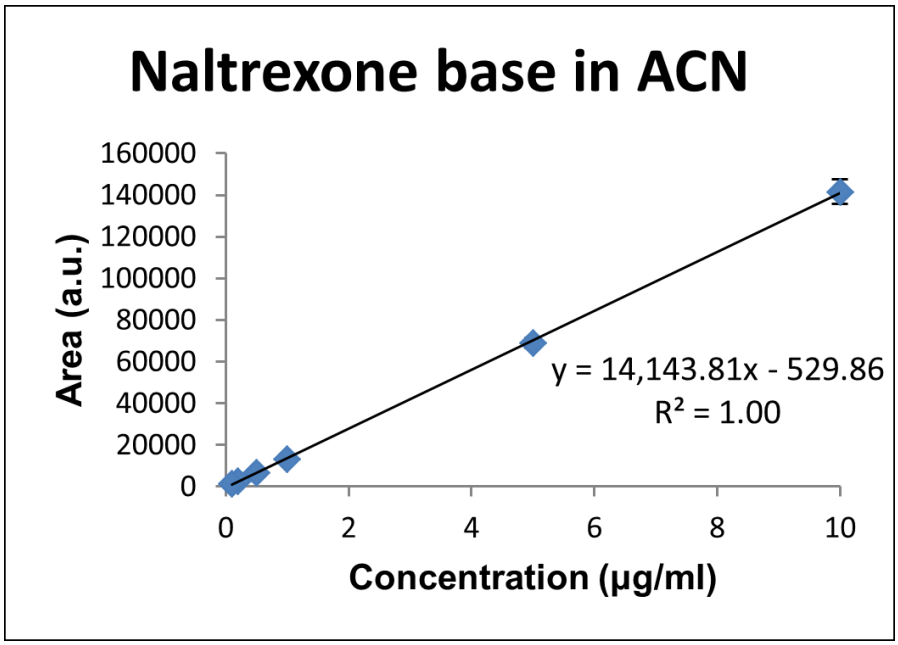

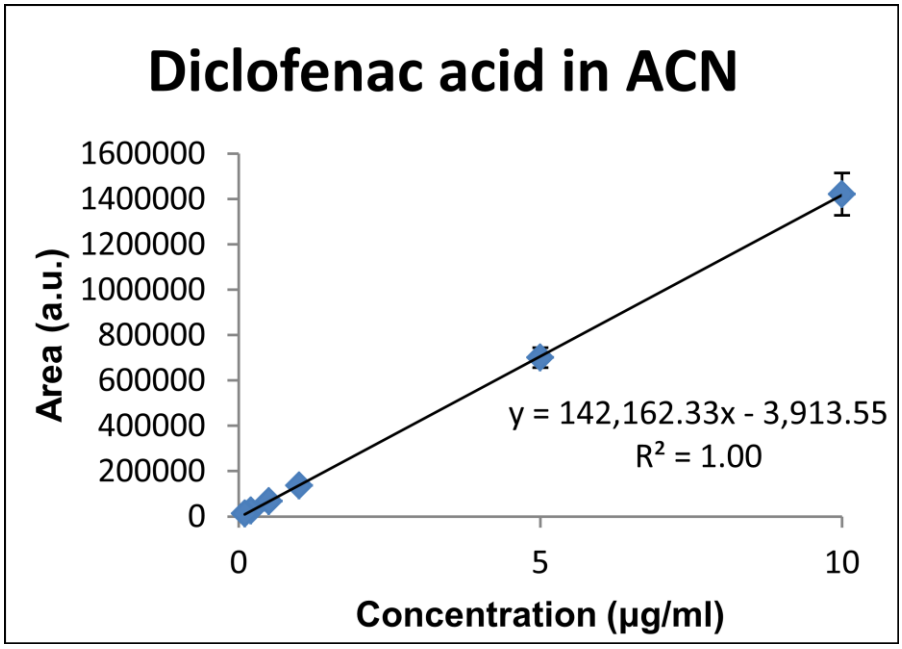

Figure II.2 HPLC standard curves of NTX and DIC in ACN. n=3 for all concentrations

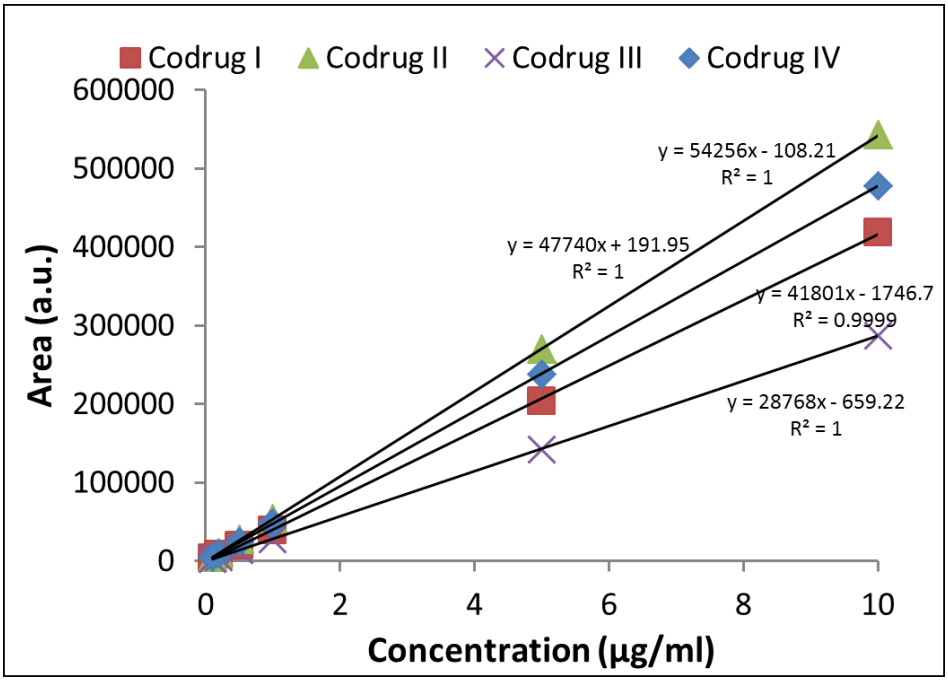

Figure II.3 Sample HPLC standard curves of codrugs in ACN

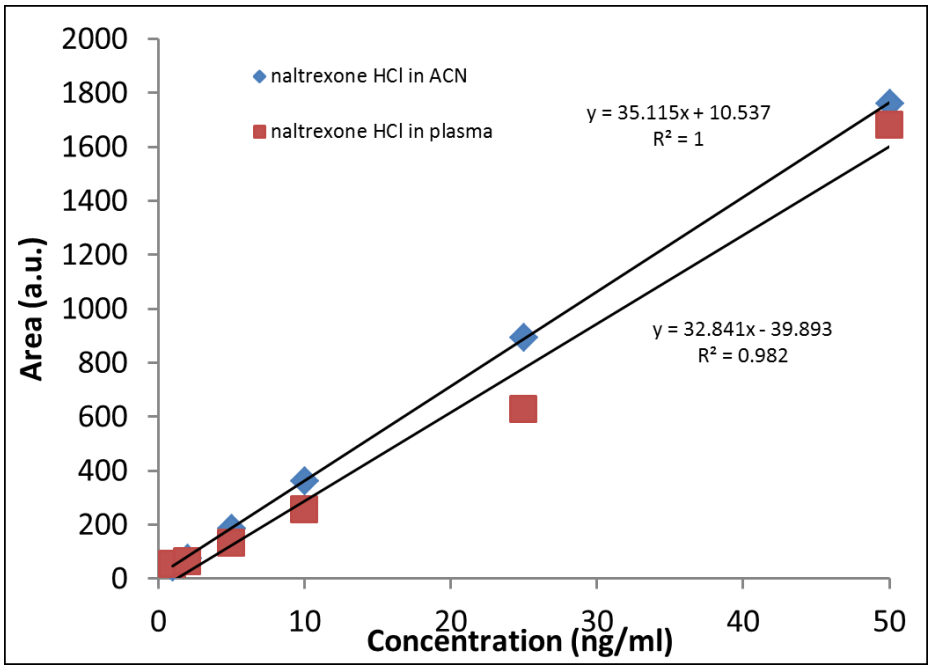

Figure II.3 Sample LCMS/MS standard curves of NTX in ACN and HGP plasma

References

1. Flynn G. 2002. Cutaneous and Transdermal Delivery - Processes and Systems of Delivery. In Anonymous Modern Pharmaceutics, Fourth Edition,: Informa Healthcare.
2. Prausnitz MR, Langer R 2008. Transdermal drug delivery. Nat Biotech 26:1261-1268.
3. Kim Y, Park J, Prausnitz MR 2012. Microneedles for drug and vaccine delivery. Adv Drug Deliv Rev 64:1547-1568.
4. Wermeling DP, Banks SL, Hudson DA, Gill HS, Gupta J, Prausnitz MR, Stinchcomb AL 2008. Microneedles permit transdermal delivery of a skin-impermeant medication to humans. Proceedings of the National Academy of Sciences 105:2058-2063.
5. Zhang Y, Brown K, Siebenaler K, Determan A, Dohmeier D, Hansen K 2012. Development of lidocaine-coated microneedle product for rapid, safe, and prolonged local analgesic action. Pharm Res 29:170-177.
6. Martanto W, Davis SP, Holiday NR, Wang J, Gill HS, Prausnitz MR 2004. Transdermal delivery of insulin using microneedles in vivo. Pharm Res 21:947-52.
7. Milewski M, Brogden NK, Stinchcomb AL 2010. Current aspects of formulation efforts and pore lifetime related to microneedle treatment of skin. Expert Opin Drug Deliv 7:617-629.
8. Banks S, Paudel K, Brogden N, Loftin C, Stinchcomb A 2011. Diclofenac Enables Prolonged Delivery of Naltrexone Through Microneedle-Treated Skin. Pharmaceutical Research :1-9.
9. Brogden NK, Milewski M, Ghosh P, Hardi L, Crofford LJ, Stinchcomb AL 2012. Diclofenac Delays Micropore Closure Following Microneedle Treatment in Healthy Human Subjects. Journal of Controlled Release 163(2):220-9.
10. Banks SL, Pinninti RR, Gill HS, Paudel KS, Crooks PA, Brogden NK, Prausnitz MR, Stinchcomb AL 2010. Transdermal delivery of naltrexol and skin permeability lifetime after microneedle treatment in hairless guinea pigs. J Pharm Sci 99:3072-3080.
11. Gupta J FAU - Gill, Harvinder,S., FAU GH, FAU AS, Prausnitz MR 0606. Kinetics of skin resealing after insertion of microneedles in human subjects. Journal of controlled release : official journal of the Controlled Release Society JID - 8607908 .
12. Kalluri H, Banga A 2011. Formation and Closure of Microchannels in Skin Following Microporation. Pharmaceutical Research 28:82-94.
13. Brogden NK, Milewski M, Ghosh P, Hardi L, Crofford LJ, Stinchcomb AL 2012. Diclofenac delays micropore closure following microneedle treatment in human subjects. J Control Release 163:220-229.
14. Brogden NK CLINICAL EVALUTION OF NOVEL METHODS FOR EXTENDING MICRONEEDLE PORE LIFETIME. 2012 .
15. Verebey K, Volavka J, Mule SJ, Resnick RB 1976. Naltrexone: disposition, metabolism, and effects after acute and chronic dosing. Clin Pharmacol Ther 20:315-328.
16. MICROMEDEX® 1.0 (Healthcare Series).
17. Alkermes Vivitrol (naltrexone for extended release injectable suspension) http://www.vivitrol.com/.
18. Mauro T, Holleran WM, Grayson S, Gao WN, Man MQ, Kriehuber E, Behne M, Feingold KR, Elias PM 1998. Barrier recovery is impeded at neutral pH, independent of ionic effects: implications for extracellular lipid processing. Arch Dermatol Res 290:215-222.
19.. https://scifinder.cas.org. Copyright © 2012 American Chemical Society
20. Schmid-Wendtner MH, Korting HC 2006. The pH of the Skin Surface and Its Impact on the Barrier Function. Skin Pharmacology and Physiology 19:296-302.

21. Milewski M, Yerramreddy TR, Ghosh P, Crooks PA, Stinchcomb AL 2010. In Vitro Permeation of a Pegylated Naltrexone Prodrug Across Microneedle-Treated Skin. J Control Release 146:37-44.
22. Milewski M, Stinchcomb A 2011. Vehicle Composition Influence on the Microneedle-Enhanced Transdermal Flux of Naltrexone Hydrochloride. Pharmaceutical Research 28:124-134.
23. Strasinger CL, Scheff NN, Stinchcomb AL 2008. Prodrugs and codrugs as strategies for improving percutaneous absorption. Expert Rev Dermatol 3:221-233.
24. Grubauer G, Feingold KR, Harris RM, Elias PM 1989. Lipid content and lipid type as determinants of the epidermal permeability barrier. J Lipid Res 30:89-96.
25. Grubauer G, Feingold KR, Elias PM 1987. Relationship of epidermal lipogenesis to cutaneous barrier function. J Lipid Res 28:746-52.
26. Scheindlin S 2004. Transdermal drug delivery: PAST, PRESENT, FUTURE. Mol Interv 4:308-312.
27. Prausnitz MR, Mitragotri S, Langer R 2004. Current status and future potential of transdermal drug delivery. Nat Rev Drug Discov 3:115-124.
28. Abelin T, Buehler A, Muller P, Vesanen K, Imhof PR 1989. Controlled trial of transdermal nicotine patch in tobacco withdrawal. Lancet 1:7-10.
29. Paudel KS, Milewski M, Swadley CL, Brogden NK, Ghosh P, Stinchcomb AL 2010. Challenges and opportunities in dermal/transdermal delivery. Therapeutic Delivery 1:109-131.
30. http://www.fluzone.com/. 2013.
31. Harding CR 2004. The stratum corneum: structure and function in health and disease. Dermatol Ther 17 Suppl 1:6-15.
32. Oesch F, Fabian E, Oesch-Bartlomowicz B, Werner C, Landsiedel R 2007. Drug-Metabolizing Enzymes in the Skin of Man, Rat, and Pig. Drug Metabolism Reviews 39:659-698.
33. Pendlington RU, Williams DL, Naik JT, Sharma RK 1994. Distribution of xenobiotic metabolizing enzymes in skin. Toxicology in Vitro 8:525-527.
34. Hikima T, Maibach HI, Tojo K 2006. SKIN ENZYMES DISTRIBUTION IN TRANSDERMAL DRUG DELIVERY. AIChE .
35. Sugibayashi K, Hayashi T, Morimoto Y 1999. Simultaneous transport and metabolism of ethyl nicotinate in hairless rat skin after its topical application: the effect of enzyme distribution in skin. J Controlled Release 62:201-208.
36. Storm JE, Collier SW, Stewart RF, Bronaugh RL 1990. Metabolism of xenobiotics during percutaneous penetration: role of absorption rate and cutaneous enzyme activity. Fundam Appl Toxicol 15:132-141.
37. Barry BW 2001. Novel mechanisms and devices to enable successful transdermal drug delivery. European Journal of Pharmaceutical Sciences 14:101-114.
38. Flynn GL, Stewart B 1988. Percutaneous drug penetration: Choosing candidates for transdermal development. Drug Dev Res 13:169-185.
39. Kalia YN, Naik A, Garrison J, Guy RH 2004. Iontophoretic drug delivery. Advanced Drug Delivery Reviews 56:619-658.
40. Ledger PW Skin biological issues in electrically enhanced transdermal delivery. Advanced Drug Delivery Reviews 9:289-307.
41. Mitragotri S, Blankschtein D, Langer R 1995. Ultrasound-mediated transdermal protein delivery. Science 269:850-853.
42. Prausnitz MR 2004. Microneedles for transdermal drug delivery. Advanced Drug Delivery Reviews 56:581-587.
43. Henry S, McAllister DV, Allen MG, Prausnitz MR 1998. Microfabricated microneedles: a novel approach to transdermal drug delivery. J Pharm Sci 87:922-5.

44. Gill HS, Prausnitz MR 2007. Coated microneedles for transdermal delivery. J Controlled Release 117:227-237.
45. Park J, Allen MG, Prausnitz MR 2005. Biodegradable polymer microneedles: Fabrication, mechanics and transdermal drug delivery. J Controlled Release 104:51-66.
46. Burton SA, Ng CY, Simmers R, Moeckly C, Brandwein D, Gilbert T, Johnson N, Brown K, Alston T, Prochnow G, Siebenaler K, Hansen K 2011. Rapid intradermal delivery of liquid formulations using a hollow microstructured array. Pharm Res 28:31-40.
47. Martanto W, Moore JS, Kashlan O, Kamath R, Wang PM, O'Neal JM, Prausnitz MR 2006. Microinfusion using hollow microneedles. Pharm Res 23:104-13.
48. Martanto W, Moore JS, Couse T, Prausnitz MR 2006. Mechanism of fluid infusion during microneedle insertion and retraction. J Control Release 112:357-61.
49. Banks SL 2008. Transdermal delivery of naltrexone by minimally invasive microneedle array application: permeation enhancement of a water soluble compound across a lipophilic barrier.
50. Yan G, Warner KS, Zhang J, Sharma S, Gale BK 2010. Evaluation needle length and density of microneedle arrays in the pretreatment of skin for transdermal drug delivery. Int J Pharm 391:7-12.
51. Brogden NK, Ghosh P, Stinchcomb AL Submitted December 2012. Development of in vivo impedance spectroscopy techniques for measurement of micropore formation. Journal of Investigative Dermatology .
52. Ito Y, Yoshimura M, Tanaka T, Takada K 2012. Effect of lipophilicity on the bioavailability of drugs after percutaneous administration by dissolving microneedles. J Pharm Sci 101:1145-1156.
53. Potts RO, Guy RH 1995. A predictive algorithm for skin permeability: the effects of molecular size and hydrogen bond activity. Pharm Res 12:1628-1633.
54. Banks S, Pinninti R, Gill H, Crooks P, Prausnitz M, Stinchcomb A 2008. Flux Across Microneedle-treated Skin is Increased by Increasing Charge of Naltrexone and Naltrexol In Vitro. Pharmaceutical Research 25:1964-1964.
55. Li G, Badkar A, Nema S, Kolli CS, Banga AK 2009. In vitro transdermal delivery of therapeutic antibodies using maltose microneedles. Int J Pharm 368:109-115.
56. Harvey AJ, Kaestner SA, Sutter DE, Harvey NG, Mikszta JA, Pettis RJ 2011. Microneedle-based intradermal delivery enables rapid lymphatic uptake and distribution of protein drugs. Pharm Res 28:107-116.
57. Daddona PE, Matriano JA, Mandema J, Maa YF 2011. Parathyroid hormone (1-34)-coated microneedle patch system: clinical pharmacokinetics and pharmacodynamics for treatment of osteoporosis. Pharm Res 28:159-165.
58. Donnelly RF, Singh TR, Tunney MM, Morrow DI, McCarron PA, O'Mahony C, Woolfson AD 2009. Microneedle arrays allow lower microbial penetration than hypodermic needles in vitro. Pharm Res 26:2513-2522.
59. Gupta J FAU - Felner, Eric,I., FAU FE, Prausnitz MR 0917. Minimally invasive insulin delivery in subjects with type 1 diabetes using hollow microneedles. Diabetes technology & therapeutics JID - 100889084 .
60. Kaushik S, Hord AH, Denson DD, McAllister DV, Smitra S, Allen MG, Prausnitz MR 2001. Lack of pain associated with microfabricated microneedles. Anesth Analg 92:502-504.
61. Haq MI, Smith E, John DN, Kalavala M, Edwards C, Anstey A, Morrissey A, Birchall JC 2009. Clinical administration of microneedles: skin puncture, pain and sensation. Biomed Microdevices 11:35-47.

62. Bal SM, Caussin J, Pavel S, Bouwstra JA 2008. In vivo assessment of safety of microneedle arrays in human skin. European Journal of Pharmaceutical Sciences 35:193-202.
63. Gupta J, Park SS, Bondy B, Felner EI, Prausnitz MR 2011. Infusion pressure and pain during microneedle injection into skin of human subjects. Biomaterials 32:6823-6831.
64. Gill HS, Denson DD, Burris BA, Prausnitz MR 2008. Effect of Microneedle Design on Pain in Human Volunteers. The Clinical Journal of Pain 24:585-594 10.1097/AJP.0b013e31816778f9.
65. Finnin BC, Morgan TM 1999. Transdermal penetration enhancers: Applications, limitations, and potential. J Pharm Sci 88:955-958.
66. Barry BW 1987. Mode of action of penetration enhancers in human skin. J Controlled Release 6:85-97.
67. Thong HY, Zhai H, Maibach HI 2007. Percutaneous penetration enhancers: an overview. Skin Pharmacol Physiol 20:272-282.
68. Benson HA 2005. Transdermal drug delivery: penetration enhancement techniques. Curr Drug Deliv 2:23-33.
69. Kurihara-Bergstrom T, Knutson K, DeNoble LJ, Goates CY 1990. Percutaneous absorption enhancement of an ionic molecule by ethanol-water systems in human skin. Pharm Res 7:762-766.
70. Feingold KR 2009. The outer frontier: the importance of lipid metabolism in the skin. J Lipid Res 50 Suppl:S417-22.
71. Feingold KR 2007. Thematic review series: skin lipids. The role of epidermal lipids in cutaneous permeability barrier homeostasis. J Lipid Res 48:2531-2546.
72. Man MQ M, Feingold KR, Thornfeldt CR, Elias PM 1996. Optimization of physiological lipid mixtures for barrier repair. J Invest Dermatol 106:1096-1101.
73. Elias PM, Tsai J, Menon GK, Holleran WM, Feingold KR 2002. The Potential of Metabolic Interventions to Enhance Transdermal Drug Delivery. J Investig Dermatol Symp Proc 7:79-85.
74. Harris IR, Farrell AM, Grunfeld C, Holleran WM, Elias PM, Feingold KR 1997. Permeability Barrier Disruption Coordinately Regulates mRNA Levels for Key Enzymes of Cholesterol, Fatty Acid, and Ceramide Synthesis in the Epidermis. J Investig Dermatol 109:783-787.
75. Tsai J, Guy RH, Thornfeldt CR, Gao WN, Feingold KR, Elias PM 1996. Metabolic approaches to enhance transdermal drug delivery. 1. Effect of lipid synthesis inhibitors. Journal of Pharmaceutical Sciences 85:643-648.
76. Li YZ, Quan YS, Zang L, Jin MN, Kamiyama F, Katsumi H, Tsutsumi S, Yamamoto A 2009. Trypsin as a novel potential absorption enhancer for improving the transdermal delivery of macromolecules. J Pharm Pharmacol 61:1005-1012.
77. Li YZ, Quan YS, Zang L, Jin MN, Kamiyama F, Katsumi H, Yamamoto A, Tsutsumi S 2008. Transdermal delivery of insulin using trypsin as a biochemical enhancer. Biol Pharm Bull 31:1574-1579.
78. Kim YC, Late S, Banga AK, Ludovice PJ, Prausnitz MR 2008. Biochemical enhancement of transdermal delivery with magainin peptide: modification of electrostatic interactions by changing pH. Int J Pharm 362:20-28.
79. Stella V, Borchardt R, Hageman M, Oliyai R, Maag H, Tilley J. 2007. Prodrugs: Challenges and rewards Part 1, 1st ed.: Springer.
80. Ettmayer P, Amidon GL, Clement B, Testa B 2004. Lessons learned from marketed and investigational prodrugs. J Med Chem 47:2393-2404.
81. Rautio J, Kumpulainen H, Heimbach T, Oliyai R, Oh D, Jarvinen T, Savolainen J 2008. Prodrugs: design and clinical applications. Nat Rev Drug Discov 7:255-270.

82. Vaddi HK, Banks SL, Chen J, Hammell DC, Crooks PA, Stinchcomb AL 2009. Human skin permeation of 3-O-alkyl carbamate prodrugs of naltrexone. Journal of Pharmaceutical Sciences 98:2611-2625.
83. Haranath KV, Mohamed OH, Jianhong C, Stan LB, Peter AC, Audra LS 2005. Human skin permeation of branched-chain 3-0-alkyl ester and carbonate prodrugs of naltrexone. Pharm Res 22:758-65.
84. Hammell DC, Hamad M, Vaddi HK, Crooks PA, Stinchcomb AL 2004. A duplex "Gemini" prodrug of naltrexone for transdermal delivery. Journal of Controlled Release 97:283-290.
85. Stinchcomb AL, Swaan PW, Ekabo O, Harris KK, Browe J, Hammell DC, Cooperman TA, Pearsall M 2002. Straight-chain naltrexone ester prodrugs: Diffusion and concurrent esterase biotransformation in human skin. Journal of Pharmaceutical Sciences 91:2571-2578.
86. Kiptoo PK, Paudel KS, Hammell DC, Hamad MO, Crooks PA, Stinchcomb AL 2008. In vivo evaluation of a transdermal codrug of 6-beta-naltrexol linked to hydroxybupropion in hairless guinea pigs. European journal of pharmaceutical sciences : official journal of the European Federation for Pharmaceutical Sciences 33:371-9.
87. Cynkowski T, Cynkowska G, Walters KA. 2007. Codrugs: Potential Therapies for Dermatological Diseases. In Anonymous : Informa Healthcare. p 255-266.
88. Lau WM, White AW, Gallagher SJ, Donaldson M, McNaughton G, Heard CM 2008. Scope and limitations of the co-drug approach to topical drug delivery. Curr Pharm Des 14:794-802.
89. Singer AJ, Clark RAF 1999. Cutaneous Wound Healing. N Engl J Med 341:738-746.
90. Eming SA, Krieg T, Davidson JM 2007. Inflammation in wound repair: molecular and cellular mechanisms. J Invest Dermatol 127:514-525.
91. Kanzler MH, Gorsulowsky DC, Swanson NA 1986. Basic mechanisms in the healing cutaneous wound. J Dermatol Surg Oncol 12:1156-1164.
92. Menon GK, Feingold KR, Elias PM 1992. Lamellar Body Secretory Response to Barrier Disruption. J Investig Dermatol 98:279-289.
93. Zhai H, Maibach HI 2002. Occlusion vs. skin barrier function. Skin Res Technol 8:1-6.
94. Grubauer G, Elias PM, Feingold KR 1989. Transepidermal water loss: the signal for recovery of barrier structure and function. Journal of Lipid Research 30:323-33.
95. Li G, Badkar A, Kalluri H, Banga AK 2010. Microchannels created by sugar and metal microneedles: characterization by microscopy, macromolecular flux and other techniques. J Pharm Sci 99:1931-41.
96. Kolli CS, Banga AK 2008. Characterization of solid maltose microneedles and their use for transdermal delivery. Pharm Res 25:104-113.
97. KALLURI, #160, H., BANGA, K. A. 2009. Microneedles and transdermal drug delivery, Paris, FRANCE: Editions de santé.
98. Bal S, Kruithof AC, Liebl H, Tomerius M, Bouwstra J, Lademann J, Meinke M 2010. In vivo visualization of microneedle conduits in human skin using laser scanning microscopy. Laser Physics Letters 7:242-246.
99. Coulman SA, Birchall JC, Alex A, Pearton M, Hofer B, O'Mahony C, Drexler W, Povazay B 2011. In vivo, in situ imaging of microneedle insertion into the skin of human volunteers using optical coherence tomography. Pharm Res 28:66-81.
100. Elias PM 2005. Stratum corneum defensive functions: an integrated view. J Invest Dermatol 125:183-200.
101. Holleran WM, Takagi Y, Imokawa G, Jackson S, Lee JM, Elias PM 1992. beta-Glucocerebrosidase activity in murine epidermis: characterization and localization in relation to differentiation. Journal of Lipid Research 33:1201-1209.

102. Takagi Y, Kriehuber E, Imokawa G, Elias PM, Holleran WM 1999. β-Glucocerebrosidase activity in mammalian stratum corneum. Journal of Lipid Research 40:861-869.
103. Simmons DL, Botting RM, Hla T 2004. Cyclooxygenase isozymes: the biology of prostaglandin synthesis and inhibition. Pharmacol Rev 56:387-437.
104. Fecker LF, Stockfleth E, Nindl I, Ulrich C, Forschner T, Eberle J 2007. The role of apoptosis in therapy and prophylaxis of epithelial tumours by nonsteroidal anti-inflammatory drugs (NSAIDs). British Journal of Dermatology 156:25-33.
105. Bastos-Pereira AL, Lugarini D, Oliveira-Christoff A, Avila TV, Teixeira S, Pires Ado R, Muscara MN, Cadena SM, Donatti L, Cristina da Silva de Assis,H., Acco A 2010. Celecoxib prevents tumor growth in an animal model by a COX-2 independent mechanism. Cancer Chemother Pharmacol 65:267-276.
106. Tegeder I, Pfeilschifter J, Geisslinger G 2001. Cyclooxygenase-independent actions of cyclooxygenase inhibitors. FASEB J 15:2057-2072.
107. Davidson JM, Breyer MD 2003. Inflammatory Modulation and Wound Repair. J Investig Dermatol 120:xi-xii.
108. Futagami A, Ishizaki M, Fukuda Y, Kawana S, Yamanaka N 0000. Wound Healing Involves Induction of Cyclooxygenase-2 Expression in Rat Skin. Lab Invest 82:1503-1513.
109. Muller-Decker K, Hirschner W, Marks F, Furstenberger G 2002. The Effects of Cyclooxygenase Isozyme Inhibition onIncisional Wound Healing in Mouse Skin. 119:1189-1195.
110. Kampfer H, Brautigam L, Geisslinger G, Pfeilschifter J, Frank S 2003. Cyclooxygenase-1-coupled prostaglandin biosynthesis constitutes an essential prerequisite for skin repair. J Invest Dermatol 120:880-890.
111. Cordero JA, Alarcon L, Escribano E, Obach R, Domenech J 1997. A comparative study of the transdermal penetration of a series of nonsteroidal antiinflammatory drugs. J Pharm Sci 86:503-508.
112. Mao-Qiang M, Mauro T, Bench G, Warren R, Elias PM, Feingold KR 1997. Calcium and potassium inhibit barrier recovery after disruption, independent of the type of insult in hairless mice. Exp Dermatol 6:36-40.
113. Feingold K 2002. In This Issue: Regulation of Permeability Barrier Homeostasis. 119:986-986.
114. Alcoholism. 2013.
115. Alcohol Use and Health. 2013.
116. Results from the 2011 National Survey on Drug Use and Health:Summary of National Findings. 2012. Substance Abuse and Mental Health Services Administration .
117. Alcohol, the Brain, and Be h a v ior Mechanisms of Addiction. 2013.
118. Anton RF, O'Malley SS, Ciraulo DA, Cisler RA, Couper D, Donovan DM, Gastfriend DR, Hosking JD, Johnson BA, LoCastro JS, Longabaugh R, Mason BJ, Mattson ME, Miller WR, Pettinati HM, Randall CL, Swift R, Weiss RD, Williams LD, Zweben A, COMBINE Study Research Group 2006. Combined pharmacotherapies and behavioral interventions for alcohol dependence: the COMBINE study: a randomized controlled trial. JAMA 295:2003-2017.
119. Fuller RK, Hiller-Sturmhofel S 1999. Alcoholism treatment in the United States. An overview. Alcohol Res Health 23:69-77.
120. Naassila M, Hammoumi S, Legrand E, Durbin P, Daoust M 1998. Mechanism of Action of Acamprosate. Part I. Characterization of Spermidine-Sensitive Acamprosate Binding Site in Rat Brain. Alcoholism: Clinical and Experimental Research 22:802-809.

121. Mann K, Lehert P, Morgan MY 2004. The Efficacy of Acamprosate in the Maintenance of Abstinence in Alcohol-Dependent Individuals: Results of a Meta-Analysis. Alcoholism: Clinical and Experimental Research 28:51-63.
122. Wright TM, Myrick H 2006. Acamprosate: a new tool in the battle against alcohol dependence. Neuropsychiatr Dis Treat 2:445-453.
123. Lee Y, Park S, Kim Y, Kim D, Jeong J, Myrick H, Kim Y 2005. Effects of naltrexone on the ethanol-induced changes in the rat central dopaminergic system. Alcohol and Alcoholism 40:297-301.
124. Revia (Naltrexone) drug information. 2013.
125. Vivitrol (Naltrexone XR Inj). 2013.
126. Vivitrol alert F2.
127. Porter SJ, Somogyi AA, White JM 2000. Kinetics and inhibition of the formation of 6?-naltrexol from naltrexone in human liver cytosol. Br J Clin Pharmacol 50:465-471.
128. McCaul ME, Wand GS, Rohde C, Lee SM 2000. Serum 6-Beta-Naltrexol Levels Are Related to Alcohol Responses in Heavy Drinkers. Alcoholism: Clinical and Experimental Research 24:1385-1391.
129. Volpicelli JR, Rhines KC, Rhines JS, Volpicelli LA, Alterman AI, O'Brien CP 1997. Naltrexone and Alcohol Dependence: Role of Subject Compliance. Arch Gen Psychiatry 54:737-742.
130. Volpicelli JR, Alterman AI, Hayashida M,O'Brien CP 1992. NAltrexone in the treatment of alcohol dependence. Archives of General Psychiatry 49:876-880.
131. O'Malley SS, Jaffe AJ, Chang G, Schottenfeld RS, Meyer RE, Rounsaville B 1992. Naltrexone and Coping Skills Therapy for Alcohol Dependence: A Controlled Study. Arch Gen Psychiatry 49:881-887.
132. Volpicelli JR, Watson NT, King AC, Sherman CE, O'Brien CP 1995. Effect of naltrexone on alcohol "high" in alcoholics. Am J Psychiatry 152:613-615.
133. Covey LS, Glassman AH, Stetner F 1999. Naltrexone Effects on Short-Term and Long-Term Smoking Cessation. Journal of Addictive Diseases 18:31-40.
134. Elias PM, Cooper ER, Korc A, Brown BE 1981. Percutaneous Transport in Relation to Stratum Corneum Structure and Lipid Composition. J Investig Dermatol 76:297-301.
135. FAU BJ, Meinardi MM 0925. The 500 Dalton rule for the skin penetration of chemical compounds and drugs. Experimental dermatology JID - 9301549 .
136. Chen L, Han L, Lian G Recent advances in predicting skin permeability of hydrophilic solutes. Adv Drug Deliv Rev .
137. Gomaa YA, Morrow DIJ, Garland MJ, Donnelly RF, El-Khordagui LK, Meidan VM 2010. Effects of microneedle length, density, insertion time and multiple applications on human skin barrier function: Assessments by transepidermal water loss. Toxicology in Vitro 24:1971-1978.
138. Li G, Badkar A, Nema S, Kolli CS, Banga AK 2009. In vitro transdermal delivery of therapeutic antibodies using maltose microneedles. Int J Pharm 368:109-115.
139. Milewski M, Pinninti RR, Stinchcomb AL 2012. Naltrexone salt selection for enhanced transdermal permeation through microneedle-treated skin. J Pharm Sci 101:2777-2786.
140. Broughton G,II, Janis JE, Attinger CE 2006. The Basic Science of Wound Healing. Plast Reconstr Surg 117.
141. Schneider LA, Korber A, Grabbe S, Dissemond J 2007. Influence of pH on wound-healing: a new perspective for wound-therapy? Arch Dermatol Res 298:413-420.
142. Gethin G 2007. The significance of surface pH in chronic wounds. Wounds UK 3:52.
143. scifinder.cas.org: American chemical society.
144. National Institute on Alcohol Abuse and Alcoholism http://www.niaaa.nih.gov.

145. PDR 1996. , second ed., New Jersey: Medical economics.
146. Milewski M 2012. MICRONEEDLE-ASSISTED TRANSDERMAL DELIVERY OF NALTREXONE SPECIES:*IN VITRO*PERMEATION AND*IN VIVO*PHARMACOKINETIC STUDIES.
147. Ghosh P, Pinninti RR, Hammell DC, Paudel KS, Stinchcomb AL Accepted January 2013. Development of a codrug approach for sustained delivery across microneedle treated skin. J Pharm Sci .
148. Paudel KS, Nalluri BN, Hammell DC, Valiveti S, Kiptoo P, Hamad MO, Crooks PA, Stinchcomb AL 2005. Transdermal delivery of naltrexone and its active metabolite 6-β-naltrexol in human skin in vitro and guinea pigs in vivo. Journal of Pharmaceutical Sciences 94:1965-1975.
149. Hadgraft J, Valenta C 2000. pH, pKa and dermal delivery. Int J Pharm 200:243-247.
150. Potts RO, Guy RH 1992. Predicting skin permeability. Pharm Res 9:663-669.
151. Milewski M, Stinchcomb AL 2012. Estimation of Maximum Transdermal Flux of Nonionized Xenobiotics from Basic Physicochemical Determinants. Mol Pharm .
152. Curdy C, Kalia YN, Falson-Rieg F, Guy RH 2000. Recovery of human skin impedance in vivo after iontophoresis: effect of metal ions. AAPS PharmSci 2:E23.
153. Swift RM 1999. Medications and Alcohol
Craving. NIAAA 23:207.
154. Swift R 2010. Medications Acting on the Dopaminergic System in the Treatment of Alcoholic Patients. Curr Pharm Des 16:2136-2140.
155. Hulse GK, Basso MR 2000. The association between naltrexone compliance and daily supervision. Drug and Alcohol Review 19:41-48.
156. Alkermes.
157. Feingold KR, Schmuth M, Elias PM 0000. The Regulation of Permeability Barrier Homeostasis. J Invest Dermatol 127:1574-1576.
158. Laneuville O, Breuer DK, Dewitt DL, Hla T, Funk CD, Smith WL 1994. Differential inhibition of human prostaglandin endoperoxide H synthases-1 and -2 by nonsteroidal anti-inflammatory drugs. Journal of Pharmacology and Experimental Therapeutics 271:927-934.
159. Prusakiewicz J, Ackermann C, Voorman R 2006. Comparison of Skin Esterase Activities from Different Species. Pharmaceutical Research 23:1517-1524.
160. Roberts ME, Mueller KR 1990. Comparisons of in vitro nitroglycerin (TNG) flux across yucatan pig, hairless mouse, and human skins. Pharm Res 7:673-676.
161. Gelfuso GM, Gratieri T, Souza JG, Thomazine JA, Lopez RFV 2011. The influence of positive or negative charges in the passive and iontophoretic skin penetration of porphyrins used in photodynamic therapy. European Journal of Pharmaceutics and Biopharmaceutics 77:249-256.
162. Barbero AM, Frasch HF 2009. Pig and guinea pig skin as surrogates for human in vitro penetration studies: A quantitative review. Toxicology in Vitro 23:1-13.
163. Banks S, Paudel K, Brogden N, Loftin C, Stinchcomb A Diclofenac Enables Prolonged Delivery of Naltrexone Through Microneedle-Treated Skin. Pharmaceutical Research 28:1211-1219.
164. Chin Y, Weber Jr WJ, Voice TC 1986. Determination of partition coefficients and aqueous solubilities by reverse phase chromatography—II: Evaluation of partitioning and solubility models. Water Res 20:1443-1450.
165. Dittert LW, Higuchi T 1963. Rates of hydrolysis of carbamate and carbonate esters in alkaline solution. J Pharm Sci 52:852-857.
166. Webster R, Didier E, Harris P, Siegel N, Stadler J, Tilbury L, Smith D 2007. PEGylated proteins: evaluation of their safety in the absence of definitive metabolism studies. Drug Metab Dispos 35:9-16.

167. Ran Y, He Y, Yang G, Johnson JLH, Yalkowsky SH 2002. Estimation of aqueous solubility of organic compounds by using the general solubility equation. Chemosphere 48:487-509.
168. Davis SP, Martanto W, Allen MG, Prausnitz MR 2005. Hollow metal microneedles for insulin delivery to diabetic rats. IEEE Trans Biomed Eng 52:909-15.
169. Andersen F, Hedegaard K, Petersen TK, Bindslev-Jensen C, Fullerton A, Andersen KE 2006. The hairless guinea-pig as a model for treatment of cumulative irritation in humans. Skin Research & Technology 12:60-67.
170. Carter PJ 2011. Introduction to current and future protein therapeutics: A protein engineering perspective. Exp Cell Res 317:1261-1269.
171. Pavlou AK, Reichert JM 2004. Recombinant protein therapeutics[mdash]success rates, market trends and values to 2010. Nat Biotech 22:1513-1519.
172. Smith PL, Wall DA, Gochoco CH, Wilson G 1992. (D) Routes of delivery: Case studies: (5) Oral absorption of peptides and proteins. Adv Drug Deliv Rev 8:253-290.
173. Dubey S, Perozzo R, Scapozza L, Kalia YN 2011. Noninvasive transdermal iontophoretic delivery of biologically active human basic fibroblast growth factor. Mol Pharm 8:1322-1331.

VITA

Priyanka Ghosh

Birthplace: Calcutta, India

EDUCATION AND TRAINING

Bachelor of Technology in Biotechnology May 2008

West Bengal University of Technology

PROFESSIONAL POSITIONS

1. Graduate Research Assistant, Department of Pharmaceutical Sciences, University of Maryland School of Pharmacy, Baltimore, MD (January, 2012-Present)
2. Graduate Research Assistant, Department of Pharmaceutical Sciences, University of Kentucky College of Pharmacy, Lexington, KY (July, 2009- December, 2011)
3. Teaching Assistant, Department of Pharmaceutical Sciences, University of Kentucky, College of Pharmacy, Lexington, KY (August 2008-June 2009)

PUBLICATIONS

1. P. Ghosh, N.K. Brogden, A.L. Stinchcomb **"Effect of formulation pH on transport of naltrexone species and pore closure in microneedle enhanced transdermal drug delivery".** 2013 May 13. [Epub ahead of print]

2. N. K. Brogden, P. Ghosh, L. Hardi, L. J. Crofford, A. L. Stinchcomb **"Development of in vivo impedance spectroscopy techniques for measurement of micropore formation following microneedle insertion"**. Published in Journal of Pharmaceutical Sciences (2013) Jun;102(6):1948-56

3. P. Ghosh, R.R. Pinninti, D.C. Hammell, K. S. Paudel, A.L. Stinchcomb **" Development of a codrug approach for sustained drug delivery across microneedle treated skin"**. Published in Journal of Pharmaceutical Sciences 2013 May;102(5):1458-67
4. N. K. Brogden, M. Milewski, P. Ghosh, L. Hardi, L. J. Crofford, A. L. Stinchcomb **"Diclofenac Delays Micropore Closure Following Microneedle Treatment in Healthy Human Subjects"**. Published in Journal of Controlled Release (2012) 163(2):220-9
5. M. Milewski, T. Yerramreddy, P. Ghosh, P. A. Crooks, A. L. Stinchcomb **"*In vitro* permeation of PEGylated naltrexone prodrug across microneedle-treated skin"** Published in Journal of Controlled Release (2010) 146(1):37-44
6. K. S. Paudel, M. Milewski, C.L. Swadley, N. K. Brogden, P. Ghosh, A. L. Stinchcomb **"Challenges and Opportunities in Dermal/Transdermal Delivery"** Published in Therapeutic Delivery (2010) Jul;1(1):109-131

MANUSCRIPTS SUBMITTED

1. P. Ghosh, D.Lee, K.B.Kim, A.L. Stinchcomb **"Optimization of naltrexone diclofenac codrugs for sustained drug delivery across microneedle treated skin".** Revisions submitted to Pharmaceutical Research, May 2013
2. M. Milewski, K. S. Paudel, N. K. Brogden, P. Ghosh, S.L. Banks, D.C. Hammell, A. L. Stinchcomb **"Microneedle-assisted percutaneous delivery of naltrexone hydrochloride in Yucatan minipig: in vitro-in vivo correlation".** Submitted to Molecular Pharmaceutics, May 2013

AWARDS AND HONORS

- **University of Maryland Pharmaceutical Sciences Graduate Program representative** at GPEN conference 2012
- **AAPS Dermatopharmaceutics Steering Committee Group member** (2012 – present)
- **DIA Annual meeting selected poster presentation,** (June 2012)
- **UKY Graduate School Academic Year Fellowship recipient** (2011-2012)
- **UKY Graduate Student Interdisciplinary Conference,** 3rd position in oral presentations, 2011

Priyanka Ghosh

Student's signature

April 24, 2013

Date